Pannexin 1 Channel Regulation and Function,

Relevance to Both Normal Physiology and Disease

Janelle Latham Weaver
Harrisonburg, VA

Masters of Science in Biological and Physical Sciences, University of Virginia, Charlottesville, VA

Bachelors of Science in Biomedical Engineering, University of Virginia, Charlottesville, VA

A Dissertation Presented to the Graduate Faculty of the University of Virginia in Candidacy for the Degree of Doctor of Philosophy

---

Department of Pharmacology
University of Virginia
May, 2016

Douglas A. Bayliss, Ph.D. (Advisor)

Norbert Leitinger, Ph.D.

Patrice G. Guyenet, Ph.D.

Kodi S. Ravichandran, Ph.D.

Mark P. Beenhakker, Ph.D.

Vesna Jevtovic-Todorovic, M.D., Ph.D., M.B.A.

Slobodan M. Todorovic, M.D. Ph.D.

ABSTRACT

Pannexin 1 (Panx1) channels are widely expressed membrane proteins that are thought to mediate adenosine triphosphate (ATP) release from many cell types. Through this capability, Panx1 can perpetuate puringeric signaling events, which are crucial for intra and intercellular communication in many physiologic contexts. Despite interest in the channels, there are still many unknowns regarding Panx1 – specifically how is the channel activity regulated *in vivo*, and how and where do these channels have a physiologic or pathophysiologic role? In this dissertation, I present three sets of results that expand on these gaps in the current literature. First, I report on the identification of a novel post-translational modification of the channel. Next, I ask whether the channel has a role in neuropathic pain and expand on the mechanism of how Panx1 might contribute to this condition. Finally, I look at a daily, more physiologic role for Panx1. These three sections represent significant advances to the field of pannexin channels and introduce many new opportunities for future studies.

DEDICATION PAGE

I am very fortunate to have had the opportunity to be a graduate student, and this work was made possible only through the outstanding people and organizations that are a part of my life.

To my husband Brian: I am most grateful for you and your company through this challenging period. You kept me sane and balanced with your calm manner of approaching everything. I would not have been able to complete this journey without your encouragement.

To my advisor Dr. Doug Bayliss: thank you so much for the opportunity to work with you and for your patience with my "adolescence" as a scientist. I am inspired by your commitment to integrity and the pursuit of truth, and your high expectations have challenged me to do my best. I also appreciate your flexibility with pursing the topics presented in this dissertation as well as other topics; most of my work has not been part of the mainstream investigations of the lab, but yet you fully supported these projects.

I am also grateful to my parents for instilling in me a strong sense of curiosity, a respect for hard work and honestly, and an ability to approach problems in a resourceful and logical manner.

Eva, Tash and Sanja: thank you all for your time, expertise and feedback on these projects. Each of you is an inspiration through your

dedication to your work as well as your willingness to help others on a daily basis.

Dr. Vesna Jevtovic-Todorovic and Dr. Slobodan Todorovic, thank you for giving me a start in a laboratory and continuing to work with me on pain projects for a long time afterwards. I was especially fortunate to work with you all as you are two successful physician scientists, and to observe the daily struggles and rewards of balancing these two very difficult careers.

To our collaborators in the Ravichandran, the Desai, the Leitinger and the Isakson labs: you are a great group of people. It is refreshing to work with collaborators who are so willing to think critically about projects that are sometimes outside of their own interest areas.

Thank you also to Dr. Norbert Leitinger, Dr. Kodi Ravichandran, Dr. Slobodan Todorovic, and Dr. Vesna Jevtovoic-Todorvic for allowing me to spend time in your labs when the project required equipment and resources beyond what were available in the Bayliss lab.

I am also grateful to the committee members not yet mentioned (Dr. Mark Beenhakker and Dr. Patrice Guyenet). Thank you for your time and your feedback about this project. Having folks not in the pain or pannexin fields on my committee was truly helpful, and you all often contributed some of the more insight comments at those meetings.

To my MSTP friends (especially Samantha and Monica), thanks for all the fun times together and for being there when things were rough. The walks, coffee breaks and chats were some of the highlights of my weeks.

Jolene, Dori, Tammy and Deborah: administrators keep this rusty academic machinery moving. That is no easy task. Thank you all for explaining all the paperwork and procedures that run this place. And particularly Jolene – I will miss our early morning conversations and sharing an office with you.

To the underhoos Jin, Joyce and Greg: best of luck on your future endeavors in medicine and engineering. I really enjoyed having you all in the lab. Your excellent questions and eagerness to work harder kept me focused and motivated on the tasks at hand.

Thanks to all the core facilities at UVA, including those associated with the Pannexin Interest Group (the mouse core run by Dr. Ulrike Lorenz and molecular biology core run by Dr. Bimal Desai) and the UVA-wide cores (The Flow Cytometry Core, the Advanced Microscopy Core and the Research Histology Core). Special thanks to Stacey Guillot and Sheri Vanhoose for performing difficult histology tasks on those teeny-tiny mouse peripheral nerves, sometimes even on short notice.

There were many training programs that contributed to my growth as a student (as well as my funding) including the UVA Medical Scientist Training Program, the Pharmacology Graduate Program (and the

Pharmacology Department in general), and the Cell and Molecular Biology Training Grant. In addition, I was fortunate to receive an F31 fellowship from the NINDS of which I am very grateful to the NIH and to all the taxpayer dollars that supported it.

Finally, a special thanks to our mouse subjects. There were at least 600 that underwent surgeries for these projects (this is probably an underestimate). They did not volunteer, but I hope that I made their time in the experiments as pleasant and as short as possible. And more importantly, I hope that the information they yielded was collected appropriately in order to best benefit others. In addition, thank you to the vivarium staff (Virginia, Hope, Bonnie and others) for caring for the mice every day.

TABLE OF CONTENTS

LIST OF FIGURES

LIST OF TABLES

ABBREVIATIONS

1H-[1,2,4]Oxadiazolo[4,3-a]quinoxalin-1-one ..... ODQ

Adenosine triphosphate ..... ATP

Carbenoxolone ..... CBX

Central nervous system ..... CNS

Chronic constrictive injury CCI

Diethylammonium (Z)-1-1(N, N-diethylamino)diazen-1-ium-1,2-diolate .....

..... DEA-NONOate

DL-Dithiothreitol ..... DTT

Dulbecco's modified eagle medium ..... DMEM

G protein-coupled receptors ..... GPCRs

Human embryonic kidney ..... HEK

N-ethylmaleimide ..... NEM

Nitric oxide ..... NO

Pannexin 1 ..... Panx1

Paw withdrawal latency ..... PWL

Primary mouse aortic endothelial cells ..... mAECs

Reduced L- glutathione ..... GSH

Single-nucleotide polymorphism ..... SNP

S-nitrosoglutathione ..... GSNO

Spared nerve injury ..... SNI

Trovafloxacin ..... Trovan

CHAPTER 1
Introduction

This first chapter will introduce what is known regarding pannexin channels, particularly with respect to post-translational modifications, pain and other central nervous system (CNS) related conditions. This chapter will also point out some pertinent areas where additional work is needed, as well as where there is confusing or misleading information in the field.

1.1 Channel properties

The name pannexin is derived from the prefix "pan" meaning "all" in conjunction with "nexus" or "connection" due to the close relation between this family of proteins and the gap junction-forming proteins connexins (1). "Pan" does indeed accurately describe Panx1, since it is expressed in almost every cell type examined to date (2,3). The other two family members, Pannexin 2 and Pannexin 3, have a more limited tissue distribution. While work on these other two channels will be of interest in the coming years, this dissertation is focused solely on Panx1.

It is important to note that although pannexin channels were identified by their homology to known gap junction proteins, Panx1 does not form gap junctions *in vivo* (4). The channel may form gap junctions in heterologous expression systems, where the channel is over-expressed and the

endogenous extracellular loop glycosylation of the channel is disrupted (2,5). Presumably, this extracellular glycosylation pattern would actually prohibit docking of two channels on adjacent cells *in vivo* thus limiting Panx1 to form only the "hemichannel" (or channel in this case) (6).

So if Panx1 is a channel, what are the known electrophysiological properties of this channel? Although this is a simple question, the properties of Panx1 as a channel are largely undefined or debated. First, the channel has been reported to contain a large-diameter pore based on its ability to pass molecules of up to 1KDa (7) including large DNA-binding dyes such as Yo-Pro and To-Pro (8,9) and purines like ATP (10) and UTP (9). The channel is thought to be non-selective, however there has also been a report claiming that Panx1 is an anion selective channel (11). This possibility is of interest considering that many dyes thought to be Panx1 permeable are indeed anionic as is ATP. The particular report is unfortunately limited by a technical flaw - the evidence of anionic permeability relies on the assumption that charged replacement molecules cannot permeate the channel and this assumption is unfounded (particularly if the channel pore is as large as some believe it to be). Another recent report suggested that Panx1 could form two main configurations – one high conductance state with less selective permeability and another as a low conductance, anionic selective channel (12). While this model does attempt to reconcile various viewpoints from different groups, it is unlikely considering that this work utilizes supra-physiologic K^+ concentrations to stimulate the channels, and neglects to

include several pertinent controls (including data from untransfected cells). In addition, work from our own lab and others (13-15) in mammalian expression systems do not substantiate the existence of a high conductance (500 pS) channel, which is primarily observed in oocytes (10). Thus, it is likely that various expression systems and recording conditions yield different results, and this complicates the basic definition of Panx1 channel properties.

Despite the ambiguities with respect to channel properties, there is good agreement about the basic structural configuration of the channel. In particular, several lines of evidence point to a hexameric structure of the channel (16) including unpublished work by our lab and collaborators at the University of Virginia. The predicted topology of each subunit consists of 4 transmembrane domains near the N-terminus and a longer intracellular C-terminal domain (1,6). The pore-forming region may consist of the first two transmembrane domains as well as the far C-terminal region of the protein (17) which could swing up into the pore in a "ball and chain" fashion to restrict channel conductance (18). While the structural properties of this channel are well-understood, solving the crystal structure would be very exciting (particularly under the various activation mechanisms of the channel, see next section).

With respect to pharmacologic properties, Panx1 is inhibited by a wide range of compounds, some of which are also known to block connexin channels and others which are more unique inhibitors of the channel (19).

Unique inhibitors, however, is not meant to imply "selective" or even "potent" as all of the Panx1 blockers identified to date also have other targets and/or are used in micromolar to millimolar concentrations. Carbenoxolone (CBX) is a glycyrrhetinic acid compound and is one of the most commonly used Panx1 channel blockers. At higher concentrations, it can inhibit connexin channels and also 11β-hydroxysteroid dehydrogenase (20,21). Nonetheless, its high water solubility (up to 100 mg/mL (22)) and relatively fast inhibition kinetics in recording studies make it a popular choice among pannexin researchers. Probenecid and other membrane transport inhibitors also inhibit Panx1 (23). Probenecid can be useful as it does not block connexin channels, however it is nearly insoluble in water (24) and has a much higher IC_{50} for inhibition of Panx1 (92 μM versus 0.69 μM for CBX in anti-FAS treated Jurkat cells (9)). Another chemically distinct and recently identified compound that inhibits Panx1 is the fluoroquinolone antibiotic Trovafloxacin (Trovan) (25). Trovan has the unique effect of blocking Panx1 in a voltage-dependent manner, inhibiting only the inward current while largely sparing the outward current. Additionally, the IC_{50} of Trovan is comparable to that of CBX (14,25) and it has the advantage of good blood-brain-barrier permeability (26). A disadvantage of this drug is its low water solubility (<25 mg/mL (27)). Finally, it is important to mention the ^{10}Panx1 peptide, which is often described as a selective inhibitor of Panx1 (7,19). This peptide was designed to mimic the extracellular loop of Panx1. In connexin channels, these loop-mimicking peptides prevent docking of two adjacent hemichannels and thus

the formation of a patent gap junction; as Panx1 does not form gap junctions, an extracellular loop-mimic peptide design would not be expected to inhibit Panx1 channels. Accordingly, the ^{10}Panx1 peptide may inhibit Panx1 via a steric effect rather than a sequence-specific mechanism (28) and unfortunately, this effect is not specific to Panx1 as ^{10}Panx1 inhibits connexin channels as well (7).

Lastly, it is important to note that the channel is indeed located on the extracellular plasma membrane (16,29-31). There are some reports of expression of the channel in the endoplasmic reticulum (6,32), however this observation is often either in the context of over-expression systems and/or with fluorescently-tagged versions of the channel, and this large tag could change the natural cellular localization of the channel. One report of endogenous Panx1 localized to intracellular organelles does exist (33), and it would be ideal to see this report followed up in other cell types with other Panx1 antibodies as the selectivity of Panx1 antibodies is notoriously enigmatic (34). If the channel is expressed in the endoplasmic reticulum, its function at that location is currently unknown.

1.2 Suspected modes of regulation

As with the basic properties of pannexin channels, understanding of Panx1 regulation is still primitive. Panx1 opening and closing is likely to be tightly regulated, as uncontrolled activity could have dire consequences for

the cell and surrounding tissue (e.g., depleting vital intracellular ATP stores and/or initiating an inflammatory response). Interestingly, one difference between mouse and human pannexin channels is that human Panx1 only produces current after activation (9,18). And with both species, ATP is only released after channel stimulation (10,35). This implies that for Panx1 to have a physiologic function (particularly related to ATP release and purinergic signaling), there must be controlled activation of the channel. In fact, there have been several modes of channel regulation identified already to date, with other mechanisms likely to be discovered in the coming years. These regulation mechanisms have been extensively reviewed by others (13,36,37). I will highlight a few mechanisms here that may be of importance to our work.

One frequently mentioned mode of regulation is via coupling of pannexin channels to purinergic receptors, specifically to P2X7. Purinergic receptors bind purines (like ATP, UTP and others) and are separated into two main classes based on mechanism of action; P2X receptors are ligand-gated cation channels while P2Y receptors are G-protein coupled (38). Interaction between Panx1 and receptors of these types is particularly remarkable as the channel could secrete the receptor ligand and act in an autocrine (in addition to paracrine) fashion, amplifying the initial purinergic signaling event.

Some purinergic receptors (P2X4 and P2X7) undergo a poorly understood change in conductance after stimulation with ligand and this

change may be connected to Panx1 (39). While the initial response of P2X7 to ATP is a small cationic conductance, the currents shift after minutes to a higher conductance, less selective state. One theory regarding this phenomenon is that the change is intrinsic to the receptor-channel, and that the pore of the P2X channel actually dilates upon prolonged stimulation, allowing nonselective passage of ions. An alternative theory posits that coupling could occur between the P2X7 receptor and Panx1 so that opening of Panx1 is actually responsible for the apparent change in electrical properties (40). Several reports replicated this coupling effect (8,41), which may occur via calcium or another second messenger (42,43). Notably, most of these findings of Panx1 acting as the large, nonselective, "P2X7 pore" used a rat P2X7 construct or mouse macrophages. At the same time, several other groups were unable to reproduce the finding that Panx1 is the P2X7 pore or had conflicting results (44-47). The point of distinction may be due to the fact that the P2X7 pore phenomenon may have a different identity depending on the cellular context (39) or perhaps that P2X7 variants support different degrees of coupling. For example, single-nucleotide polymorphisms (SNPs) that disrupt P2X7 pore formation are found in particular mouse strains (like the commonly used C57BL/6 strain) and in subsets of the human population as well (41,48,49). In addition, there also exist several splice variants of P2X7, which hinder large pore formation in various cell types (50,51). In sum, whether and how Panx1 couples to P2X7 remains under debate (specifically, whether Panx1 opening can account for the "pore dilation" of

P2X7), but it is likely that coupling may occur in certain species and cell types which have permissive P2X7 variants. In specific mouse lines (like C57BL/6), P2X7 and Panx1 will be unable to couple.

In addition to coupling to P2X receptors, Panx1 may also be activated via other receptors, specifically G-protein coupled receptors of the Gq type. Several of these types of receptors activate Panx1 channels including α1 adrenoreceptors (52), histamine H1 receptors (53), the thrombin receptor PAR-1 (54), thromboxane receptors (55), and P2Y6 (56). While the exact manner of channel activation is still being examined, some groups suspect that this coupling may occur via phospholipase C and intracellular calcium (57) while others implicate Rho kinases (58) or cAMP/PKA (55). Our group is also investigating this question and assessing various alternative hypotheses for the activation mechanism. We identified the second intracellular loop as being the vital for activation via this mechanism (52) and found that mutation of a specific tyrosine (Y198) to alanine can completely disrupt α1 adrenoreceptor-dependent activation of the channel. This mutation and activation mechanism will be discussed further in Chapter 3.

Another mechanism of activation involves caspase-mediated cleavage of the C-terminal tail of Panx1 (9,18). This cleavage event can be associated with cell apoptosis, opening the channel to release the "find me" signal ATP and recruit phagocytic cells to the area (9). As mentioned above, the C-terminal portion of the channel may be located near the presumed pore of

the channel (17). Indeed, cleavage and removal of the C-tail activates the channel whether or not apoptosis is occurring; this suggests that modulation of this region of the protein could be critical for a broad range of channel activation mechanisms (18).

Several post-translational modifications can regulate Panx1 channel function (reviewed in (59)). First, the channel can contain multiple glycosylation forms located on the first extracellular loop (6). Not only can these glycosylation patterns potentially prevent gap junction formation between two adjacent pannexin channels, these extracellular modifications are also implicated in channel trafficking. Specifically, the most complex glycosylation state of the channel promotes Panx1 trafficking to the cell surface and other less complex glycosylation states are more intracellular. However, there also exist several mutant forms of the channel that lack the most complex glycosylation state and yet still traffic normally to the cell surface (35,60).

Phosphorylation of the channel by Src kinase is another proposed activation mechanism, specifically facilitated by upstream activation of NMDA receptors (61,62), P2X7 receptors (42) and/or type 1 TNF receptors (63). The presumed phosphorylation target is Y308 in the intracellular C-terminal portion of the channel (61,62).

Finally, three other mechanisms of activation are worth mentioning: mechanical stretch (10), membrane depolarization (2) and high extracellular

K^+ (10,30). With respect to these mechanisms, however, it is important to note that how these stimuli act on the channel is currently unknown. In addition, our single channel recordings show that Panx1 is not a voltage-gated channel (unpublished data). Also, in our hands at the University of Virginia, high K^+ does not stimulate opening of the channel as measured by dye uptake in native channels (unpublished data).

Despite significant progress in the area of Panx1 regulation, two key questions remain. First, what are the endogenous mechanisms of channel inhibition that prevent the negative consequences of excess ATP efflux? I examine a novel mechanism of channel inhibition in Chapter 2 of this dissertation. And second, of these potential channel regulations, which are relevant *in vivo*, and under what physiologic or pathophysiologic settings? I address this question specifically with respect to neuropathic pain in Chapter 3, and I present a new idea for a physiologic function of Panx1 in Chapter 4.

1.3 Functions of Panx1: phenotypes despite low expression

As mentioned above, the expression of Panx1 is widespread, having been detected in most tissues (2,3). It is highly expressed in the brain in particular, although the level of expression peaks during the late embryonic period and then rapidly drops off into adulthood (64). This expression pattern implies a role for the channel in development but surprisingly, the global

Panx1 knockout mouse is largely normal under unstressed conditions (see Chapter 3 and also (65)).

One exception, where Panx1 has a role in normal physiology, is in the regulation of vascular function (52,66). In these studies, smooth muscle cell specific knockout of Panx1 caused nocturnal hypotension, presumably due to a disruption of α1 adrenoreceptor-mediated Panx1 opening (and subsequent vasoconstriction supported by ATP release). Panx1 channels may also support synaptic plasticity, as global Panx1 knockout mice had impaired spatial learning and object recognition (67,68). In the coming years, it will be interesting to see if more physiologic roles are found for Panx1.

A number of phenotypes do readily appear, however, after the mice are subjected to various stressors or stimuli. Many of these identified phenotypes deal with CNS functions and inflammation, and these will be summarized below.

Within the nervous system, pathophysiologic functions of the channel result in several diverse phenotypes. One of the earliest observed roles for pannexin channels was in brain ischemia (69,70), where double Panx1-Panx2 knockout mice are largely protected from damage after ischemic insult (71). Other reports implicate Panx1 in epilepsy (72-74), the carotid body response to hypoxia (75), death of enteric neurons due to colitis (76), migraine (77), glaucoma (78), multiple sclerosis (79), and perhaps even schizophrenia (80).

Another role for Panx1 is in the development of neuropathic pain. A handful of papers (41,81-83) and reviews (84,85) have suggested this role, however there are some key limitations to these studies that are worth mentioning. Before detailing these limitations, I first want to summarize the key features of neuropathic pain as this is a major topic of Chapter 3.

Neuropathic pain is a type of chronic pain condition that results from direct damage to the nervous system (86,87). This damage can be caused by trauma (e.g., sciatica, operative injury), metabolic aberrations (e.g., diabetes, vitamin B12 deficiency), or toxic insults (e.g., chemotherapeutic agents, heavy metals). The results of this damage are painful symptoms defined as allodynias (a painful response to normally non-painful stimuli) and hypersensitivities (an increased sensitivity to stimuli that is already painful). Patients often describe the symptoms as chronic burning, tingling sensations, and a heightened sensitivity to touch or temperature (e.g., pain when putting on socks). Unfortunately, for many patients these symptoms are unresponsive to most of the front-line medications for neuropathic pain (86). Ongoing, under-treated symptoms lead to a host of related psychosocial conditions, including loss of sleep, poor job performance, addiction to pain medications, and depression (88-90). The monetary costs from the treatment of neuropathic pain and these associated conditions are immense, constituting a significant portion of the $635 billion spent annually in the US on chronic pain (91). In addition, neuropathic pain is widespread with an estimated prevalence of upwards of 17% (88).

In recent years, there has been a remarkable amount of convincing work implicating ATP and purinergic signaling in neuropathic pain (38). The current molecular model of neuropathic pain posits that P2X4 receptors promote brain-derived neurotrophic factor release in the dorsal horn of the spinal cord (92), leading to altered pain processing and an increased propagation of pain signals into the CNS (93). Other purinergic receptors contribute to neuropathic pain as well, including P2X3 (94,95), P2X7 (96) and P2Y12 (97). While the downstream players of these pathways are well characterized, the initial source of ATP necessary to stimulate P2X4 and other purinergic receptors has not been identified. This unknown element of the model led us to test the hypothesis that Panx1 could contribute to neuropathic pain development, and therefore could be the missing source of ATP after nerve injury (see Chapter 3). In fact, this was such a strong, compelling hypothesis that unbeknownst to us, several other groups were testing similar hypotheses which have since been published (41,81-83).

The first published work examined the relationship of SNPs in various mouse lines to pain behavior after spared nerve injury (41). One of the most prominent associations between genetics and pain was with a SNP in the P2X7 receptor that disrupts P2X7 pore formation (and presumably Panx1 opening (48)). While this paper implicated Panx1 via the association with P2X7, an independent role for the channel was not specifically addressed. The next publications did attempt to establish a role for Panx1 in pain, however the primary data was heavily - or in two of the cases, entirely -

dependent on notoriously nonselective Panx1 blockers (81-83). These papers certainly represent important contributions to the understandings of neuropathic pain, but the use of these nonselective blockers prevents the formation of definitive conclusions. Additionally, mechanisms by which the channel promotes neuropathic pain were suggested in those works (e.g., via P2X7 or NMDA receptors (84)), but again not directly tested. In Chapter 3, we confirm that Panx1 function contributes to neuropathic pain and further attempt to understand the mechanism behind this phenomenon.

A final area of interest is Panx1 and inflammation. This topic has been extensively reviewed by others (98-100), but it is important to note that Panx1 channels are implicated in many inflammation-related processes. These processes include releasing ATP to act as a "find me" signal for apoptotic cells (9), migration of immune cells (101,102), T lymphocyte activation (103,104), and possibly inflammasome activation (105,106) although this is debated by others (101,107). As an aside, neuropathic pain is also heavily dependent on both peripheral and central inflammation, and the interaction between these recruited inflammatory cells at various locations along sensory processing pathways promotes the development of neuropathic pain (93,108-110).

1.4 Dissertation preview

This introduction highlighted the fact that there are still many unanswered questions regarding Panx1 (Figure 1.1). The following dissertation does not attempt to address any of these major questions as a whole; rather, it is an evaluation of several of these key questions separated into three distinct narratives. The first section investigates a novel post-translational modification of Panx1 (Chapter 2). The second is a continuation of early work on the channel regarding neuropathic pain, and seeks to confirm and expand those initial findings on this pathophysiologic function of the channel (Chapter 3). The last part consists of a preliminary investigation into a novel physiologic role for Panx1 in sleep (Chapter 4). Finally, Chapter 5 will review each of these findings with respect to future work and overall conclusions.

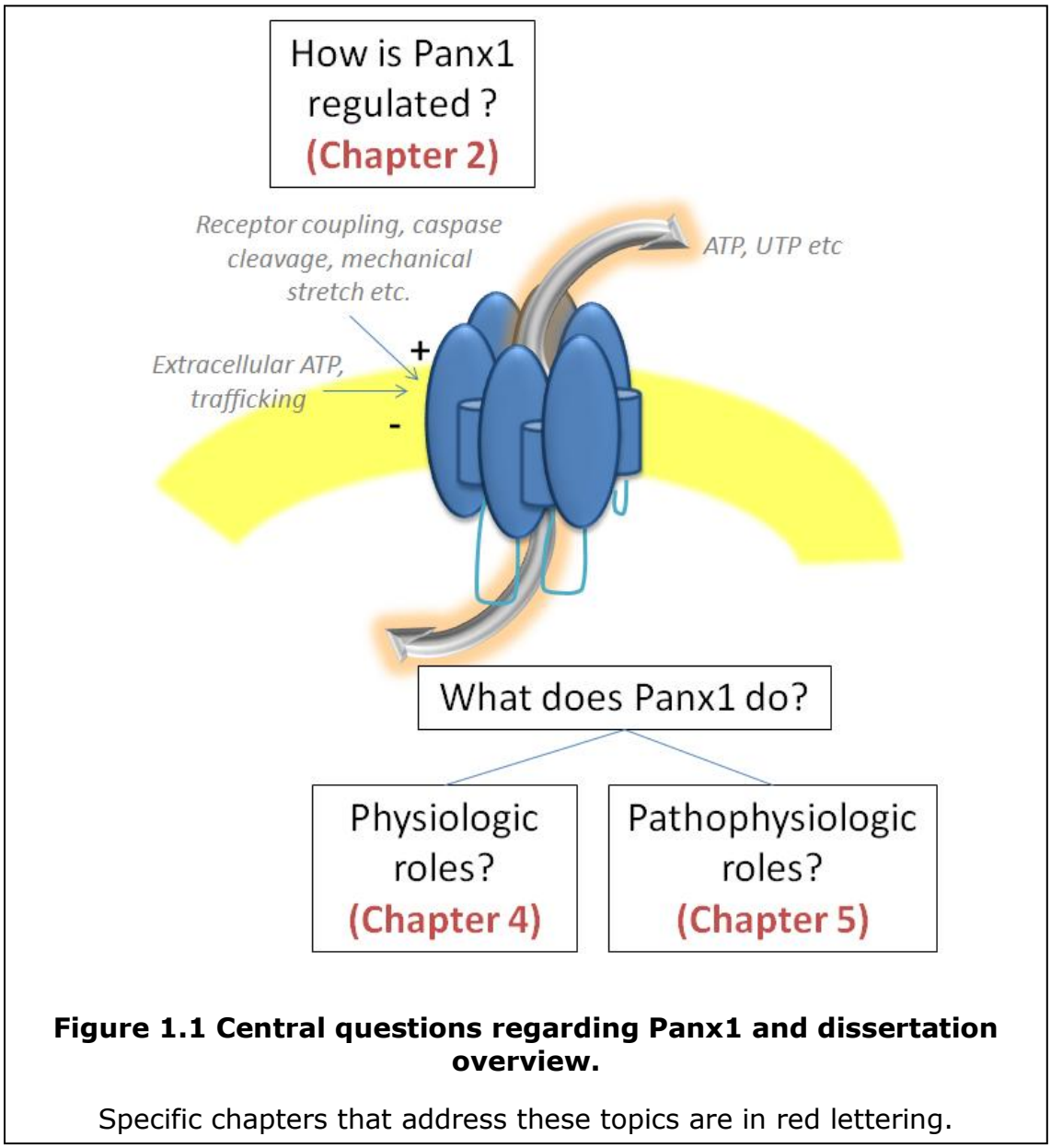

Figure 1.1 Central questions regarding Panx1 and dissertation overview.

Specific chapters that address these topics are in red lettering.

CHAPTER 2

S-nitrosylation inhibits pannexin 1 channel function

This chapter is modified from the following publication and represents the work of myself along with Alex Lohman from the Brant Isakson lab as co-first-authors:

Lohman, A.W., Weaver, J.L.*, Billaud, M., Sandilos, J.K., Griffiths, R., Straub, A.C., Penuela, S., Leitinger, N., Laird, D.W., Bayliss, D.A., Isakson, B.E. (2012). S-nitrosylation inhibits pannexin 1 channel function. Journal of Biological Chemistry 287(27): 39602-12. [PMID: 24634817]*

Please note: I was responsible for performing all patch clamping experiments. Western blots, biotin switch assays, histology and ATP release assays were conducted by Alex Lohman.

2.1 Introduction

As described in Section 1.2, there are several known modes of Panx1 channel activation including membrane stretch and depolarization (10), activation of α1-adrenorecptors (10,66) and PAR-1 receptors (54), and by cleavage of its intracellular C-tail by activated caspases 3 and 7 (9,18). Since sustained ATP release from cells is detrimental to cell viability, it is crucial that the activity of these channels be tightly regulated to prevent depletion of ATP. Even as novel forms of Panx1 channel activation continue to emerge,

mechanisms leading to inhibition of these channels remain poorly understood.

Inhibition of the channel could potentially occur via several mechanisms including alterations in channel trafficking, allosteric modulation, inactivation/deactivation or other forms of post-translational modification (of which there are many). Allosteric modulation and inactivation/deactivation may not apply in the case of Panx1 as these channels do not appear to be ligand-gated or voltage-gated. Evidence has arisen indicating that the channel is post-translationally modified by glycosylation at asparagine 254, an event thought to regulate trafficking of Panx1 channels to the plasma membrane (31,111). However, alterations in these glycosylation events are restricted to heterologous expression systems (and often observed in mutant proteins), and have not been observed dynamically or spontaneously with the endogenous channel. Panx1 channels can also be irreversibly modified during apoptosis by cleavage of the intracellular C-tail by caspases (9,18), allowing release of ATP that serves as a "find-me" signal for monocyte recruitment and phagocytosis. Despite the recognition of these modification events, there are no indentified reversible post-translational modifications involved in the regulation of Panx1 channel activity at the plasma membrane.

Protein S-nitrosylation is a reversible post-translational modification in which nitric oxide (NO) moieties are covalently bound to reactive cysteine thiols via an S-nitrosothiol bond. S-nitrosylation can have profound effects on

protein function with modification of even a single cysteine residue dramatically altering protein activity (112,113). This modification is known to regulate the activity of several membrane channels including, among others, connexin43 (Cx43) gap junctions and hemichannels (112,114), the cardiac slowly activating delayed rectifier potassium channel KCNQ1 (115), the transient receptor potential channel TRPC5 (116) and the ryanodine receptor type 1 (113). Notably, Cx43, a constituent of gap junction channels with a similar membrane topology and oligomerization state as Panx1, is modified by S-nitrosylation at a single cysteine residue in small arteries leading to an increase in channel permeability to second messengers (112).

Panx1 contains several cysteine residues that may play important roles in the regulation of channel function. As Panx1 is highly expressed in tissues rich in NO, such as the vasculature and nervous system, we sought to determine if Panx1 can be post-translationally modified by S-nitrosylation and whether this modification can affect channel activity.

2.1 Experimental procedures

2.1.1 Chemicals and reagents

Reduced L- glutathione (GSH), DL-Dithiothreitol (DTT), N-ethylmaleimide (NEM) and 1H-[1,2,4]Oxadiazolo[4,3-a]quinoxalin-1-one (ODQ) were purchased from Sigma (St Louis, MO). Diethylammonium (Z)-1-1(N, N-diethylamino)diazen-1-ium-1,2-diolate (DEA-NONOate) was

purchased from Cayman chemicals (Ann Arbor, MI) and prepared by dissolving in 10 mM NaOH. S-nitrosoglutathione (GSNO) was prepared by incubating reduced GSH with sodium nitrate. CBX, Biotin-HPDP and EZ-link sulfo-NHS-LC-biotin were purchased from ThermoFisher (Waltham, MA).

2.1.2 Cell culture and transfections

Human embryonic kidney (HEK) 293T cells were cultured in Dulbecco's modified eagle medium (DMEM) High Glucose (Gibco) supplemented with 10% fetal bovine serum (Life Technologies, Carlsbad, CA), 1% penicillin/streptomycin, 1% L-glutamine and 1% non-essential amino acids and maintained at 37°C in a humidified 5% CO_2 incubator. All cells were used for experiments at passage ≤ 20. Primary mouse aortic endothelial cells (mAECs) were purchased from Cell Biologics (Chicago, IL), cultured in ECM-MV media and maintained at 37°C in a humidified 5% CO_2 incubator. All mAECs were used for experiments at passage ≤ 8 as per the manufacturer's recommendations.

Cells at 80-90% confluency were transfected with plasmids or siRNAs using the Lipofectamine 2000 reagent (Invitrogen, Carlsbad, CA) following the manufacturers protocol. For electrophysiology experiments, cells were co-transfected with the Panx1 pcDNA3.1 plasmid and green fluorescent protein (2.5 µg of Panx1 plasmid with 0.5 µg of pEGFP) and plated onto poly-L-lysine-coated glass coverslips 24 hours later. The cells were returned to the

incubator and allowed to adhere for at least 1 hour prior to use. Recordings were conducted within 1 day of plating.

2.1.3 Plasmid generation and site-directed mutagenesis

Full length murine Panx1 coding region was amplified by PCR from a Panx1-EGFP-N1 plasmid, previously described in (6), using the following primers: forward – 5'caaatgggcggtaggcgtgt 3', reverse – 5' cttgtggccgtttacgtcgc 3'. The PCR product was digested (*HindIII* and *BamHI*) and ligated into pcDNA3.1. The final construct was sequenced to confirm proper insertion. Single cysteine-to-alanine mutations were performed in the Panx1 pcDNA3.1 construct using the QuikChangeII Site-Directed Mutagenesis Kit (Agilent Technologies, Santa Clara, CA) and double cysteine-to-alanine mutations were constructed using the QuikChange Multi Site-Directed Mutagenesis Kit (Agilent Technologies) following the manufacturer's protocol.

2.1.4 Biotin switch assay

The biotin switch assay was performed as previously described (112,117). Briefly, cell monolayers were treated with 100 μM GSNO, 50 μM DEA-NONOate or vehicle for 10 minutes at 37°C. Monolayers were then washed with PBS, cells lysed in RIPA buffer containing protease inhibitors and protein quantified using the Bradford technique. Proteins were precipitated with acetone and pelleted by centrifugation for 5 minutes at 10,000xg. Pellets were resuspended and free cysteine thiols were blocked with NEM for

20 minutes at 50°C. Proteins were then precipitated as described above to remove excess NEM and S-nitrosylated cysteines were reduced with 1 mM ascorbate in the presence of 1mM $Cu^{2+}$and biotinylated with biotin-HPDP for 1 hour at room temperature. Biotinylated proteins were then pulled down with streptavidin-agarose beads for 1 hour at room temperature and subjected to SDS PAGE and Western blotting for detection of S-nitrosylated Panx1. For negative controls, ascorbate was omitted from the assay which prevented reduction of S-nitrosothiols and subsequent biotinylation.

2.1.5 Electrophysiology

Whole cell voltage-clamp recordings were performed as described (18). Recordings were obtained at room temperature with 3-5 MΩ Sylgard-coated borosilicate glass patch pipettes and an Axopatch 200B amplifier (Molecular Devices, Sunnyvale, CA). The internal solution contained 30 mM tetraethylammonium chloride, 100 mM $CsMeSO_4$, 4 mM NaCl, 1 mM $MgCl_2$, 0.5 mM $CaCl_2$, 10 mM HEPES, 10 mM EGTA, 3 mM ATP-Mg and 0.3 mM GTP-Tris (pH 7.3). The bath solution was composed of 140 mM NaCl, 3 mM KCl, 2 mM $MgCl_2$, 2 mM $CaCl_2$, 10 mM HEPES and 10 mM glucose (pH 7.3). Bath solutions containing 50 μM CBX, 1 mM DTT, and 100 μM DEA NONOate (bubbled with 100% O_2) were flowed over the cells at a rate of approximately 2 mL/min while 100 μM GSNO, 100 μM GSH, or 100 μM GSH with 100 μM H_2O_2 were pipetted directly into the bath under stop-flow conditions. Ramp

voltage clamp commands were applied at 5-s intervals using pCLAMP software and a Digidata 1322A digitizer (Molecular Devices). Peak currents were taken at +80 mV and the percent inhibition was calculated by dividing the decrease in peak current by the total Panx1 current (defined by its CBX sensitivity). We quantified the DTT-reversible component of GSNO/DEA-inhibited current to define the fraction of current inhibition that was due to S-nitrosylation.

2.1.6 ATP release assay

HEK293T cells or mAECs were plated in 24 well plates coated with 0.01% poly-L-lysine or 0.2% gelatin, respectively. HEK293T cells at 80-90% confluency were transfected with plasmids encoding $Panx1^{WT}$ or Panx1 cysteine mutants for 24 hours. For ATP release experiments, the media was removed from each well and cells were carefully washed 2 times with warm Krebs-HEPES buffer containing 2 mM Ca^{2+} and 1% BSA. Cells were then incubated in fresh Krebs-HEPES buffer for 30 minutes at 37°C to allow degradation of any ATP released as a result of mechanical stimulation imparted by changing the media. Ecto-nucleotidases were then inhibited by incubating cell monolayers with 300 μM ARL 67156 (Tocris, Bristol, UK) for 30 minutes at 37°C. ATP release was stimulated from HEK293T cells by depolarizing the cells with 100 mM KCl for 1 minute or from mAECs by treatment with 1 U/mL mouse thrombin for 5 minutes (as previously described (54)). To evaluate the effect of NO donors on ATP release, cells

were pretreated with 100 μM GSNO or 50 μM DEA NONOate for 10 minutes. For controls, cells were pretreated with 100 μM GSH or 50 μM CBX. For experiments using mAECs, cells were either allowed to grow to confluency or transfected at 80-90% confluency with two siRNAs targeting Panx1 (Ambion, ThermoFisher) (66) for 48 hours to knockdown endogenous Panx1. Following stimulation of ATP release, 75 μL of the cell supernatant was collected and placed immediately on ice. All samples were briefly centrifuged and 50 μL of each sample was transferred to a 96-well plate. Using a FluoStar Omega luminometer, 50 μL of luciferin:luciferase reagent (ATP bioluminescence assay kit HSII; Roche, Risch-Rotkreuz, Switzerland) was injected into each well and luminescence was immediately recorded. ATP concentration in each sample was calculated from a standard curve for all experiments. Data are expressed as a % change in ATP release from control (unstimulated cells) conditions or a % inhibition of ATP release by GSNO for experiments on HEK293T cells expressing Panx1 cysteine mutants.

2.1.7 Cell surface protein biotinylation

HEK293T cells were transfected to express $Panx1^{WT}$ or Panx1 cysteine mutants as described above and grown to confluency in 6-well plates. For experiments examining the effect of NO donors on Panx1 membrane expression, confluent monolayers were treated for various times (0-10 minutes) with GSNO. Cells were washed once with cold PBS then incubated with cold DMEM (without FBS) and 50 μM CBX at 4°C for 30 minutes. CBX

was added to prevent biotin from passing through Panx1 channels, which would label intracellular proteins. Cells were then washed with PBS and incubated at 4°C for 1 hour in cold PBS (1.5 mL/dish) containing EZ-link-sulfo-NHS-LC-biotin (1 mg/mL) and CBX (50 μM). The cells were then washed again with PBS and lysed in PBST (PBS + 0.5-1% Triton-X 100) containing protease inhibitors. Total protein was quantified using the Bradford technique and equal amounts of protein were incubated with Streptavidin-agarose beads for 2 hours at 4°C to pull down biotinylated proteins. Beads were then washed 5 times with PBST, spun down and bound proteins eluted by incubation with laemmli buffer. Eluted proteins were subjected to SDS-PAGE and Western blotting for detection of Panx1.

2.1.8 Immunofluorescence microscopy

Transfected HEK cells were fixed in 4% PFA for 15 minutes and subjected to standard immunocytochemistry as previously described (66). Images were obtained with an Olympus Fluoview 1000 laser scanning confocal microscope.

2.1.9 cGMP assay

Transfected HEK cells were incubated with ODQ (10 μM) for 20 minutes prior to treatment with GSNO (100 μM) or vehicle for 10 minutes at 37°C. Cells were then isolated and lysed in buffer provided in the cGMP XP®

Assay kit (Cell Signaling, Danvers, MA) and the assay was performed according to manufacturer's protocol. A standard curve of known cGMP concentrations was constructed and used to calculate cGMP concentrations in the experimental samples.

2.1.10 Data analysis

Results are presented as means ± s.e.m. Statistical significance was determined by $p < 0.05$ using a Mann-Whitney U-test or Kruskal-Wallis test followed by Dunn's test for multiple comparisons.

2.2 Results

2.2.1 Panx1 can be S-nitrosylated

To determine if Panx1 can be S-nitrosylated, we transfected HEK293T cells with a plasmid encoding murine Panx1 and treated the cells with two independent NO donors: S-nitrosoglutathione (GSNO) or diethylamine NONOate (DEA NONOate). This provides a useful model system for examination of Panx1 modifications since we find that endogenous Panx1 is undetectable in these cells (118). In addition, Western blot analysis did not reveal any expression of nitric oxide synthase (NOS) isoforms in these cells (Figure 2.1A), providing a clean model system with little to no background NO from endogenous sources.

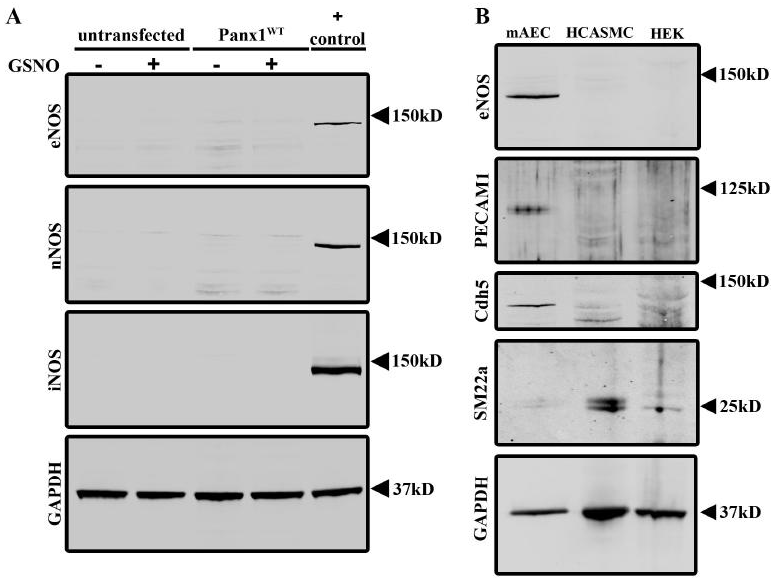

Figure 2.1 Expression of NOS isoforms in HEK cells and validation of the mAEC phenotype.

(A) Western blots of HEK cell lysates for eNOS, nNOS and iNOS. + control for eNOS was human coronary artery endothelial cells, for nNOS was mouse brain and iNOS was activated macrophages. (B) Western blots of mAEC lysates for the endothelial cell markers eNOS, PECAM-1, Cdh5. Human coronary artery smooth muscle cells were used as a negative control and positively identified by their expression of SM22α.

Application of 100 μM GSNO or 50 μM DEA NONOate for 10 minutes induced S-nitrosylation of Panx1 as detected by the biotin switch assay (Figure 2.2). Treating cells with a reducing agent (DTT, 1 mM) immediately following GSNO or DEA NONOate treatment to reduce S-nitrosothiols prevented biotinylation in this assay. In addition, S-nitrosylation of Panx1 was not observed in untransfected cells or when the ascorbate step was omitted to prevent unmasking of S-nitrosylated cysteines for subsequent biotinylation. The biotin switch assay can detect proteins with cysteine modifications in addition to S-nitrosylation, and GSNO is capable of also modifying cysteine thiols by S-glutathionylation. Therefore, we treated $Panx1^{WT}$ expressing HEK cells with reduced glutathione (GSH, 100 μM), which can induce S-glutathionylation but not S-nitrosylation. Importantly, we did not observe Panx1 modification by GSH in these cells (Figure 2.2A). Protein S-glutathionylation occurs more readily under conditions of oxidative stress, but we did not observe any Panx1 cysteine modification when $Panx1^{WT}$ expressing cells were exposed to reduced GSH in the presence of 100 μM H_2O_2. This further supports a role for Panx1 S-nitrosylation over S-glutathionylation (Figure 2.2B). Taken together, these results indicate that Panx1 can be S-nitrosylated.

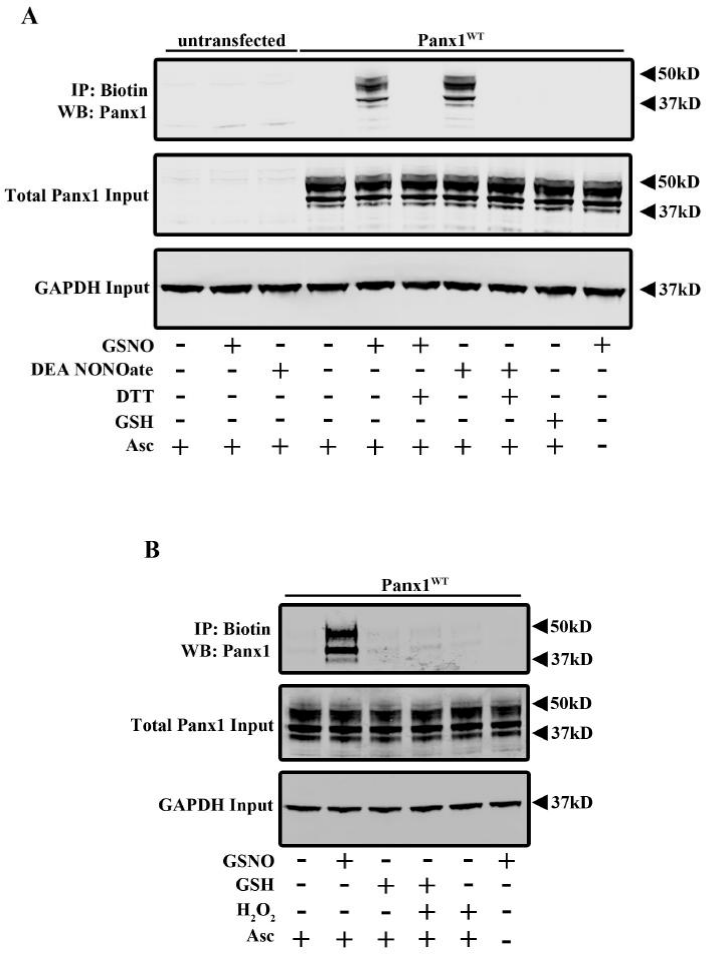

Figure 2.2 S-nitrosylation of Panx1 by GSNO.

(A) Biotin switch assay on untransfected and Panx1^{WT} expressing HEK cells treated with 100 μM GSNO ± 1 mM DTT, 50 μM DEA-NONOate ± 1 mM DTT, or 100 μM GSH. Ascorbate (-Asc) was omitted from the biotin switch assay for the negative control. (B) Biotin switch assay on Panx1^{WT} expressing HEK cells treated with 100 μM GSNO, 100 μM GSH ± 100 μM H2O2, or 100 μM H_2O_2 alone.

2.2.2 S-nitrosylation inhibits Panx1 channel function

To determine the functional consequences of S-nitrosylation on Panx1 channel activity, we examined effects of GSNO and DEA NONOate on whole cell currents from $Panx1^{WT}$ expressing HEK cells. The peak current evoked by voltage ramp protocols (at +80 mV) was strongly inhibited by GSNO (Figure 2.3A and Figure 2.3B). Importantly, and as expected for an effect mediated by S-nitrosylation, GSNO-mediated current inhibition was completely reversed by the reducing agent, DTT (Figure 2.3A and Figure 2.3B). The current restored by DTT was inhibited by the Panx1 channel blocker, CBX and displayed a current-voltage relationship characteristic of Panx1 (Figure 2.3B); note that GSNO-mediated inhibition was evident over the entire voltage range, including at rest potentials. We quantified the DTT-reversible component of GSNO-inhibited current, relative to the CBX-sensitive current, as a measure of the percentage of Panx1 current that was reduced by S-nitrosylation (~63%, Figure 2.3C). The DTT-reversible inhibition was significantly greater following GSNO treatment, by comparison to that following GSH or GSH with H_2O_2 application, consistent with the biotin switch data which suggested that the channel was modified by S-nitrosylation rather than S-glutathionylation. We also observed DTT-reversible current inhibition following application of DEA NONOate (e.g., see Figure 2.4A-B). However, the response with DEA NONOate was less consistent than with GSNO (n=2 of 6 cells tested), and effects of the compound were not more evident when applied at higher concentrations (up to 1 mM) or at elevated temperature

(30°C). There was no significant activation of current by DTT in Panx1-expressing cells that had not been treated with NO donors, and there were no detectable CBX-sensitive currents in untransfected cells (data not shown).

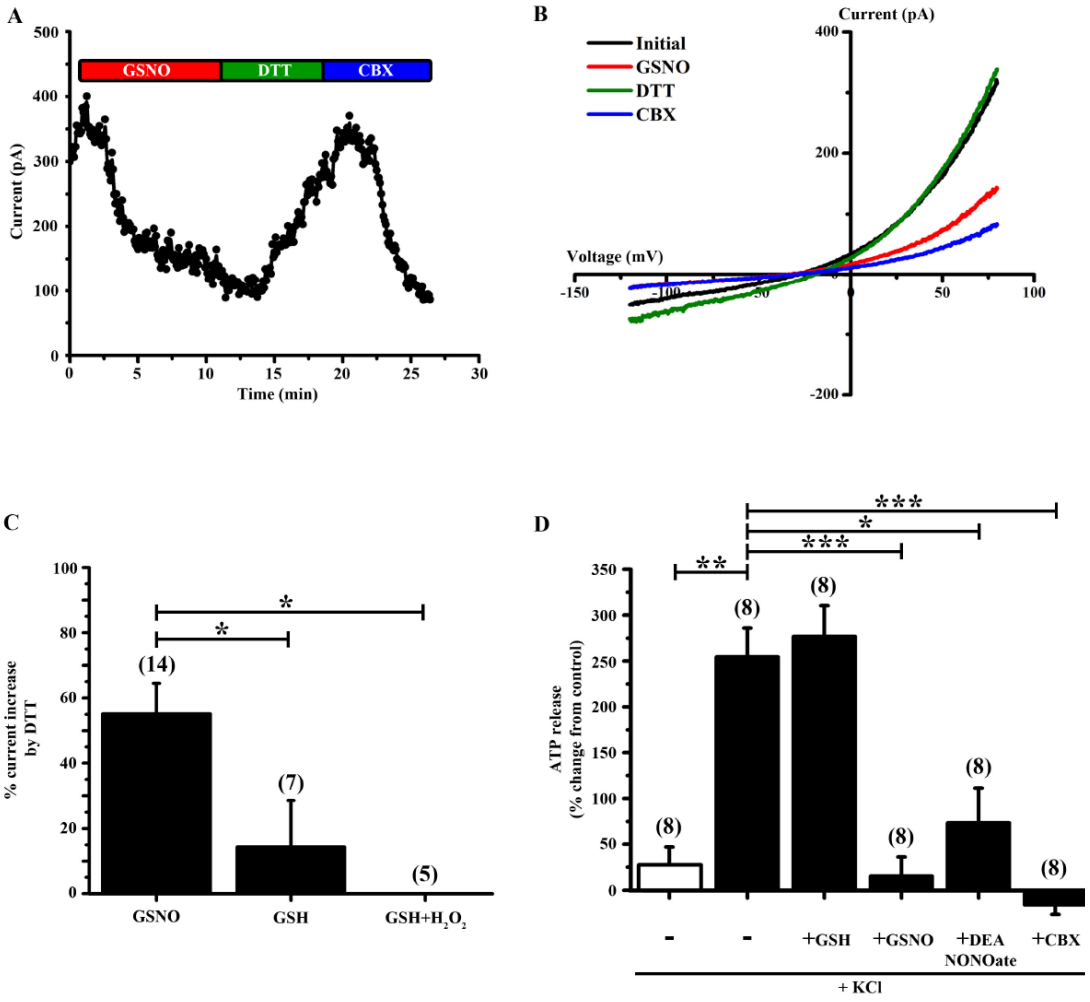

Figure 2.3 GSNO inhibits Panx1 currents.

(A) Time series showing peak Panx1 whole cell current amplitude during application of 100 μM GSNO, DTT and CBX. (B) I/V curves of Panx1 currents from Panx1^{WT} expressing HEK cells under control conditions (black trace), following application of 100 μM GSNO (red trace), 1 mM DTT (green trace) and CBX (blue trace). (C) Summary data showing the percent of Panx1 current inhibition by GSNO, GSH or GSH with H_2O_2 that was reversible by DTT. D. ATP release assay from untransfected (white bar) and Panx1WT expressing (black bars) HEK cells. Data represents cells treated with 100 mM KCl following pretreatment with 100 μM GSNO, 50 μM DEA NONOate, 100 μM GSH or 50 μM CBX. All data are presented as a % change in ATP release compared to control (-KCl). n-values are indicated in brackets. *, $p<0.05$; **, $p<0.001$; ***, $p<0.0001$

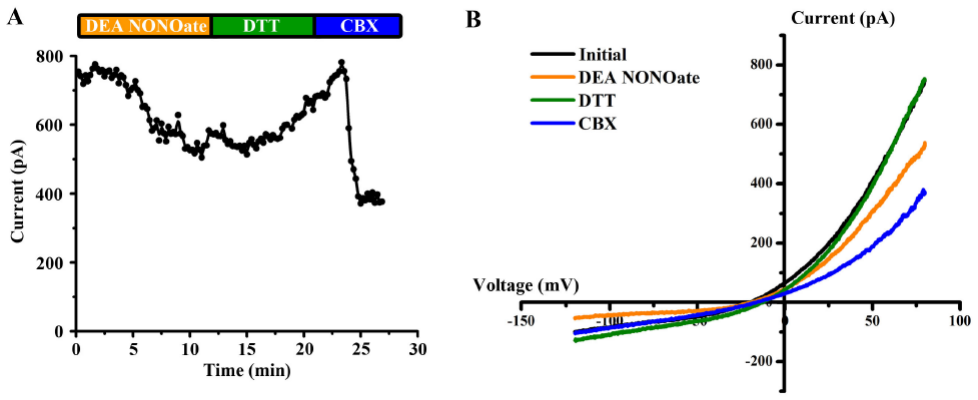

Figure 2.4 Panx1 current inhibition by DEA NONOate.

(A) Time series showing peak Panx1 whole cell current amplitude during application of 100 μM DEA NONOate, DTT and CBX. (B) I/V curves of Panx1 currents from $Panx1^{WT}$ expressing HEK cells under control conditions (black trace), following application of 100 μM DEA NONOate (orange trace), 1 mM DTT (green trace) and CBX (blue trace).

In addition to S-nitrosylation, increases in NO can activate soluble guanylate cyclase (sGC) and promote downstream cGMP-dependent phosphorylation cascades. Therefore, we examined whether GSNO treatment activated sGC in our cells and if this contributed to GSNO-mediated Panx1 current inhibition. Western blot analysis revealed endogenous expression of sGC in our HEK cells that was not affected by transfection with the murine Panx1 plasmid or by treatment with GSNO (Figure 2.5A). While GSNO did not affect the expression of sGC, we observed a significant increase in intracellular cGMP concentration following GSNO treatment in $Panx1^{WT}$ expressing HEK cells that could be blocked by pretreatment with the sGC inhibitor ODQ (Figure 2.5B). To rule out the possibility that GSNO was exerting its functional effects on Panx1 currents by activation of cGMP-dependent signaling cascades, we pretreated $Panx1^{WT}$ expressing HEK cells with 20 μM ODQ and examined the effect of GSNO on Panx1 currents. Importantly, ODQ had no effect on Panx1 current inhibition by GNSO (Figure 2.5C). Taken together, these data indicate that NO can inhibit Panx1 currents by a mechanism distinct from cGMP signaling, likely by S-nitrosylation of the channel.

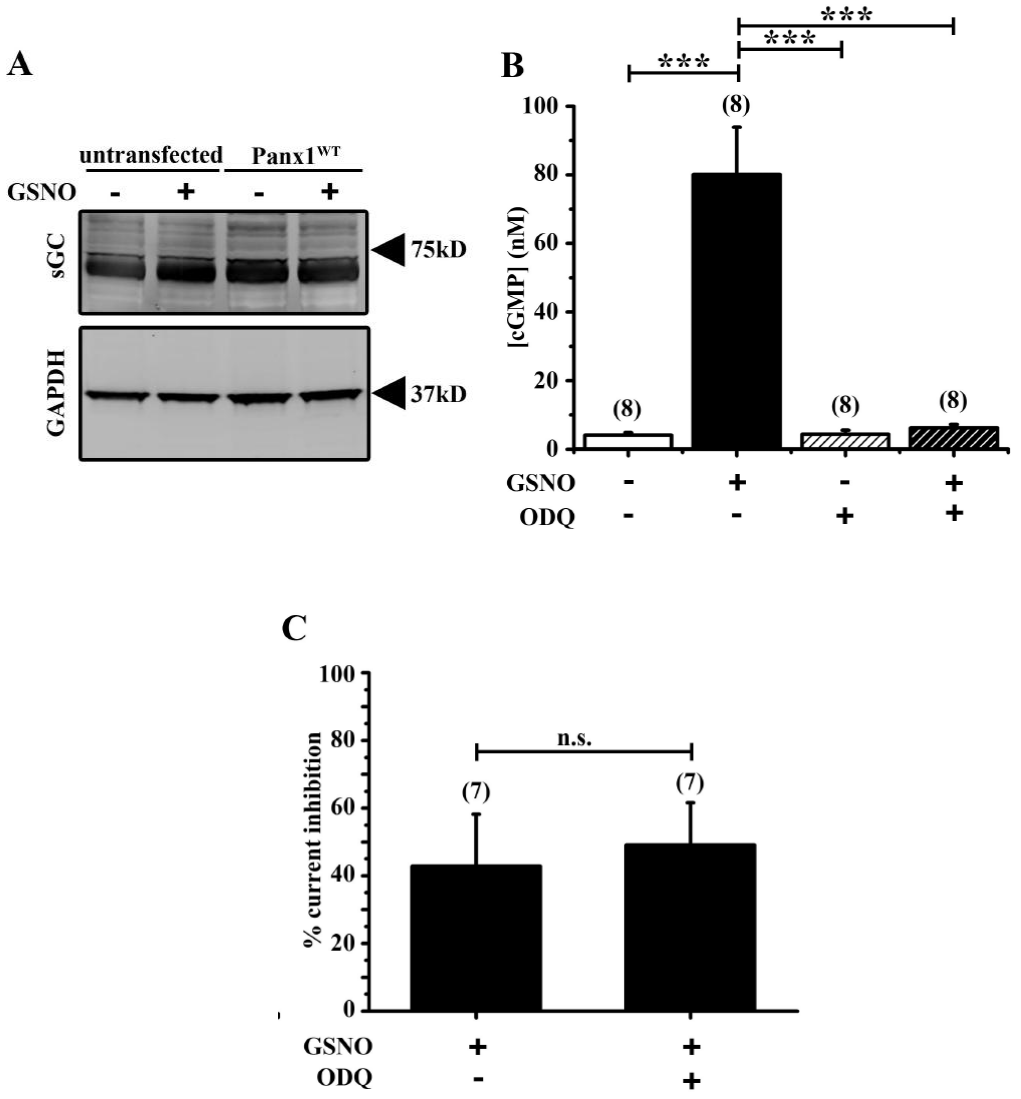

Figure 2.5 Intracellular cGMP signaling does not contribute to GSNO mediated Panx1 current inhibition.

(A) Western blot for soluble guanylate cyclase (sGC) expression in untransfected or Panx1^{WT} expressing HEK cells in following treatment with 100 μM GSNO or vehicle. (B) cGMP assay of Panx1WT expressing HEK cells treated with 100 μM GSNO or vehicle and the sGC inhibitor ODQ. ***, $p<0.0001$. C. Effect of sGC inhibition by ODQ on Panx1 current inhibition by GSNO. Numbers in brackets represent n-values for each experiment.

While our electrophysiology experiments provide strong evidence that Panx1 channel currents can be inhibited by S-nitrosylation, we also sought to determine if ATP release from Panx1^{WT} expressing HEK cells is functionally affected by S-nitrosylation. Based on previous reports indicating the ability of Panx1 channels to release ATP in response to high extracellular K^+ (10), we treated Panx1^{WT} expressing HEK cells with 100 mM KCl and observed a significant increase in ATP release into the extracellular medium that was strongly inhibited by CBX (Figure 2.3D). There was no significant change in ATP release from untransfected HEK cells following KCl stimulation, indicating that Panx1 expression was required for ATP release in these cells. Importantly, treatment of Panx1^{WT} expressing HEK cells with 100 μM GSNO or 50 μM DEA NONOate attenuated the depolarization-evoked ATP release, consistent with our observations on the effects of these NO donor molecules on Panx1 channel currents. Moreover, pretreatment with GSH had no effect on ATP release from these cells (Figure 2.3D).

To examine the possibility that the reduction in Panx1 current and ATP release following treatment with our NO donors was due to reduced expression of these channels at the plasma membrane, we performed a membrane biotinylation assay on Panx1^{WT} expressing HEK cells treated with GSNO for a time course from 0 to 10 minutes, a time frame consistent with the observed inhibitory effects on Panx1 currents. Treatment of cells with GSNO did not affect Panx1 expression at the plasma membrane (Figure 2.6A). Moreover, treatment of Panx1^{WT} expressing HEK cells with GSNO for

10 minutes had no effect on Panx1 membrane localization as assessed by immunofluorescence microscopy (Figure 2.6B). Together, these data indicate that the inhibitory effect of S-nitrosylation on Panx1 channels is unlikely to reflect decreased plasma membrane expression of the channel.

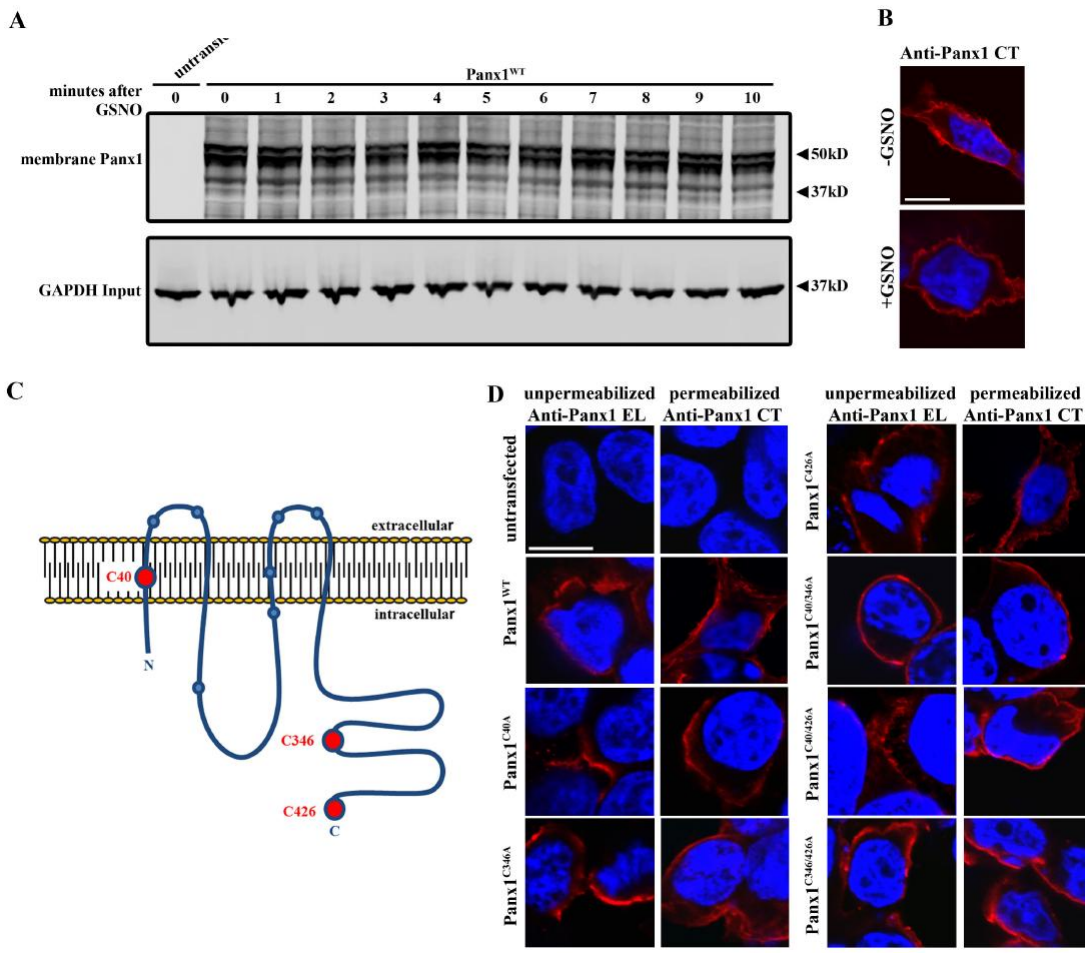

Figure 2.6 Panx1 cysteine mutants traffic to the plasma membrane.

(A) Cell surface biotinylation assay of Panx1 from Panx1^{WT} expressing HEK cells following treatment with 100 μM GSNO for 0-10 minutes. (B) Immunofluorescence of Panx1^{WT} expressing HEK cells treated with or without 100μM GSNO for 10 minutes. Red is Panx1 and blue is DAPI stained nuclei. (C) Topology map of Panx1 showing the predicted location of cysteine residues (circles). The red circles indicate the three cysteines that were mutated to alanines within the Panx1 polypeptide (C40A, C346A and C426A). (D) Immunofluorescence of HEK cells depicting Panx1 mutants at the plasma membrane. Samples were processed for immunofluorescence either under non-permeabilizing conditions and labeled with an antibody directed against the second extracellular loop of Panx1 (anti-Panx1 EL), or under permeabilizing conditions and labeled with an antibody against the C-terminus of Panx1 (anti-Panx1 CT). Red is Panx1, blue is DAPI stained nuclei. Scale bar is 10 μm in all images.

2.2.3 Multiple cysteine resides contribute to Panx1 inhibition by S-nitrosylation

To determine which cysteines are modified by S-nitrosylation and contribute to Panx1 inhibition, we generated several cysteine-to-alanine mutations in murine Panx1 by site-directed mutagenesis. A topology map of Panx1 indicating the cysteines in which we made alanine substitutions (red circles) is shown in Figure 2.6C. We identified target cysteines through a combination of experimental and computational evidence. Previous studies have reported increased Panx1 channel currents upon mutation of C40 or C346, suggesting that these residues may be intimately involved in channel regulation (17,60). The C-terminal tail, which contains an additional cysteine (C426), may also be important for channel regulation as its removal increases channel activity (18). Additionally, we used the scan-x post-translational modification prediction method (119) to rank the highest probability S-nitrosylation sites, which pointed to C40 as the most likely S-nitrosylation site. Therefore, we constructed single cysteine-to-alanine substitutions at these sites ($Panx1^{C40A}$, $Panx1^{C346A}$ and $Panx1^{C426A}$). To ensure that mutation of these single cysteines did not affect trafficking to the plasma membrane, we performed immunofluorescence microscopy on mutant expressing cells under non-permeabilizing conditions with an antibody directed against the second extracellular loop of Panx1 (anti-Panx1 EL) and under permeabilizing conditions with an antibody directed against the intracellular C-tail (anti-Panx1 CT). We found that all Panx1 cysteine mutants

were able to reach the plasma membrane (see Figure 2.6D and recordings of Cys-substituted channels below). In addition, there was no significant difference in Panx1 holding current or basal ATP release between WT and the Panx1 cysteine mutant channels (Figure 2.7A-B). Moreover, we performed cell surface biotinylation assays on HEK cells expressing each of these Panx1 mutants and found that all localize to the membrane and their expression was not affected by treatment with GSNO (Figure 2.8A-B).

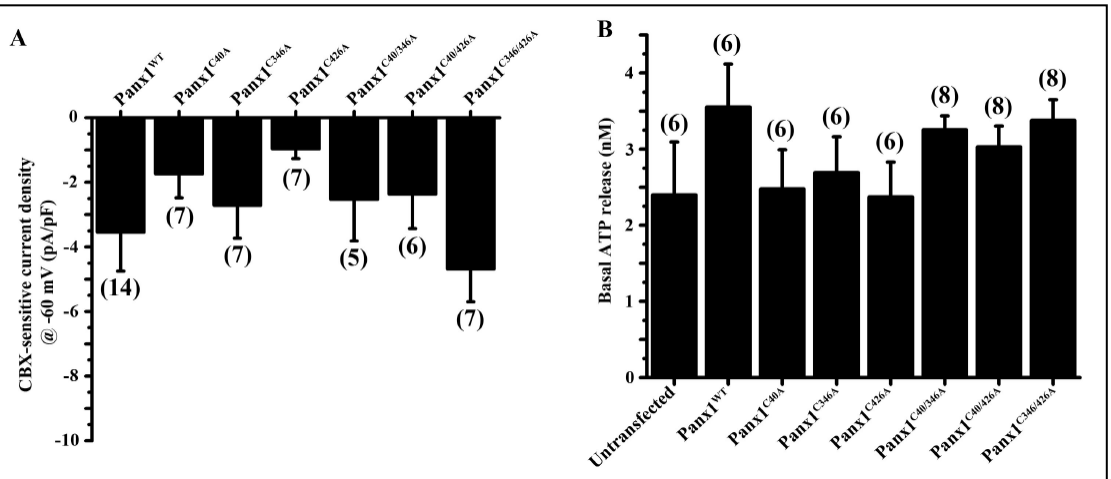

Figure 2.7 Holding currents and ATP release from WT and Panx1 cysteine mutant channels are not different.

(A) Panx1 holding currents at a holding potential of -60 mV from HEK cells expressing WT and Panx1 cysteine mutants. (B) Basal ATP release from unstimulated (-KCl) HEK cells expressing WT and Panx1 cysteine

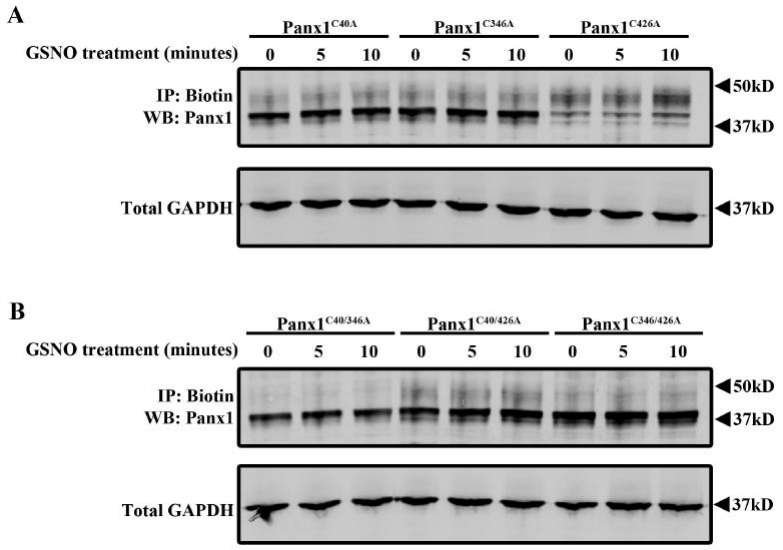

Figure 2.8 Expression of Panx1 cysteine mutants at the plasma membrane is not altered by GSNO.

(A) Cell surface biotinylation assay of Panx1 from HEK cells expressing $Panx1^{C40A}$, $Panx1^{C346A}$ or $Panx1^{C426A}$ following treatment with 100 μM GSNO for 0, 5 or 10 minutes. GAPDH was used as a loading control. (B) Cell surface biotinylation assay of Panx1 from HEK cells expressing $Panx1^{C40/346A}$, $Panx1^{C40/426A}$ or $Panx1^{C346/426A}$ following treatment with 100 μM GSNO for 0, 5 or 10 minutes. GAPDH was used as a loading control.

To determine which cysteine residue(s) are modified by S-nitrosylation, we treated HEK cells expressing Panx1 single mutant channels with 100 μM GSNO and performed biotin switch assays. Interestingly, S-nitrosylation of Panx1 was preserved in all three constructs with individual cysteine-to-alanine substitutions (Figure 2.9A). It should be noted that mutation of C40 or C346 resulted in decreased representation of the higher molecular weight glycosylation species of Panx1 in this assay (Figure 2.9A). Although all three single Cys mutant channels retained the ability to be S-nitrosylated, the inhibitory effects of GSNO on Panx1 currents were abolished specifically in Panx1^{C40A} (Figure 2.9B) and Panx1^{C346A} (Figure 2.9C) expressing cells; GSNO-mediated inhibition was preserved in Panx1^{C426A} expressing cells (Figure 2.9D). Summary data for each Panx1 single cysteine mutant is shown in Figure 2.9E indicating that mutation of C40 or C346, but not C426, significantly prevented Panx1 current inhibition by GSNO. Consistent with a lack of current inhibition by GSNO in the Panx1^{C40A} and Panx1^{C346A} mutants, ATP release from cells expressing these two Panx1 mutants was not affected by GSNO, with the Panx1^{C426A} mutant exhibiting strong inhibition (Figure 2.9). The ability of Panx1 to be S-nitrosylated in each Panx1 single cysteine mutant, with a loss of current inhibition and inhibition of ATP release by GSNO only in the Panx1^{C40A} and Panx1^{C346A} mutants, suggested that S-nitrosylation at multiple cysteine residues may be required for channel inhibition.

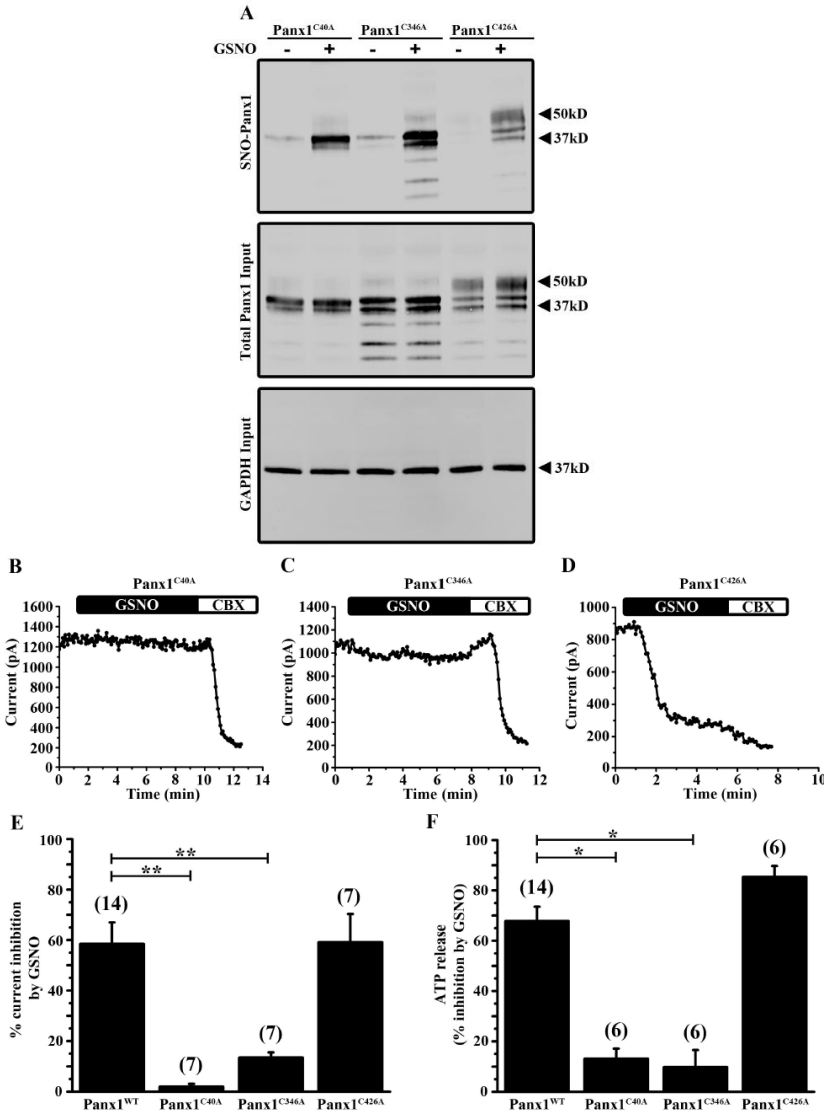

Figure 2.9 Single mutation of C40 or C346 prevents Panx1 current inhibition by GSNO.

(A) Biotin switch assay on HEK cells expressing each of the Panx1 single cysteine mutants, treated with or without 100 μM GSNO. (B-D) Time series of the peak Panx1 current amplitudes from HEK cells expressing $Panx1^{C40A}$ (B), $Panx1^{C346A}$ (C) or $Panx1^{C426A}$ (D) mutant constructs and treated with 100 μM GSNO. Transfected cells were treated with 50 μM CBX near the end of each recording, demonstrating that currents could be blocked. (E) Summary data showing the percent of Panx1 current inhibition by GSNO. (F) ATP release assay from HEK cells expressing Panx1 single cysteine mutants. Data are presented as a % inhibition of ATP release by GSNO. n-values are indicated in brackets. *, $p<0.05$; **, $p<0.001$; ***, $p<0.0001$.

To determine if multiple cysteines can be S-nitrosylated, we generated double cysteine-to-alanine substitutions in Panx1 (Panx1$^{C40/346A}$, Panx1$^{C40/426A}$ and Panx1$^{C346/426A}$) and tested the ability of GSNO to S-nitrosylate and inhibit the double mutant channels. Each of the Panx1 double cysteine mutants trafficked to the plasma membrane (Figure 2.6D). The GSNO-induced S-nitrosylation was preserved in Panx1 constructs that retained either C40 or C346, but was lost in Panx1 channels missing both C40 and C346 (Panx1$^{C40/346A}$), indicating that these two cysteines are the sites of modification (Figure 2.10A). All double mutant constructs generated CBX-sensitive Panx1 currents, but GSNO-mediated current inhibition was not observed in any of the double mutant constructs, each of which had a substitution at either C40 or C346 (Figure 2.10B-E). Consistent with this, GSNO was unable to inhibit ATP release from cells expressing any of the Panx1 double mutant constructs (Figure 2.10F). Together, these data support the idea that both C40 and C346 can be S-nitrosylated and modification at both sites is required for GSNO-mediated inhibition of Panx1.

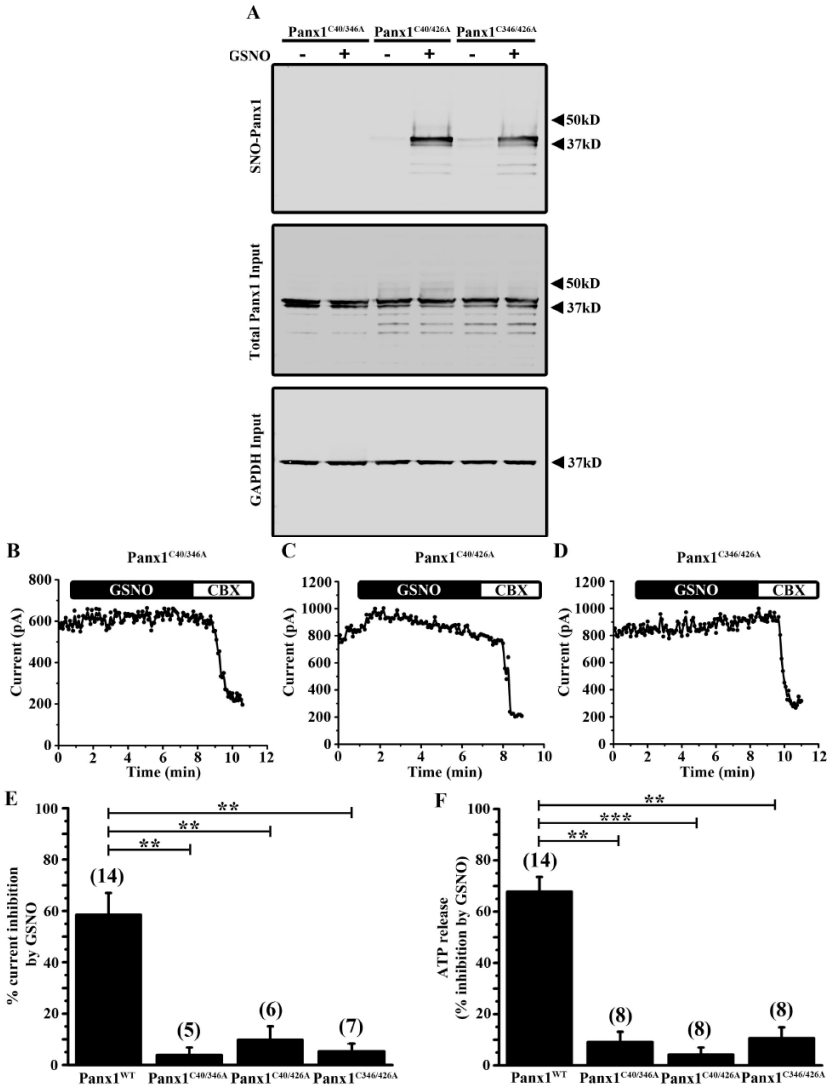

Figure 2.10 Both C40 and C346 are required to be S-nitrosylated to inhibit Panx1 currents.

(A) Biotin switch assay on HEK cells transfected with each Panx1 double cysteine mutant construct ($Panx1^{C40/346A}$, $Panx1^{C40/426A}$, $Panx1^{C346/426A}$). Panx1 mutant expressing cells were treated with or without 100 μM GSNO. (B-D) Time series of the peak Panx1 current amplitudes from HEK cells expressing $Panx1^{C40/346A}$ (B), $Panx1^{C40/426A}$ (C) and $Panx1^{C346/426A}$ (D) and treated with 100 μM GSNO. Transfected cells were treated with 50 μM CBX near the end of each recording protocol. (E) Summary data of the percent of Panx1 current inhibition by GSNO from HEK cells expressing the Panx1 double cysteine mutant constructs. (F) ATP release assay from HEK cells expressing Panx1 single cysteine mutants. Data are presented as a % inhibition of ATP release by GSNO. n-values are indicated in brackets. **, $p<0.001$; *** $p<0.0001$

2.2.4 S-nitrosylation of Panx1 in endothelial cells inhibits channel activity

Panx1 is highly expressed in endothelial cells across the arterial tree (118). Because these cells express eNOS and are exposed to large amounts of NO, we sought to determine if Panx1 can be modified by S-nitrosylation in a native cell. We utilized primary cultures of mouse aortic endothelial cells (mAEC) which express eNOS and the endothelial cell markers VE-cadherin (Cdh5) and PECAM-1 (Figure 2.1B). Treatment of mAECs with GSNO or DEA NONOate for 10 minutes induced S-nitrosylation of endogenous Panx1 (Figure 2.11A). Consistent with our HEK cell data, S-nitrosylation of Panx1 in mAECs by GSNO or DEA NONOate was reversed by treatment with DTT. Moreover, treatment with GSH alone had no effect on Panx1 cysteine modification.

To determine if S-nitrosylation of Panx1 in mAECs inhibits channel function, we conducted whole-cell patch clamp recordings and ATP release assays on mAECs. Single mAECs were patched in the whole cell configuration and Panx1 currents were identified by their sensitivity to CBX and their characteristic I/V relationship (Figure 2.11B-C). Consistent with our previous observations, peak Panx1 currents at +80 mV were significantly inhibited by GSNO and this inhibition was substantially reversed by treatment with DTT (Figure 2.11B-D). Treatment with GSH or DTT alone did not affect Panx1 current in these cells indicating that S-nitrosylation of endogenous Panx1 causes potent inhibition of channel currents. We next sought to determine

whether ATP release from Panx1 channels in mAECs was affected by S-nitrosylation. Because thrombin is a specific stimulus for ATP release from Panx1 channels in ECs (54), we stimulated mAECs with 1U/mL of thrombin for 5 minutes. Thrombin stimulation significantly increased ATP release that was inhibited by both CBX and siRNA knockdown of endogenous Panx1 (Figure 2.11E). Moreover, GSNO and DEA-NONOate significantly attenuated ATP release from mAECs, indicating that S-nitrosylation inhibits endogenous Panx1 channel function, confirming our findings from HEK cells.

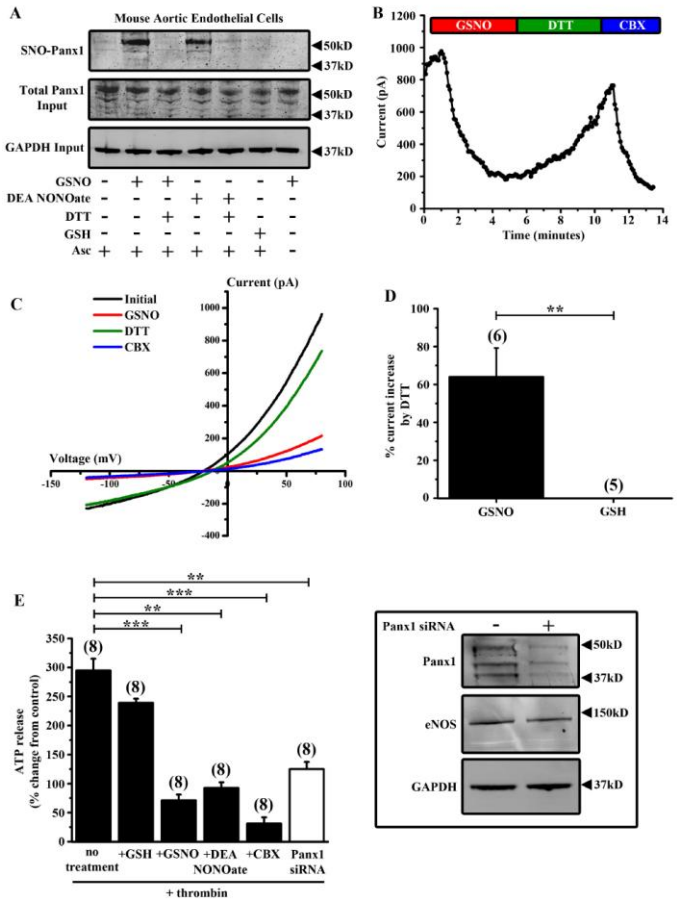

Figure 2.11 S-nitrosylation inhibits Panx1 currents and ATP release from mouse aortic endothelial cells.

(A) Biotin switch assay on primary mouse aortic endothelial cells treated with 100 μM GSNO ± 1 mM DTT, 50 μM DEA NONOate ± 1 mM DTT or 100 μM GSH. Ascorbate was omitted from the assay as a negative control. (B) Time series showing peak Panx1 whole cell current amplitude from mAECs during application of GSNO, DTT and CBX. (C) I/V curves of Panx1 currents from primary mAECs under control conditions (black trace), following application of 100 μM GSNO (red trace), 1 mM DTT (green trace) and CBX (blue trace). (D) Summary data showing the percent of Panx1 current inhibition by GSNO or GSH that was reversible by DTT. (E) ATP release assay from mAECs stimulated with 1U/mL mouse thrombin. Cells were pretreated with 100 μM GSNO, 50 μM DEA NONOate, 100 μM GSH or 50 μM CBX. A subset of cells was transfected with siRNA against mouse Panx1 to knockdown the endogenous protein. All data are presented as a % change in ATP release compared to control (-thrombin). Panel F insert depicts a Panx1 Western blot of untransfected and Panx1 siRNA transfected mAECs. eNOS and GAPDH were used as loading controls. n-values are indicated in brackets. **, $p<0.001$; *** $p<0.0001$

2.3 Discussion

In this study, we identify a novel inhibitory mechanism for Panx1 channels: we show that Panx1 can be modified by S-nitrosylation and that this post-translation modification leads to inhibition of Panx1-mediated currents and ATP release. In brief, we used a biotin switch assay to show that GSNO and DEA NONOate, NO donor molecules, induce a DTT-sensitive Panx1 modification that is consistent with S-nitrosylation; also, it was not observed when GSH was substituted for GSNO in control or oxidative conditions, ruling out an alternative glutathionylation mechanism. Likewise, inhibition of whole cell Panx1 currents by GSNO and DEA NONOate was reversed by DTT, an action that was also not mimicked by GSH. In addition, GSNO-mediated current inhibition was not dependent on sGC activity, supporting S-nitrosylation over other mechanisms that can contribute to NO actions. In support of a direct inhibitory action on the channel, substitution of either C40 or C346 on Panx1 prevented GSNO-mediated channel inhibition, while mutation of both C40 and C346 blocked S-nitrosylation of the channel. In sum, these data demonstrate that modification at these two critical cysteines is required for Panx1 channel inhibition by S-nitrosylation, and they suggest a functional role for NO in regulating the activity of Panx1 channels.

The role of Panx1 channels in ATP release from cells has been a growing area of investigation, with multiple studies identifying mechanisms by which Panx1 channels can be activated. By contrast, there remains little understanding as to how Panx1 channels are inhibited. The results of our

current study provide a novel mechanism by which Panx1 channels can be inhibited, supporting a functional role for NO in controlling the activity of Panx1 channels at the plasma membrane of cells and suggesting a way to negatively regulate ATP release from cells.

Although our results indicate an inhibitory role imparted by NO on Panx1 channels through S-nitrosylation, a recent study has implicated this reactive oxygen species in Panx1 channel activation (70). In that work, it was suggested that NO generated during oxygen-glucose deprivation can activate Panx1 channels expressed in cultured hippocampal neurons. While it is possible that NO signaling may result in differential Panx1 channel regulation in different physiological contexts, it is important to point out that the aforementioned study used calcein dye leakage as a functional readout for Panx1 channel activity. Since cultured hippocampal neurons express connexin proteins, which are both permeable to calcein dye and activated by S-nitrosylation (112,114), it is possible that the dye leakage they observed represented activity of connexins. Moreover, it is possible that cultured hippocampal neurons may express other pannexin isoforms, such as Panx2, which is highly expressed in the central nervous system (120,121). As such, other pannexin isoforms may be regulated differently by NO. In our work, we assessed S-nitrosylation and recorded whole cell currents as well as ATP release from recombinant Panx1 channels, providing direct evidence for inhibition of Panx1 by NO.

We performed cysteine mutagenesis of Panx1 to identify the specific residues required for S-nitrosylation and channel inhibition. Interestingly, the two sites that we identified as critical for this inhibitory modification -- C40 and C346 -- were previously reported to enhance activity of Panx1 channels in mutagenesis studies (60,122). In that other work, serine substitution at either C40 (122) or C346 (60) produced "leaky" or constitutively active channels. Together with our results, these observations suggest that C40 and C346 may be localized to regions that are important for dynamic up- and down-regulation of Panx1 channel activity.

We noted that mutation of either C40 or C346 affected the glycosylation state of Panx1. It is known that Panx1 exists in three forms: a core unglycosylated species (Gly0), a high-mannose species (Gly1) and a complex glycosylated form (Gly2), each contributing to the characteristic triple banding pattern on a Western blot. Mutation of C40 or C346 resulted in a marked reduction in the Gly2 species, with the protein detected mainly as Gly0 and Gly1 forms. Since glycosylation has been implicated in trafficking of Panx1 channels to the plasma membrane, we examined the cellular localization of the cysteine mutants and found that each mutant appeared on the plasma membrane surface. Even though these cysteine substitutions may have affected Panx1 glycosylation status, it is important to point out that Panx1 currents and ATP release were detected for all mutant constructs, indicating that they could form functional channels at the plasma membrane. This is constant with previous work indicating that all Panx1 Gly species can

reach the plasma membrane (31). Also, a previous study identified a loss in the Gly2 species in functional, plasma membrane-localized Panx1C346S (60).

S-nitrosylation of Panx1 channels may function physiologically as a negative feedback mechanism, mediating inhibition of channel activity following their activation to prevent chronic release of ATP. In the vasculature, endothelial cells that line the blood vessel lumen express functional Panx1 channels at the plasma membrane and multiple studies have emerged implicating these channels in ATP release (30,54,66,118,123). Recently, it was suggested that thrombin, by activation of endothelial cell PAR-1 receptors, promotes ATP release from Panx1 channels into the extracellular compartment (54). Our data utilizing mouse aortic endothelial cells indicates that thrombin-induced ATP release from these cells can be significantly inhibited by S-nitrosylation of the channel. This novel regulatory mechanism may play an important role in controlling the extent of ATP release from the vascular endothelium and therefore modulate purinergic signaling events in the vasculature. In addition, circulating erythrocytes release ATP via Panx1 into the blood vessel lumen during conditions of low oxygen tension and membrane deformation, conditions that arise in small arterioles and capillaries (30,123). Released ATP activates endothelial cell P2Y receptors causing NO generation which diffuses to and relaxes adjacent smooth muscle cells (124). It is possible that the endothelial-derived NO could also diffuse into the blood vessel lumen and S-nitrosylate erythrocyte Panx1 channels, inhibiting further ATP release and preventing excess

vasodilation. Regulation of Panx1 channels by S-nitrosylation in these cells could therefore play an important role in the matching of blood flow to tissue oxygen demand.

While the inhibitory effect of S-nitrosylation on Panx1 channel function was demonstrated, the mechanism by which this modification elicits its effects on the channel is not as clear. In this respect, our data indicate that S-nitrosylation has no effect on Panx1 cell membrane localization suggesting the possibility that channel activity is directly inhibited. Recent evidence has indicated that the C terminal tail may form a portion of the Panx1 channel pore (17) and that proteolytic cleavage of the C terminal tail increases channel currents by its removal from the Panx1 pore (18). It is possible that S-nitrosylation of C346 and C40 promotes a conformation that stabilizes the C-terminal:pore interaction, and thus the channel closed state. Future studies utilizing structural and biophysical techniques may reveal the precise mechanism by which Panx1 S-nitrosylation inhibits the channel. Nonetheless, our data has provided novel evidence for a post-translational mechanism inhibiting Panx1 channels at the plasma membrane.

CHAPTER 3

Hematopoietic pannexin 1 function is critical for neuropathic pain

This chapter is modified from the following publication, which is under review at the time of preparation of this thesis:

Weaver, J.L, Arandjelovic, S., Brown, G., Mendu, S., Schappe, M., Buckley, M.W., Chiu, Y.H., Shu, S., Kim, J.K., Chung, J., Krupa, J., Jevtovic-Todorovic, V., Desai, B.N., Ravichandran, K.S., Bayliss, D.A. (2016). Hematopoietic pannexin 1 function is critical for neuropathic pain. Manuscript under review.

Please note: Individual contributions were as follows: J.L.W. conducted all behavior tests, generated bone marrow transplants and viral re-expression of Panx1. J.L.W. and G.B. isolated semi-purified populations of cells and did RT-qPCR. S.A., M.W.B. and M.S. ran flow cytometry experiments. S.M. recorded Panx1 currents in HEK cells, assisted by J.K.. J.L.W. and M.W.B. generated adoptive transfer mice. Y.H.C. and S.S. subcloned Panx1 variants into Migr1. Y.H.C. ran western blots for Panx1. J.L.W., G.B., J.K.K. and J.C. conducted histology experiments and counted cells.

3.1 Introduction

Neuropathic pain is increasingly recognized as a major clinical and societal problem, contributing to the almost $635 billion spent annually on chronic pain in the US (87,90,91). Unlike acute pain, which is protective, neuropathic pain is a chronic, burning, "pins and needles" sensation that

does not respond well to currently available therapeutics. The refractory nature of this condition negatively impacts patient quality-of-life, leading to steep economic costs directly associated with the condition, and indirect consequences of using opiate drugs as a primary treatment option, including drug addiction and associated crime (88-90). A better understanding of the molecular and cellular bases underlying the pathogenesis of neuropathic pain can yield opportunities for more effective therapeutics.

Neuropathic pain results from physicochemical insults to the nervous system (e.g., trauma) which triggers a chronic inflammatory response and subsequent functional remodeling of peripheral and central sensory circuits that underlie the persistent pain and/or sensory hypersensitivity characteristic of the condition (108,125). Central to this prevailing model is a critical role for paracrine purinergic signaling, whereby multiple P2X and P2Y receptor subtypes mediate the complex intercellular communication driving neuropathic pain symptoms (38). Whereas various theories have been proposed for how elevated ambient ATP/UTP could trigger the downstream effects of P2 receptor activation (125), notably absent is a clear understanding of the source(s) of the nucleotide ligands – neither the relevant cell type nor the mechanism of release has been identified.

A potential pathway for nucleotide release is via the widely-expressed membrane channel Panx1 (3,10). Panx1 provides a primary means for ATP release in many cell types, and is modulated by mechanisms potentially

relevant to nerve injury. For example, Panx1 is activated by inflammatory mediators (e.g., TNFα (63)), G protein-coupled receptors (GPCRs: e.g., P2Y (53-56,66)), and apoptotic signaling (e.g., caspase cleavage (9)). The contribution of Panx1 to neuropathic pain has been suggested based largely on circumstantial evidence or the use of non-selective pharmacological tools, with suspected mechanisms of channel activation focused primarily on a proposed functional relationship between P2X7 and Panx1 (41,81,82). However, other potentially relevant channel activation mechanisms have not been tested, and the cellular site(s) of Panx1 action have not been explored.

Here, we used global Panx1 knockout mice (*Panx1*$^{-/-}$) and two models of trauma-induced neuropathy (i.e., spared nerve injury, SNI, and chronic constrictive injury of the sciatic nerve, CCI) to provide genetic evidence for a role of Panx1 in neuropathic pain. Strikingly, the hypersensitivity that typically develops after sciatic nerve injury was abrogated in *Panx1*$^{-/-}$ mice in both models. Consistent with a role for Panx1 in circulating hematopoietic cells, neuropathic pain in *Panx1*$^{-/-}$ mice could be restored by bone marrow transplantation, either with cells from *Panx1*$^{+/+}$ mice or with cells from *Panx1*$^{-/-}$ mice after ex vivo viral-mediated re-expression of wild-type Panx1; this latter rescue required the expression of Panx1 channels that could be activated by GPCRs but not by caspase cleavage. Interestingly, this pain development occurred in mice with a P2X7 variant that does not support Panx1 interactions (48) challenging previously held theories which suppose that P2X7 is required for Panx1 activation in neuropathic pain (41,81,82).

From a therapeutic standpoint, mice treated with two chemically-distinct Panx1 blockers in relevant dosing schemes were protected from pain. These data demonstrate that Panx1 expression in hematopoietic cells is both necessary and sufficient for the induction of neuropathic pain after nerve injury, and that pharmacological inhibition of Panx1 could be a viable therapeutic alternative for the prevention and/or treatment of neuropathic pain.

3.2 Methods

3.2.1 Reagents

Cell culture reagents were obtained from Life Technologies (Carlsbad, CA), subcloning reagents from New England Biolabs (Ipswich, MA), and all other reagents were purchased from Sigma Aldrich (St Louis, MO) unless specified otherwise below.

3.2.2 Mice

Adult mice of both sexes were used in this study. All mice used in these experiments were on a C57BL/6 background. *Panx1*$^{-/-}$ mice and *Panx1*$^{fl/fl}$ mice were generated and genotyped as previously described (Figure 3.1; (25)). The absence of Panx1 protein in the *Panx1*$^{-/-}$ mice was verified by Western blot in various tissues (brain, see Figure 3.1C; thymus, liver, spleen, ear, heart, data not shown). To generate various conditional knockout lines,

the following Cre-driver mice were used: GFAP-cre (Jackson Laboratories, stock#012886), Synapsin-Cre (Jackson Laboratories, stock #003966), LysM-cre (Jackson Laboratories, stock#004781), CX3CR1-cre (Jackson Laboratories stock#0025524 (126)), CD4-cre (Taconic stock#4196). Conditional knockout lines were monitored frequently for germline deletion and, if observed, breeders were replaced; we found that maintaining the Cre(+) allele exclusively on the female breeder greatly reduced the occurrence of germline deletion. In some of the bone marrow transplant experiments, mice expressing GFP under the ubiquitin promoter were used to confirm transfer efficiency (UBI-GFP mice; Jackson Laboratories, stock#004353).

3.2.3 Surgeries

To induce neuropathic pain, mice underwent spared nerve injury (SNI; (127,128)) or chronic constrictive injury of the sciatic nerve (CCI; (129,130)). Mice were anesthetized with isoflurane and received bupivacaine at the site of incision prior to surgery. After skin incision over the dorsal aspect of the upper thigh, a blunt dissection through the muscle allowed access to the sciatic nerve either at its branch point (for SNI) or proximal to the branch (for CCI). For SNI, the common fibular and tibial nerves were tightly ligated together using 6-0 sutures then cut to remove approximately 1 mm of nerve distal to the ligation point. The sural nerve was left completely

intact and untouched. For CCI, the sciatic nerve was loosely ligated (until the first contraction of the distal muscles was observed) by two 4-0 silk sutures at approximately 5 mm from the emergence of the nerve from the greater sciatic foramen. Sham operations involved exposure of the nerve with no further manipulations to it. After nerve injury or sham procedure, the incision was closed by sutures and skin glue.

3.2.4 Mechanical sensitivity

Sensitivity to touch was assessed using the standard up-down method modified for mice with von Frey filaments (Stoelting, Wood Dale, IL) of sizes 1.65 (0.008 gr of force) to 4.17 (1.4 gr of force) (131). Mice were placed in clear plexiglass containers situated on an elevated wire mesh surface and allowed to acclimate at least 30 min prior to testing. Starting with the middle filament, the filaments were applied to the lateral portion of the hindpaw (for SNI) or central hindpaw (for CCI) until the filament just bent. A response was indicated by a sharp withdrawal of the paw. An average of three trials was obtained in order to calculate the final 50% response threshold per paw, per testing day. A minimum of 10 min of rest was allowed between each trial. Day "0" testing was an average of two baselines taken on separate days.

3.2.5 Heat sensitivity

Sensitivity to heat was quantified by the Hargreaves method as the paw withdrawal latency to radiant heat (PWL, measured in seconds) as described (132,133). The measurement system consisted of a clear plastic chamber (8 x 8 x 18 cm) sitting on an elevated clear glass floor that was temperature-regulated at 30°C. Each mouse was placed in the chamber to accommodate for 30 min. A radiant heat source mounted on a movable holder beneath the glass floor was positioned to deliver heat focally to the plantar surface of either the right or left hindpaw. When the mouse withdrew the paw, the timer was shut off. To prevent thermal injury, the light beam automatically discontinued after 20 sec if the mouse failed to withdraw its paw. An average of four trials was obtained in order to calculate the PWL per paw on each day. A minimum of 10 min of rest was allowed between each trial. Day "0" testing was an average of two baselines taken on separate days.

3.2.6 Sensorimotor testing

Mice administered drugs were monitored for motor proficiency and alertness using sensorimotor testing modified from a previously described method (132,133). Three home-made apparatuses were used: an elevated ledge, an elevated platform and an inverted wire-mesh screen. The tests had a maximum cut-off time of 60 sec and were performed in the same order

(ledge, platform then inverted screen). The elevated ledge was 22 cm high and 5 mm wide. The maximum score was given if the mouse traversed the entire length of the ledge (32 cm) within the allotted time or maintained its balance on the ledge for that same period of time. The platform test used an elevated circular platform of 35 mm diameter and at a height of 31 cm. The length of time a mouse remained on the platform was measured. The maximum score was given if the mouse remained on the platform for 60 sec or if it climbed down the pole holding the platform. For the inverted screen test, the mouse was placed on a wire mesh grid measuring 17 x 50 cm (15 squares per 10 cm) and the grid was rapidly inverted so the mouse was hanging upside-down. The mouse was timed to see how long it could hang on the screen. The area underneath each apparatus was heavily padded to prevent injuries from potential falls and the mouse was allowed at least 5 min of rest between each apparatus.

3.2.7 Adoptive Transfer

Donor mice were sacrificed by CO_2 exposure, and lymph nodes and spleens were rapidly dissected into PBS with 10% FBS. Single cell suspensions were made by pressing the tissue through 70 μm nylon mesh and T cells separated by negative selection using a Pan T cell Isolation Kit (Miltenyl Biotech, San Diego, CA). Cells were resuspended in RPMI and 2x106 cells were given via tail vein injection to each adult Rag1KO mouse

(Jackson Laboratories stock#00216). Mice underwent SNI 10 days after the transfer. After injury, spleens and lymph nodes were collected from some of the mice to confirm the efficiency of the reconstitution by FACS.

3.2.8 Bone marrow transplants

Donor mice were sacrificed by CO_2 exposure, hindlimb bones extracted and flushed with PBS. The bone marrow cells were then washed, filtered through 70 μm mesh and resuspended in PBS so that each recipient mouse received $3x10^6$ cells via tail vein injection. Recipient mice were irradiated with 2 doses of 600 rads using a Shepherd Mark irradiator. The irradiations occurred on the same day separated by 4 h and injections of new bone marrow cells were given approximately 24 h after the final irradiation. The recipients were maintained antibiotic water (80 mg/mL sulfmethoxazole and 0.37 mM trimethoprim) for one week before and four weeks after irradiation. All experiments, including SNI surgeries, occurred ten weeks after the irradiation.

3.2.9 Generation of viral constructs and particles

Viral vectors for expression of Panx1 in bone marrow cells were sub-cloned into Migr1, a vector previously described for ex vivo infection of bone marrow cells ((134); Addgene plasmid #27490). Briefly, pcDNA3.1 vectors containing the three versions of Panx1 (Panx1(WT), Panx1(TEV), Panx1(YA))

were cut with HindIII, incubated with DNA polymerase I (Klenow) to produce blunt ends then digested with EcoRI. Migr1 (cut with XhoI then incubated with DNA polymerase I followed by digestion with EcoRI) was ligated with the gel-extracted band (of the expected size) from the pcDNA3.1 digest. After transformation of One Shot Stbl3 competent cells (ThermoFisher, Waltham, MA), plasmids were purified and sequenced. The final vectors were packaged by the University of Michigan Vector Core using transient transfection of the plasmids pUMVC-Gag/Pol (Aldevron and the University of Michigan vector core) and pCl-VSVg envelope (Addgene #1733).

3.2.10 Virally infected bone marrow chimeras

Methods for ex vivo infection of bone marrow cells and reconstitution in irradiated mice were modified from a previously described method (134,135). Donor *Panx1*$^{-/-}$ mice were pretreated with 2 mg of 5-fluorouracil for 4 days prior to bone marrow harvest. The RBCs were lysed, and the remaining cells resuspended at a concentration of 1x106 cells per ml and cultured overnight in a 37°C humidified incubator with 5% CO_2. Media consisted of IMDM supplemented with 15% FBS, 2 mM glutamax, 1% penicillin/streptomycin, 50 µM β-mercaptoethanol, 5 ng/mL IL3 (Peprotech, Rockyhill, NJ), 5 ng/mL IL6 (Peprotech) and 50 ng/mL of stem cell factor (R&D Systems, Minneapolis, MN). Cells were replated the next day with the inclusion of 4 mg/mL polybrene (Millipore, Darmstadt, Germany) and at a

density of $2x10^6$ cells per mL. Spin innoculation then occurred at 1300G and 20°C in a table-top centrifuge for 2 h using 1 mL of virus concentrate per 3 mL of cells. Cells were then returned to the incubator overnight and the spin inoculation was repeated the next day. After 16 h, the cells were resuspended in PBS and injected via tail vein to lethally irradiated mice (see above for details) at a minimum of 500,000 cells per mouse.

3.2.11 Isolation and enrichment of peritoneal macrophages

Adult *LysM-Cre::Panx1$^{fl/fl}$* and *CX3CR1-Cre::Panx1$^{fl/fl}$* mice of either genotype were euthanized by CO_2 exposure and injected with 10 mL PBS delivered via a 28G needle into the peritoneal cavity immediately after confirmation of death (136). The fluid was collected via a 23G needle and the cells washed, resuspended in DMEM-F12 media (supplemented with 10% FBS, 10 mM L-gluatmine, 1% penicillin/streptomycin), plated and incubated at 37°C with 5% CO_2 for 3 days. The media was changed daily and on the last day, cells were lysed in the 6-well plate and the exudate collected for RT-qPCR analysis.

3.2.12 Isolation and enrichment of astrocytes

Four to 6 day-old pups of the *GFAP-Cre::Panx1$^{fl/fl}$* line were sacrificed by rapid decapitation under ketamine-xylazine anesthesia (375 and 25 mg/kg i.m.). Cortices were dissected into HBSS, meninges removed and the

tissue minced into 1 mm pieces. Brains were then digested in 0.25% trypsin at 35°C for 30 min followed by gentle trituration of the tissue in glass pipettes of increasingly smaller sizes. The resulting suspension was filtered through a 70 µm mesh and astrocytes were enriched using an anti-glast 1 microbead kit (Miltenyl Biotech) and the positive-selection procedure on an AutoMacs Pro machine (Miltenyl Biotech) according to the manufacturer's protocol. This procedure yielded approximately 2-fold enrichment for astrocytes in the final positive selection as assessed by RT-qPCR for genes specific to astrocytes and other brain cells (neurons and microglia, details listed below; data not shown).

3.2.13 Isolation and enrichment of neurons

Five day-old pups of the *Syn-Cre::Panx1*$^{fl/fl}$ line were sacrificed by rapid decapitation under ketamine-xylazine anesthesia (375 and 25 mg/kg i.m.). Whole brains were dissected into DMEM/F12 media, meninges removed and the tissue minced into 1 mm pieces. Brains were then digested in 120U/ml papain (Worthington Biochemical Corporation) at 30°C for 30 min followed by gentle trituration of the tissue in glass pipettes of increasingly smaller sizes. The resulting cells were spun at 200G for 4min, then resuspended in Neurobasal media supplemented with 2% B27 and 0.5 mM Glutamax. Cells were plated at a concentration of $1x10^6$ cells per mL on poly-l-lysine coated 6-well plates with partial media changes every 4 days. After 8

days, the cells were incubated for 48-72 h with 1 μM cytosine β-D-arabinofuranoside hydrochloride to inhibit the growth of any contaminating cells. Cells were lysed directly in the 6-well plate and the exudate collected for RT-qPCR analysis. This procedure reportedly generates semi-purified neuronal cultures (~50% neuronal cells (137,138)).

3.2.14 Isolation and enrichment of T cells

Adult *CD4-Cre::Panx1*$^{fl/fl}$ mice were sacrificed by CO_2 exposure, and lymph nodes and spleens were rapidly dissected into PBS with 10% FBS. Single cell suspensions were made by pressing the tissue through 70 μm nylon mesh and T cells separated by negative selection using a Pan T cell Isolation Kit (Miltenyl Biotech). Cells were pelleted, lysed and saved for further RT-qPCR analysis.

3.2.15 Quantitative real-time PCR

Cells were isolated by various methods as described above. mRNA was extracted using a Trizol reagent and a RNAeasy minkit (Qiagen, Hilden, Germany). Equal quantities of mRNA were reverse transcribed using the iScript cDNA synthesis kit (Biorad, Hercules, CA). 25-100 ng of cDNA was then added to a 96-well plate in triplicates and analyzed using a CFX Connect Real-Time PCR Detection System (Biorad). For expression of Panx1, Taqman probes and iTaq Universal Probes Supermix was used (ThermoFisher, probe

Mm00450900_m1 for Panx1, probe Mm01545399_m1 for HPRT, and probe Mm99999915_g1 for GAPDH). To assess the efficiency of various cell isolation methods, iQ SYBR green Supermix (Biorad) and primers for the following transcripts were used (Table 3.1 Primers): Slc1a3 for astrocytes, Itgam for microglia, and Map2 for neurons and β-actin or GAPDH as housekeeping genes. Template and primer dilutions, melt curves and amplicon sizes were used to verify primer specificity. For all RT-qPCR data, cycles to threshold were analyzed using a $2^{-\Delta Ct}$ normalization procedure (139).

Table 3.1 Primers

Name	PrimerBank ID	GenBank Accession ID	5’ to 3’ sequence	Amplicon size
Slc1a3 forward	24233554a1	NM_148938	ACCAAAAGCAACGGAGAAGAG	144
Slc1a3 reverse			GGCATTCCGAAACAGGTAACTC	
Itgam forward	6680484a1	NM_008401	ATGGACGCTGATGGCAATACC	203
Itgam reverse			TCCCCATTCACGTCTCCCA	
Map2 forward	28981317a1	NM_008632	GCCAGCCTCAGAACAAACAG	146
Map2 reverse			AAGGTCTTGGGAGGGAAGAAC	
β-actin forward	6671509a1	NM_007393	GGCTGTATTCCCCTCCATCG	154
β-actin reverse			CCAGTTGGTAACAATGCCATGT	
GAPDH forward	6679937a1	NM_008084	AGGTCGGTGTGAACGGATTTG	123
GAPDH reverse			TGTAGACCATGTAGTTGAGGTCA	
5’ Panx homology arm	N/a	N/a	AGGAACCATTCTGCAGGACAGGAA	See Figure 3.1
Common reverse	N/a	N/a	TTATCATAGCAACAGAAATTCTAAGACAGGAATAT	See Figure 3.1
Exon 3 reverse	N/a	N/a	GCTGCAGAGAAGCGCCAGAAGAGTGCG	See Figure 3.1Figure 1.1

3.2.16 Immunohistochemistry

Mice were anesthetized, perfused with PBS followed by 4% PFA and tissue removed. For analysis of spinal cord sections, the tissue was left in PFA for two additional nights then 30 μm sections were cut from the lumbar prominence on a vibrating microtome (VT1000s, Leica Microsystems, Wetzlar Germany). Free-floating sections were washed in TS, blocked in 10% normal horse serum then incubated with rabbit anti-pp38 (Cell Signaling Technologies, Danvers, MA; 1:1000) for two nights at 4°C followed by incubation with unconguated goat anti-rabbit (Jackson ImmunoResearch, West Grove, PA; 1:50 for 90 min at room temperature) and finally FITC conjugated anti-goat secondary antibody (Jackson ImmunoResearch; 2 h at room temperature). A second primary antibody of rabbit anti-Iba1 (Wako, Osaka, Japan; 1:600) was then used for two nights at 4°C followed by rhodamine conjugated anti-rabbit secondary antibody (Jackson ImmunoResearch; 2 h at room temperature). Sections were then dehydrated, mounted on glass slides and cover-slipped.

For peripheral nerve analysis, tissues were post-fixed overnight and embedded in paraffin. 5 μm thick longitudinal sections were mounted on slides, which were deparaffinized and underwent either H&E staining or immunohistochemistry. For immunohistochemistry, antigen retrieval occurred via 10 mM sodium citrate (pH 6.0) in a pressure cooker for 30 min. Slides were then washed, blocked in 10% normal horse serum in TBS (2 h at room temperature), endogenous peroxidases blocked with 0.3% H_2O_2 and

incubated overnight in rabbit anti-Iba1 (1:500). The next day, the slides were incubated with secondary antibody (biotinylated anti-rabbit , 1:1000 for 2 h, Jackson ImmunoResearch) followed by processing with Elite ABC reagents (Vector Laboratories, Burlingame, CA) and a DAB substrate kit (Vector Laboratories). Slides were finally dehydrated and cover-slipped.

3.2.17 Toluidine blue analysis

Mice were anesthetized, perfused with PBS followed by 4% PFA and the distal segments of the sciatic nerve extracted. After overnight fixation at 4°C, samples were then postfixed in 1% osmium tetroxide, dehydrated in a series of graded alcohols and embedded in epon. Semi-thin (0.5 μm) transverse sections were cut on an ultramictrome (Leica Ultracut), stained with toluidine blue and cover-slipped.

3.2.18 Image acquisition and analysis

Slides were examined under an epifluroescence microscope (Zeiss Axioimager Z1; Oberkochen, Germany) with motorized stage using Neurolucida software (MBF Bioscience, Williston, VT). For Iba1-facilitated analysis of microglia activation, the morphology of the cells allowed for determination of activation state, where activated cells had rounded cell bodies and short processes (140). For analysis of the injured sciatic nerve, the longitudinal slice was considered representative of the injury if the H&E

stained section adjacent to it demonstrated signs of injury (red blood cells, tissue fibrous, and Iba1-postive macrophages surrounding the cut end); only tissue enclosed by the perineural sheath and within 500 μm of the end was analyzed. For toludine blue analysis, nerves were counted as intact profiles if the myelin appeared as a continuous, round structure with a clear axon center; nerves were counted as degenerating profiles if the cross-section was a myelin ovoid or it appeared as a dark, irregular profile that lacked axoplasm. Data are presented as average values of 3-5 slices for dorsal horn sections, 1-2 representative section for peripheral nerves and dorsal root ganglia.

3.2.19 Flow Cytometry

Mice were sacrificed by CO_2 exposure and the following tissues collected for flow cytometry analysis: blood was collected via cardiac puncture, followed by immediate lysis of red blood cells; spleens were rapidly dissected into RPMI with 10% FBS, and the bone marrow was collected by flush using a 23G needle (BD Biosciences, Franklin Lakes, NJ). Single cell suspensions were made by pressing the tissues through a 70 μm nylon mesh (ThermoFisher). Cellular composition and expression of GFP was analyzed after staining with antibodies specific for CD3, CD4, CD8, CD19, Thy1.2, CD11b, Ly6C and Ly6G. All antibodies used were obtained from eBioscience (San Diego, CA). Flow cytometry was performed using FACSCanto II (BD

Biosciences) and the results were analyzed with the FlowJo software (TreeStar Inc., Ashland, OR).

3.2.20 Electrophysiology

HEK293T cells were transfected with mPanx1 retroviral plasmids (Panx1(WT), Panx1(TEV) and Panx1(YA)) using Lipofectamine 3000 (Invitrogen, Carlsbad, CA). After ~12h, cells were transferred on coverslips, allowed to attach and used for whole cell patch clamp recordings. To isolate Panx1 currents, the extracellular solution contained (in mM): 140 NaCl, 3 KCl, 2 $MgCl_2$, 2 $CaCl_2$, 110 Glucose and 10 HEPES (pH 7.3). The internal (pipette) solution contained (in mM): 100 CsMeSO3, 30 Tetra Ethyl Ammonium Chloride (TEA-Cl), 4 NaCl, 1 $MgCl_2$, 0.5 $CaCl_2$, 10 EGTA, 3 ATP-Mg, 0.3 GTP-Tris and 10 HEPES (pH adjusted to 7.3 with CsOH). Whole cell currents were measured using a configuration that included an Axopatch 200B (Molecular Devices, Sunnyvale, CA), Digidata 1440A (Molecular Devices) and pClamp acquisition software (Molecular Devices). Whole cell currents were recorded while applying a voltage ramp protocol (-100 mV to 80 mV in 1.5s; holding potential -50 mV). Extracellular solution containing CBX (50 μM) was perfused after the outwardly-rectifying Panx1 currents stabilized. The acquired signals were filtered at 1 kHz and sampled at 2 kHz for digitization. Data were normalized to cell capacitance (from the amplifier

circuits) and quantified as current density (pA/pF) at +80 mV and -60 mV. All recordings were carried out at room temperature.

3.2.21 Western blots

Cerebral cortices of mice were dissected in cold dissection buffer (26 mM $NaHCO_3$, 3 mM KCl, 1.25 mM NaH_2PO_4, 10 mM glucose, and 2 mM $MgCl_2$) and lysed in a protein extraction buffer (50 mM Tris, 150 mM NaCl, pH 7.4, 1% Triton X-100, 0.2% SDS, a cocktail of protease inhibitors, 5 mM NaF, and 10 mM $NaVO_3$) by using TissueLyser II (Qiagen). Protein samples were separated by SDS-PAGE, transferred onto 0.45 µm nitrocellulose membranes (Amersham) and blocked with 5% non-fat dry milk dissolved in a tris-based buffer (10 mM Tris, 150 mM NaCl, and 0.1% Tween 20, pH 7.4) at room temperature for 1 h. Endogenously expressed Panx1 proteins were detected by incubating with anti-Panx1 antibodies (C-terminus (6)), and anti-α-tubulin (T9026, Sigma Aldrich) antibodies were used as loading controls. Amersham ECL horseradish peroxidase (HRP)-linked secondary antibodies (GE Healthcare, Little Chalfont, United Kingdom) and Amersham ECL Western blotting dectection reagent were used to visualize immunoreactive signals on Amersham Hyperfilm ECL (GE Healthcare).

3.2.22 Statistics

All behavioral data and image analysis was conducted by experimenters blinded to animal genotype or condition. Data are presented as means ± s.e.m. Statistical comparisons were performed using GraphPad Prism using the indicated tests, with $p<0.05$ considered statistically significant. N.S. in figures stands for not significant.

3.2.23 Study Approval

All animal use was approved by the University of Virginia Animal Care and Use Committee, and all handling and procedures were performed in adherence to the National Institutes of Health Guide for the Care and Use of Laboratory Animals.

3.3 Results

3.3.1 Panx1$^{-/-}$ mice are protected from the hypersensitivity that typically accompanies nerve injury

To assess whether Panx1 contributes to neuropathic pain, we obtained global Panx1 knockout mice (*Panx1*$^{-/-}$) from a C57BL/6-derived ES cell line in which loxP sites were engineered to flank exon 3 of the Panx1 gene (obtained from the KOMP and described previously (25); Figure 3.1A-C). In addition, because C57BL/6 mice contain a non-synonymous SNP in P2X7 (Leu451) that disrupts the ability of the receptor to activate the Panx1

channel (41,48), any effect of Panx1 deletion in these mice is independent of its coupling to P2X7. Despite lacking this widely-expressed channel, *Panx1*$^{-/-}$ mice had no gross abnormalities or other apparent differences from wild-type littermates (*Panx1*$^{+/+}$ mice) as previously reported for other lines of Panx1 knockout mice (65), and heterozygous breedings yielded the expected Mendelian distribution of genotypes. Importantly, *Panx1*$^{-/-}$ mice did not demonstrate any significant differences in normal (uninjured) sensitivity to heat or mechanical stimuli (Figure 3.1D and E), ruling out systemic defects in nociception.

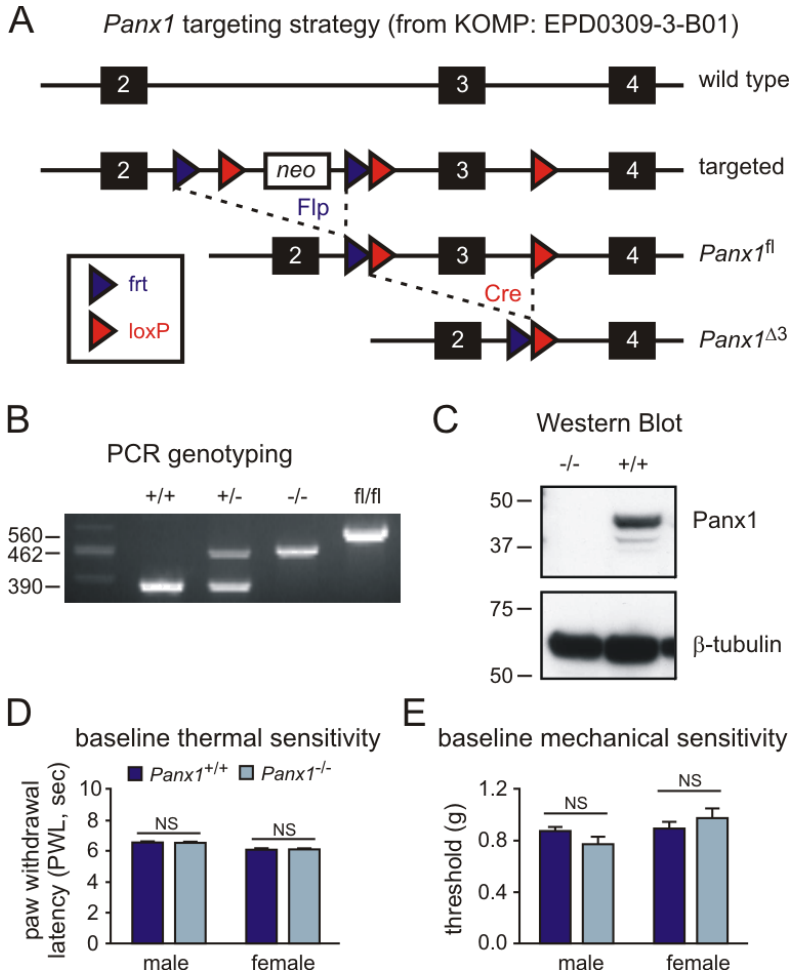

Figure 3.1 Development of Panx1-deleted mice.

(A) Targeting strategy for conditional and deleted Panx1 alleles. (B) PCR genotyping of wild-type, deleted and floxed alleles. (C) Western blot of brain tissue depicting loss of Panx1 protein in *Panx1*$^{-/-}$ mice. (D, E) *Panx1*$^{-/-}$ mice have normal heat (D, n=10-21) and mechanical (E, n=25-43) sensitivity in the absence of injury (ns, $p>0.05$ for genotype by two-way ANOVA).

Hypersensitivity to sensory stimuli is a common feature of neuropathic pain, with patients mainly complaining of increased sensitivity to touch (141,142). To induce mechanical hypersensitivity indicative of neuropathic pain, we performed unilateral spared nerve injury (SNI) surgery on wild-type (*Panx1*$^{+/+}$) and Panx1-deleted mice (*Panx1*$^{-/-}$) and assessed mechanical sensitivity over the next 28 days (schematic in Figure 3.2A). As expected, *Panx1*$^{+/+}$ mice developed robust and persistent mechanical hypersensitivity ipsilateral to the injured sciatic nerve beginning between 4 to 7 days and continuing until at least 28 days after surgery, as evidenced by a decrease in the threshold for response to stimulation by von Frey filaments (Figure 3.2C, left, and Figure 3.2D). In marked contrast to wild-type mice, *Panx1*$^{-/-}$ mice were completely protected over the entire 28 day testing period (Figure 3.2C, right, and Figure 3.2D). Importantly, no change in mechanical sensitivity was seen in the paw contralateral to the nerve injury for either genotype over the course of the experiment; moreover, sham-operated mice exhibited no change in mechanical hypersensitivity in either paw over an equivalent time period (Figure 3.2B). Thus, Panx1-deleted mice are resistant to SNI-induced pain.

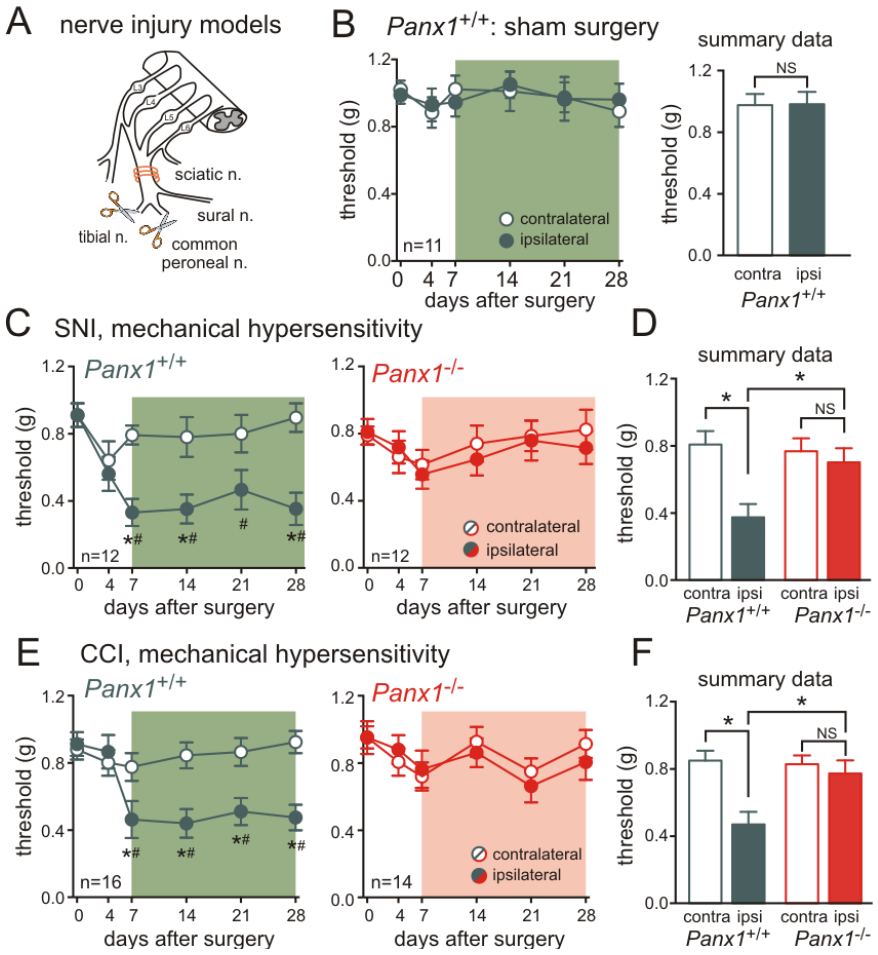

Figure 3.2 *Panx1*$^{-/-}$ mice are resistant to SNI-induced mechanical hypersensitivity.

(A) Diagram depicting the SNI surgery (with sparing of the sural nerve) and CCI surgery. (B) Absence of mechanical hypersensitivity in *Panx1*$^{+/+}$ mice undergoing sham surgery (ns, two-way RM ANOVA). (C) Wild-type littermates underwent unilateral SNI and developed mechanical hypersensitivity in the operated limb. In contrast, *Panx1*$^{-/-}$ mice were protected from mechanical hypersensitivity. (D) Summary data is the average threshold for each mouse from 7-28 days after operation (depicted by the shaded region in the time series. Summary data for (C). (E) Like SNI, mechanical hypersensitivity following CCI is completely absent in *Panx1*$^{-/-}$ mice while wild-type littermates experience robust hypersensitivity. (F) Summary data for (E). We used two-way RM ANOVA for statistical analysis, with Tukey's test for pairwise comparisons. In this and all other figures showing time course of mechanical sensitivity: # indicates $p<0.05$ versus day 0; * indicates $p<0.05$ for contralateral versus ipsilateral paw. For all figures showing summary data of sensitivity measures from POD7-28, * depicts $p<0.05$ between indicated groups and Sidak's test was used for pairwise comparison.

We used a second traumatic injury model to confirm these findings. The chronic constrictive injury of the sciatic nerve (CCI) model (depicted in Figure 3.2A) can be associated with greater variability, but it has the advantage of provoking both mechanical and heat hypersensitivity (129). Indeed, following CCI surgery, *Panx1*$^{+/+}$ mice developed both mechanical (Figure 3.2E, left, and Figure 3.2F) and heat hypersensitivity (Figure 3.3A, left and Figure 3.3B) starting between 4 to 7 days after surgery and continuing throughout the 28-day testing period. In contrast, *Panx1*$^{-/-}$ did not develop mechanical hypersensitivity (Figure 3.2E, right, and Figure 3.2F), and exhibited only mild hypersensitivity to heat (Figure 3.3A, right and Figure 3.3B). The degree of injury resulting from CCI was similar between experimental groups, since there were no differences in the number of preserved axons or degenerating profiles in semi-thin sections distal to the site of nerve injury from *Panx1*$^{+/+}$ and *Panx1*$^{-/-}$ mice (Figure 3.3C and D).

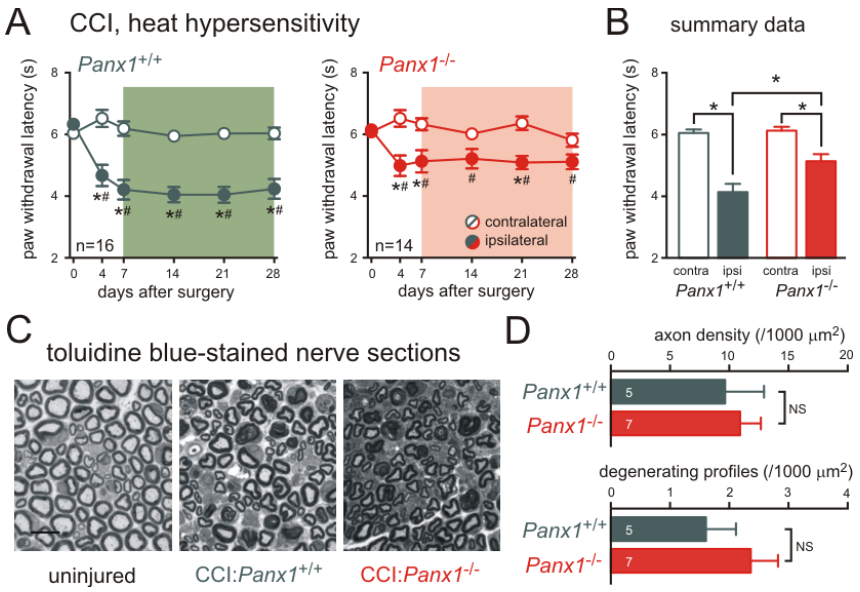

Figure 3.3 Heat hypersensitivity is blunted in *Panx1*$^{-/-}$ mice after CCI surgery.

(A) Heat sensitivity after CCI in wild-type (left, n=16) and *Panx1*$^{-/-}$ mice (right, n=14). (B) Summary data for (A). (C) Example semithin sections of the sciatic nerve distal to the CCI suture placement 7 days after surgery. Scale bar in left image is 10 μm (D) Quantification of intact axonal density (above) and degenerating neuronal profiles (below; $p>0.05$ for both parameters by unpaired two-tailed t-test). Statistical analysis of behavioral data as in Figure 3.2

Thus, hypersensitivity in two different models of traumatic nerve injury was significantly attenuated by Panx1 deletion. We focused on the more robust SNI model for subsequent experiments.

3.3.2 Panx1 expression in bone marrow cells mediates neuropathic pain

Panx1 is a major ATP release channel in many immune cells (101-103,143), and inflammatory purinergic mechanisms have been implicated in chronic neuropathic pain (38,108). We performed bone marrow transplantation studies to test the contribution of Panx1 in bone marrow cells to the appearance of nerve injury-induced neuropathic pain (study design depicted in Figure 3.4A and B). Strikingly, when *Panx1*$^{-/-}$ recipient mice were reconstituted with *Panx1*$^{+/+}$ cells from wild-type mice, the hypersensitivity following SNI was fully restored (Figure 3.4C left, and Figure 3.4D). Conversely, in wild-type mice reconstituted with *Panx1*$^{-/-}$ cells, the hypersensitivity following injury was significantly blunted, and fully resolved by the end of the test period (at 28 days post-injury, Figure 3.4C right, and Figure 3.4D). Importantly, bone marrow transplantation between donors and recipients of the same genotype did not differ in phenotype from the initial non-transplanted groups (compare Figure 3.4E and F with Figure 3.2C and D). We confirmed that cells in the circulation (not shown) and the bone marrow (Figure 3.4G and H) of transplanted mice were of donor origin by

flow cytometry using mice that ubiquitously express green fluorescent protein (UBI-GFP mice). These data indicate that expression of Panx1 in bone marrow-derived cells is sufficient for its contribution to neuropathic pain.

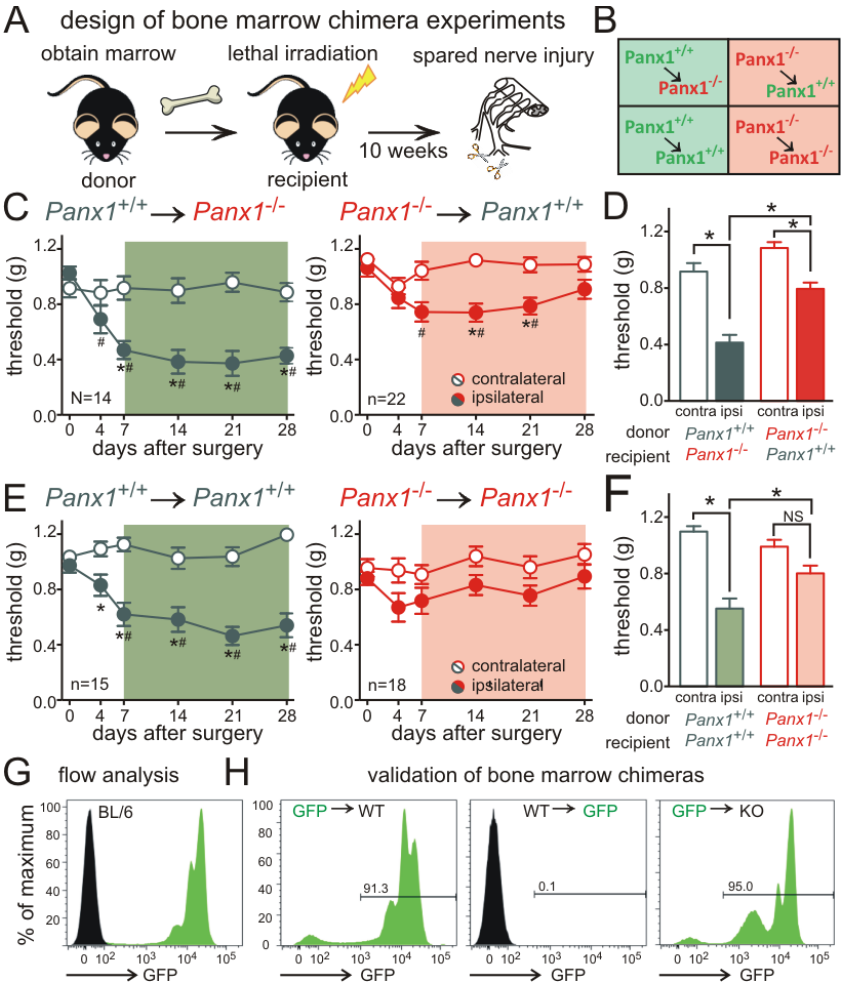

Figure 3.4 Bone marrow transplantation reveals a critical role for Panx1 in hematopoietic cells following nerve injury.

(A,B) Schematic depicting study design. (C) Mechanical hypersensitivity following SNI was restored in *Panx1*$^{-/-}$ mice reconstituted with wild-type marrow and diminished in *Panx1*$^{+/+}$ mice reconstituted with *Panx1*$^{-/-}$ marrow. (D) Summary data for (C). (E) Reconstitution of mice with cells of the same genotype. (F) Summary data for (E). (G) Flow cytometry showing GFP fluorescence in bone marrow from C57BL/6 mice or UBI-GFP mice. (H) GFP fluorescence after bone marrow transplantation of UBI-GFP cells or C57BL/6 cells into *Panx1*$^{+/+}$ or *Panx1*$^{-/-}$ mice demonstrating successful irradiation and replacement. Statistical analysis of behavioral data as in Figure 3.2

To test whether a specific cell type might be involved in the Panx1-mediated effects on SNI-induced pain, we crossed different Cre-driver lines to mice with *Panx1*$^{fl/fl}$ alleles to generate cell-type specific disruption of Panx1. In consideration of our results from the bone marrow transplants, and given the importance of macrophages/microglia in response to nerve injury (125), we crossed *Panx1*$^{fl/fl}$ mice to two different macrophage/myeloid-specific Cre lines: CX3CR1-Cre and LysM-Cre. These two Cre lines differ slightly in the extent and subtype of cells targeted with CX3CR1-cre being expressed in a greater percentage of microglia (126) and LysM-Cre being expressed more broadly in myeloid cells, including granulocytes (144). Despite the readily observed loss of Panx1 in the *CX3CR1-Cre/Panx1*$^{fl/fl}$ and *LysM-Cre/Panx1*$^{fl/fl}$ mice (Figure 3.5C and Figure 3.5F), they displayed a nerve injury-induced pain phenotype that was indistinguishable from floxed, Cre(-) littermates (Figure 3.5A, B, D and E). This suggested that the myeloid/macrophage loss of Panx1 alone is not sufficient to provide attenuation of SNI-induced pain. We then tested whether the expression of Panx1 in the T lymphocyte lineage is necessary as T cells have also been linked to neuropathic pain (108); this was achieved by crossing *Panx1*$^{fl/fl}$ mice to the CD4-Cre strain. However, *CD4-Cre/Panx1*$^{fl/fl}$ mice also did not show the attenuation of neuropathic pain that was seen with the global Panx1 knockout mice (Figure 3.5G-I). To test this in another way, we performed adoptive transfer experiments, introducing T cells from *Panx1*$^{+/+}$ and *Panx1*$^{-/-}$ mice into T/B cell-deficient Rag1KO mice (Figure 3.5J). Transferring Panx1-

deficient T cells into the Rag1KO mice failed to alter the hypersensitivity following spared nerve injury (Figure 3.5L and M). Of note, effective reconstitution of Rag1KO mice was achieved using T cells of either genotype (Figure 3.5K). Finally, to test a neuronal or glial contribution, we crossed the *Panx1*$^{fl/fl}$ mice to Syn-Cre and GFAP-Cre mice. The SNI-induced mechanical hypersensitivity was not attenuated in either of these well-established Cre lines despite demonstrable knockdown of Panx1 in semi-purified astrocyte and neuron preparations (Figure 3.6). Although, the extensive tissue-specific Panx1 deletion studies above did not implicate expression of Panx1 in a single cell type for nerve-injury induced pain, the pain attenuation observed with bone marrow cells lacking Panx1 in the transplantation studies suggests that Panx1 expression in multiple cell types and/or Panx1-mediated communication between more than one hematopoietic cell type contributes to the phenotype.

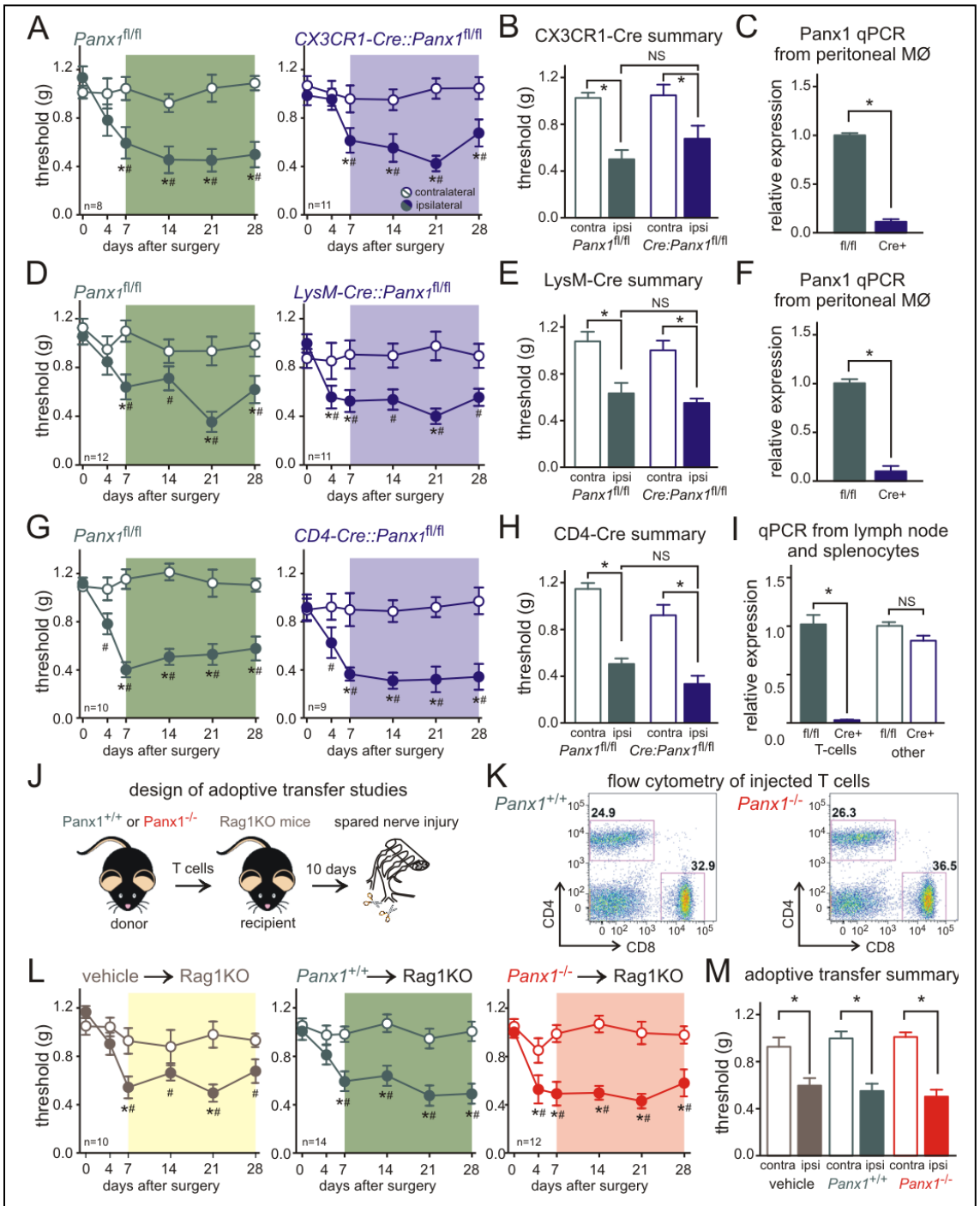

Figure 3.5 Removal of Panx1 from macrophages, myeloid cells or T cells does not prevent pain.

(A) The development of mechanical hypersensitivity in *Panx1*$^{fl/fl}$ mice or CX3CR1-Cre littermates. (B) Summary data for (A). (C) RT-qPCR for Panx1 relative to HPRT from peritoneal macrophages (n=3-7, * $p<0.05$, unpaired two-tailed t-test). (cont. on next page)

(D) The development of mechanical hypersensitivity in *Panx1*$^{fl/fl}$ mice or LysM-Cre littermates. (E) Summary data for (D). (F) RT-qPCR for Panx1 relative to HPRT from peritoneal macrophages (n=5, * $p<0.05$, unpaired two-tailed t-test). (G) The development of mechanical hypersensitivity in *Panx1*$^{fl/fl}$ mice or CD4-Cre littermates. (H) Summary data for (G). (I) RT-qPCR for Panx1 relative to HPRT from acutely isolated T cells (n=4-5, * $p<0.05$, one-way ANOVA). (J) Design of T cell adoptive transfer experiments. (K) Representative cytometry plots of CD4 (APC) and CD8 (PE) staining of Thy1.2 positive splenocytes isolated from adoptive transfer mice after SNI. (L) SNI-induced mechanical hypersensitivity in Rag1KO mice after vehicle treatment (left) or after reconstitution with *Panx1*$^{+/+}$ T cells (middle) or *Panx1*$^{-/-}$ T cells (right) (M) Summary data for (L). Statistical analysis of behavioral data as in Figure 3.2

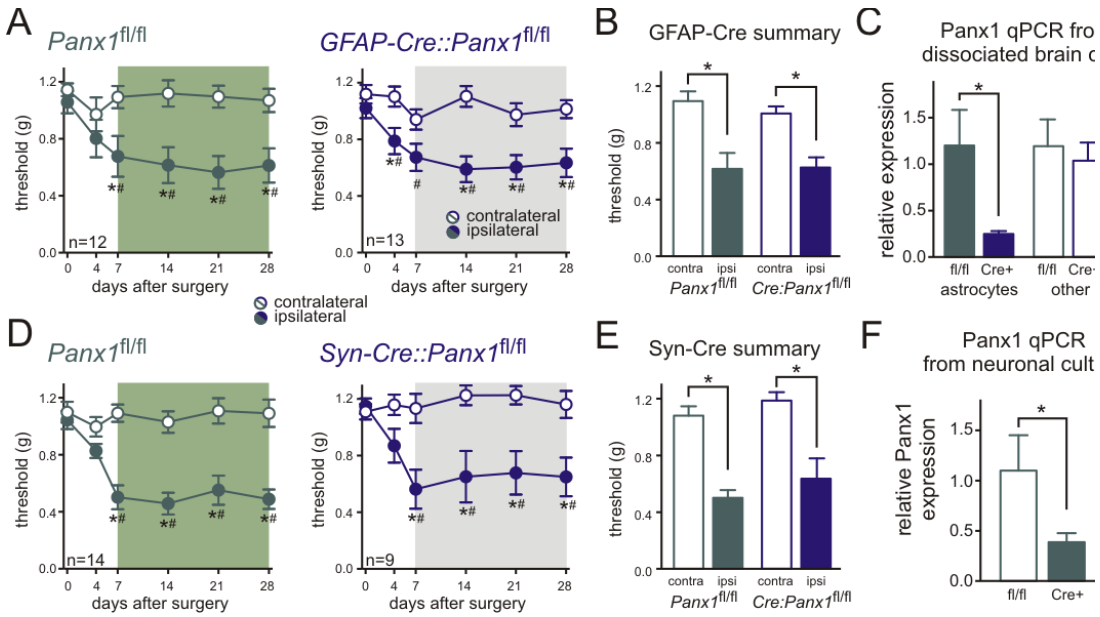

Figure 3.6 Expression of Panx1 in neurons or astrocytes alone is not required for neuropathic pain.

(A) The development of mechanical hypersensitivity in *Panx1*$^{fl/fl}$ mice or GFAP-Cre littermates (n=12-13). (B) Summary data for (A). (C) RT-qPCR for Panx1 relative to GAPDH from acutely isolated astrocytes (n=4-8, * p<0.05, one-way ANOVA). (D) The development of mechanical hypersensitivity in *Panx1*$^{fl/fl}$ mice or Syn-Cre littermates (n=9-14). (E) Summary data for (D). (C) RT-qPCR for Panx1 relative to HPRT from semi-purified neuronal cultures (n=3-8, * p<0.05, unpaired two-tailed t-test). Statistical analysis of behavioral data as in Figure 3.2

We also asked whether Panx1 deficiency alters the inflammatory cell profile within neural tissues. Prominent within this profile are macrophages, which contribute to hypersensitivity early after injury in the periphery and then at later time points from within the CNS (108,125). Resident macrophages (i.e., microglia in the CNS) as well as recruited circulating monocytes are believed to promote neuropathic pain (93,108,110). Indeed, at 7 days after injury, we observed a significant increase in the number of activated microglia in the ipsilateral spinal cord dorsal horn, relative to contralateral, as assessed by Iba1 immunostaining and characteristic morphological features (data not shown) or by co-immunostaining for Iba1 and phosphorylated p38 MAPK (pp38, an established marker of microglial activation (145)(Figure 3.7A and B). However, this ipsilateral increase in activated spinal microglia was fully retained in *Panx1*$^{-/-}$ mice. In the periphery, a significant ipsilateral:contralateral increase in the number of macrophages in the transected nerve (within 500 μm of the injured end) was observed 3 days after injury in *Panx1*$^{+/+}$ mice (Figure 3.7C upper row and Figure 3.7D and E). Notably, whereas *Panx1*$^{-/-}$ mice also had some macrophage infiltration into the cut nerve (Figure 3.7C lower row), there was no significant difference between the ipsilateral and contralateral sides. These data suggest that *Panx1*$^{-/-}$ mice may have blunted neural inflammation after injury.

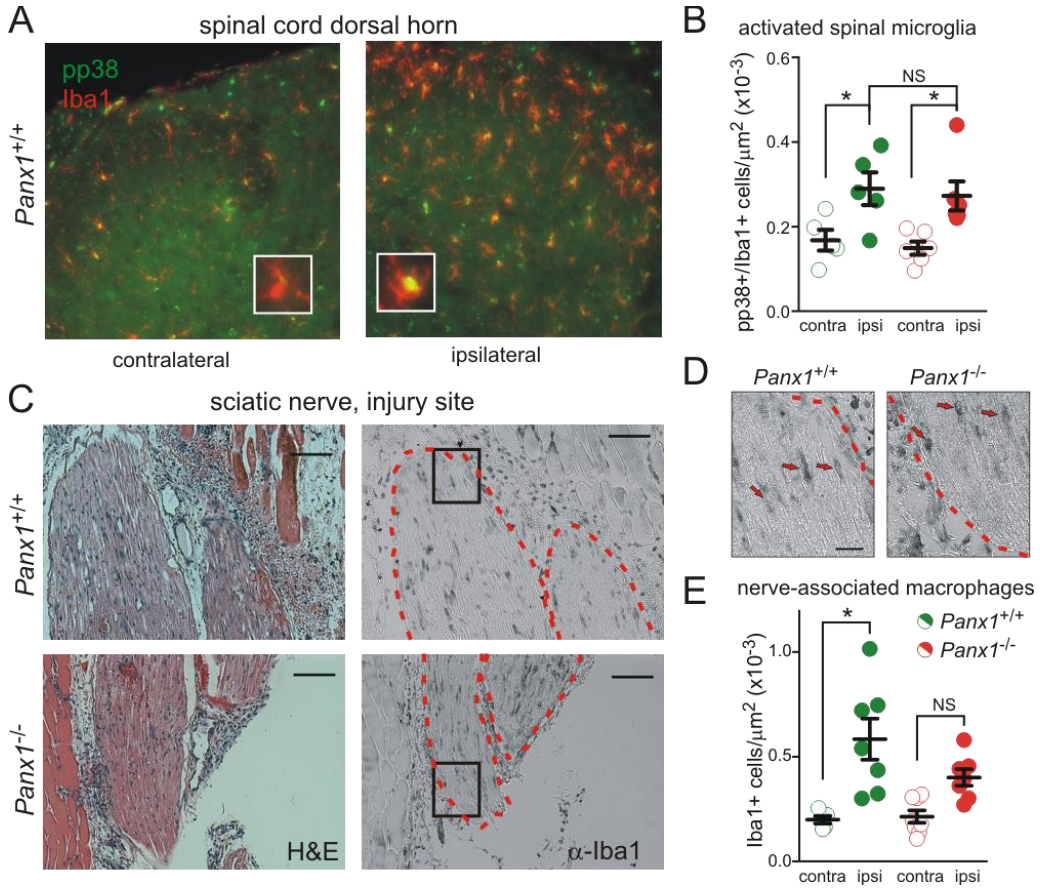

Figure 3.7 *Panx1*$^{-/-}$ mice have lessened peripheral inflammation after nerve injury.

(A) Example co-staining between Iba1 and pp38 in the dorsal horn of mice after 7 days of injury. Inset on left depicts a typical resting pp38(-) microglia, whereas inset on right shows a pp38(+), activated microglia. (B) Quantification of cells with an activated, amoeboid-like Iba1 staining with co-localization of pp38 (* $p < 0.05$, two-way ANOVA followed by pairwise comparison, n=5-6). (C) Example H&E staining of the injured sciatic nerve (left) and Iba1 staining (right). Note the effusion of red blood cells and other cells surrounding the nerve on the H&E stain, which was used to identify the cut end of the nerve. The red border depicts the region within the nerve used for further quantification Scale bar on the larger images is 100 μm and on the higher magnification image is 25 μm. (D) Example high powered images taken from the boxed region in panel (C). Black arrows are example Iba1(+) cells. (E) Quantification of macrophages within the nerve ending. (* $p<0.05$, by Kruskal-Wallis test, n=5-8).

3.3.3 A receptor-mediated Panx1 activation mechanism for SNI-induced hypersensitivity

Taking advantage of the rescue of pain we obtained with bone marrow transplantation, we addressed whether different mechanisms of Panx1 activation can be linked to neuropathic pain after nerve injury. We focused on channel activation by caspase-mediated cleavage of the Panx1 C-terminal tail and by an intracellular loop mechanism required for G protein-coupled receptor activation, as both caspases and various G protein-coupled receptors can contribute to neuropathic pain (108,146), and because activation of Panx1 by either mechanism can be disrupted by specific Panx1 mutations (9,18,52). The approach we took was to re-introduce wild-type or mutant channels into *Panx1*$^{-/-}$ hematopoietic cells by retroviral transduction to determine whether these modes of Panx1 activation affect SNI-induced hypersensitivity.

We obtained retroviral particles using an IRES-GFP vector (Migr1 (134)), that contained: the GFP reporter alone (empty vector); wild-type Panx1 (Panx1(WT)); a mutated Panx1 resistant to activation by caspase cleavage (Panx1(TEV)); or a mutated Panx1 resistant to activation by G protein-coupled receptors (Panx1Y198A (52)), here called Panx1(YA)). Transfection of HEK293 cells with each of these vectors resulted in currents with I-V characteristics indicative of Panx1 and sensitive to the Panx1 blocker CBX (Figure 3.8). We cultured bone marrow cells from donor *Panx1*$^{-/-}$ mice (134,135), infected the bone marrow cells with one of the 4 viruses

described above, and injected those virally transduced cells into lethally irradiated *Panx1*$^{-/-}$ mice (see experimental design, Figure 3.9A). Ten weeks after reconstitution, we tested these mice in the spared nerve injury model and made several interesting observations. First, reintroduction of wild-type Panx1 into the Panx1-deficient hematopoietic cells and reconstituting the Panx1-deficient mice with these cells restored the mechanical hypersensitivity to the *Panx1*$^{-/-}$ mice (Figure 3.9C and D). Based on flow cytometry analysis of GFP-expressing bone marrow cells after reconstitution, the infection appeared to affect several subtypes of cells equally (monocytes, T cells and B cells; data not shown). This recapitulated results obtained from transplanting wild-type bone marrow into Panx1-deleted mice. Second, *Panx1*$^{-/-}$ mice reconstituted with Panx1(TEV)-infected bone marrow cells, showed mechanical hypersensitivity after SNI that was comparable to that seen with Panx1(WT)-infected cells (Figure 3.9E, left, and Figure 3.9F). This suggested that caspase-mediated activation of Panx1 was not playing a role in the elicitation of pain after SNI. Third, re-expression of Panx1(YA) failed to completely rescue mechanical hypersensitivity in *Panx1*$^{-/-}$ mice following nerve injury, with essentially no difference in mechanical threshold at 28 days (Figure 3.9E, right, and Figure 3.9F). This suggested a specific requirement for Tyr-198 in Panx1 activation for neuropathic pain in this SNI mode, an intracellular loop residue implicated previously in a form of GPCR-mediated channel activation (52). Importantly, the difference in sensitivity to pain seen between the Panx1(TEV) mutant and the Panx1(YA) mutant

mutant was not due to differences in expression, as the relative expression of Panx1 restored by each of the Panx1(WT), Panx1(TEV) and Panx1(YA) viruses were not different (Figure 3.9B). These data are consistent with a GPCR-mediated channel activation mechanism in hematopoietic cells underlying Panx1 contributions to nerve injury-induced pain.

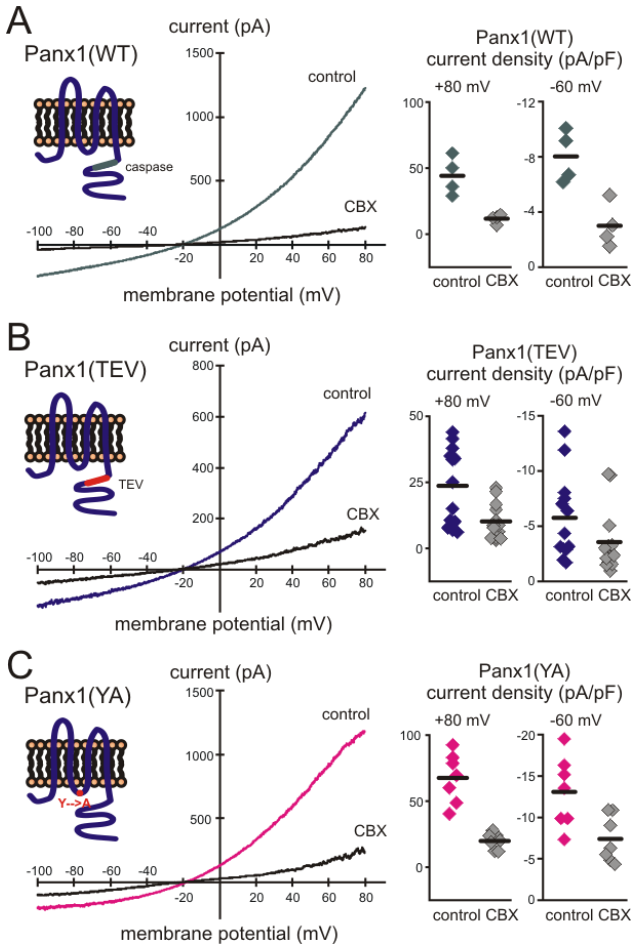

Figure 3.8 Expression of Panx1 from retroviral vectors in HEK cells.

(A-C, left) I-V curves of Panx1 currents from (A) Panx1(WT), (B) Panx1(TEV), and (C) Panx1(YA) before and after 50 μM CBX application. (A-C, right) Summary data of current densities with and without CBX for each vector calculated at +80 mV and at -60 mV.

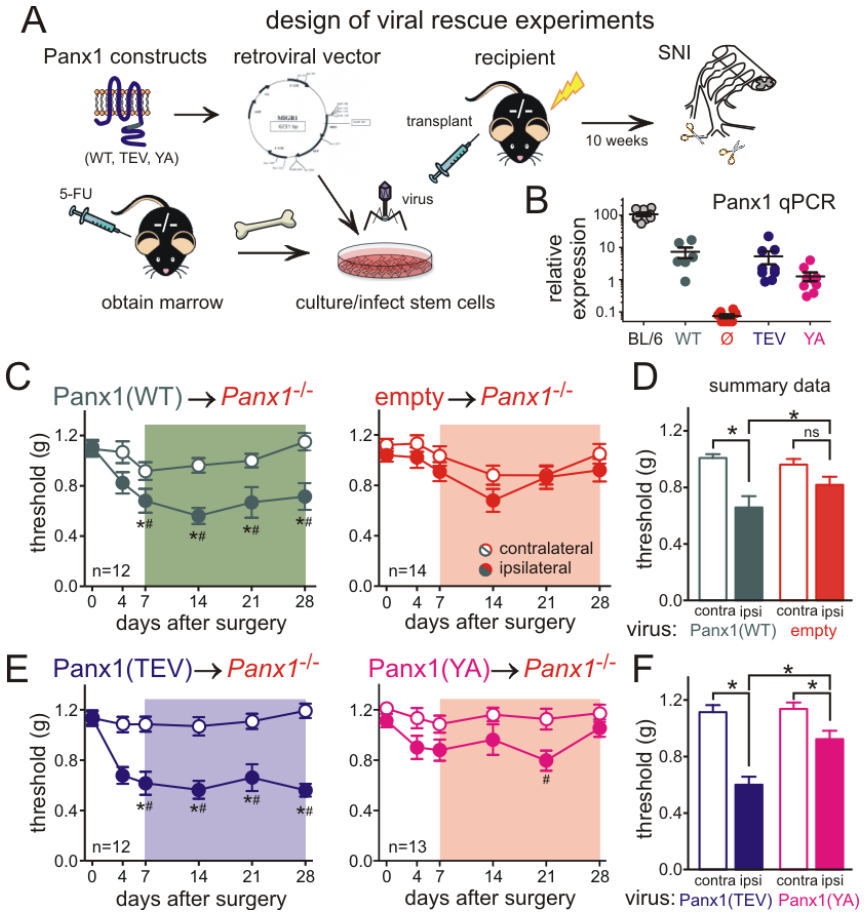

Figure 3.9 Restoration of Panx1 expression in adult Panx1-/- hematopoietic cells restores pain following nerve injury; rescue requires tyrosine 198 of Panx1.

(A) Design of viral irradiation-replacement experiments. (B) RT-qPCR for Panx1 (relative to HPRT) from bone marrow of uninfected C57BL/6 mice, or mice who received virally-infected hematopoietic cells. (C) Mechanical hypersensitivity develops fully in mice receiving cells infected with Panx1(WT), but fails to develop in empty-vector treated cells. (D) Summary data for (C). (E) Mechanical hypersensitivity develops fully in mice receiving cells infected with Panx1(TEV), but is reduced in Panx1(YA) treated cells. (F) Summary data for (E). Statistical analysis of behavioral data as in Figure 3.2

3.3.4 Pharmacological targeting of Panx1 is effective in treating hypersensitivity following nerve injury

The genetic studies presented to this point indicate that the expression of Panx1 in hematopoietic cells contributes to neuropathic pain, and that disruption of its function attenuates the pain. We next asked whether pharmacologically inhibiting Panx1 function would be a viable approach to diminish pain in wild-type mice, and thereby serve as a potential therapeutic target for the human condition. We treated mice with two chemically distinct Panx1 blockers: CBX (a classical Panx1 blocker) and Trovan (a fluoroquinolone antibiotic recently identified to inhibit Panx1 in a voltage-dependent manner (25)). First, CBX and Trovan were given systemically for 7 days in an early treatment protocol (starting 1 day prior to SNI surgery), as depicted in Figure 3.10A. Early daily treatment with either Trovan (Figure 3.10B) or CBX (Figure 3.10D) resulted in complete protection from hypersensitivity; responses in ipsilateral paws of drug-treated mice were not different from pre-operation baselines during the period of drug administration. After discontinuation of the drug, hypersensitivity developed fully (Figure 3.10B and D, see rightmost bars at day 28). We next asked whether giving drugs that block Panx1 could potentially relieve mice with an established pain phenotype (late treatment, with drugs given daily starting at least 7 days after surgery; see Figure 3.10A). Late treatment with both drugs partially relieved established hypersensitivity, recovering approximately half the decrease in mechanical threshold that followed nerve injury (Figure

3.10C and E). It is unlikely that these effects were due to some unintended effect of drug treatment (e.g., lethargy, or an inability to respond), since we found no drug-related effects on performance of mice using three different tests of motor function: elevated ledge (Figure 3.11A), elevated platform (Figure 3.11B) and inverted screen (Figure 3.11C). Thus, the observed effects of these drugs on mechanical threshold can be attributed to reduced hypersensitivity, suggesting that inhibition of Panx1 may be a viable strategy for treating neuropathic pain.

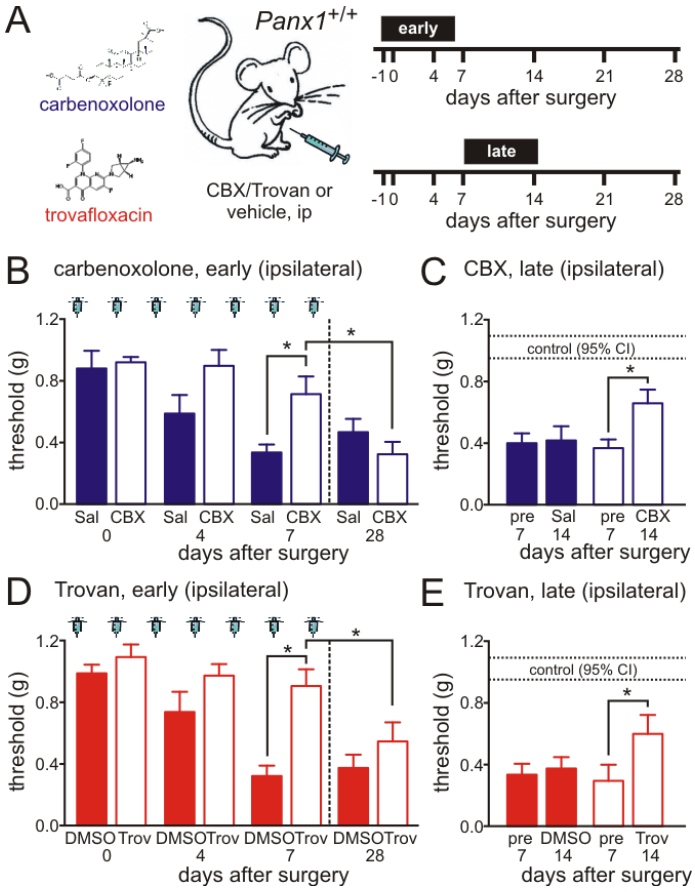

Figure 3.10 The pannexin channel inhibitors trovafloxacin (Trovan) and carbenoxolone (CBX) prevent or reverse mechanical hypersensitivity when administered systemically.

(A) Diagram depicting two dosing schemes, one before and early after nerve injury and the other after hypersensitivity is established. (B,D) The effect of early and daily IP trovan (B, 30 mg/kg in DMSO, n=10 per condition) or CBX (D, 30 mg/kg in saline, n=10-11 per condition) and the respective vehicles. Syringe cartoons above data indicate testing days where the drug was also administered. At day 7, pain development was significantly blunted by drug treatment, relative to vehicle; after the drug was withdrawn, full hypersensitivity was observed at day 28. (*, $p<0.05$ by pairwise comparison after two-way RM-ANOVA). (C,E) Changes in hypersensitivity after daily IP trovan or DMSO (C, n=12-13), and after CBX or saline (E, n=12-13). Mechanical sensitivity was partially relieved by both drugs, comparing pre- and post- treatment values (solidly colored bars are pre values; dotted lines above mark the 95% CI for the pre-operation baselines; *, $p<0.05$ pairwise comparisons following two-way RM ANOVA).

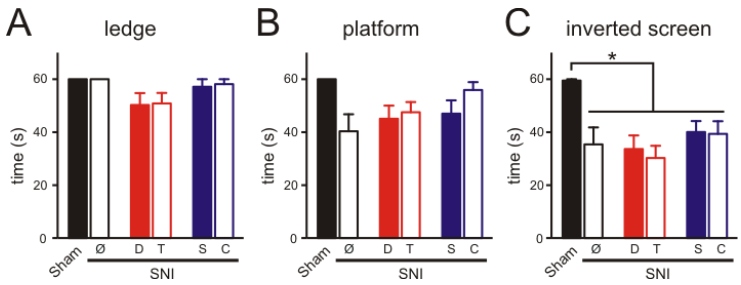

Figure 3.11 Mice treated daily with Panx1 blockers maintain sensorimotor capabilities.

(A-C) Sensorimotor function of mice after 7 days of drug (T, trovan or C, CBX) or vehicle treatment (D, DMSO or S, saline). There were no differences in performance between SNI-operated mice receiving no treatment (null symbol) or any of the 7 day drug or vehicle treatments ($p>0.05$, Kruskal Wallis test). In the last test (C, inverted screen), sham mice completed the task better than any of the SNI-operated mice (*, $p<0.05$, Kruskal Wallis test with pairwise comparisons).

3.4 Discussion

In this study, we demonstrate that Panx1 is necessary for chronic pain following traumatic nerve injury, Panx1 expression in hematopoietic cells is sufficient to account for its contribution to neuropathic pain, and that Panx1 inhibition may be an effective approach to alleviate neuropathic pain. Specifically, mice with global deletion of Panx1 fail to develop the typical mechanical and/or heat hypersensitivity that normally accompanies two different forms of sciatic nerve injury in mice, and rescue of hypersensitivity in Panx1-deleted mice was obtained with wild-type bone marrow cell transplantation. In addition, these experiments were performed in C57BL/6 mice, which express a P2X7 variant that is unable to couple to Panx1 (41,48), and Panx1 re-expression and rescue was observed with a Panx1 construct that cannot be activated caspase cleavage (9,18), excluding those channel activation mechanisms in this context. On the other hand, a Panx1(YA) channel that is resistant to activation by G protein-coupled receptors (52) did not support rescue of neuropathic pain in *Panx1*$^{-/-}$ mice. Finally, systemic administration of Panx1 blockers prior to the injury was fully protective while later treatment partially relieved established pain, indicating a role for Panx1 in both development and maintenance of neuropathic pain. Collectively, this work suggests that Panx1 activation by GPCRs in hematopoietic cells plays a major role in the onset and persistence of neuropathic pain following nerve injury, and that Panx1 should be considered as a practicable therapeutic target for this often intractable condition.

This direct genetic and pharmacological validation for the hypothesis that Panx1 contributes to neuropathic pain could be relevant to the human condition. Patients are most likely to report heightened sensitivity to touch as particularly unpleasant among the different sensory modalities affected (141,142), and, notably, we find that either Panx1 deletion or inhibition can strongly suppress nerve injury-associated mechanical hypersensitivity. Pharmacologic inhibition of the channel was effective when drugs were administered systemically, which suggests that targeting this channel may not require complicated spinal cord delivery methods (81,82). The site of action of the Panx1 blockers in our model is unclear as Trovan and CBX can both cross the blood-brain-barrier (26,147) and thus could modulate the channel within the CNS or peripherally, at the site of nerve injury. Likewise, intrathecal injection of Panx1 blockers could disrupt channel function in the spinal cord or dorsal root ganglia, but could also leak from the spinal injection site to work at peripheral sites (81,82). Nonetheless, the present demonstration of effective pain relief from systemic administration of Panx1 blockers, rather than by intrathecal delivery, presents the possibility of a more convenient translation toward clinical application. Our data also suggest that continued systemic administration of Panx1 blockers may be required for prolonged pain relief as pain sensitivity developed after the blocker was withdrawn. Encouragingly, however, attenuation of pain was achievable when blockers were provided after the establishment of pain, suggesting that treating patients already suffering from neuropathic pain with a Panx1

blocker may prove useful and worthy of further testing. It is also possible that longer term treatment, perhaps with multiple combinations of blocker dose and duration, could provide more complete relief.

Our bone marrow transplant studies highlight the importance of Panx1 in circulating hematopoietic cells for pain development following nerve injury. Specifically, the neuropathic pain phenotype was fully rescued by re-introduction of Panx1-expressing hematopoietic cells into *Panx1*$^{-/-}$ mice. A blunted and transient hypersensitivity developed after nerve injury when *Panx1*$^{-/-}$ cells were donated to *Panx1*$^{+/+}$ mice, implying some possible early contributions from a radiation-insensitive cell population (e.g., embryonic yolk sac-derived microglia or other tissue-resident macrophages). Moreover, since neuropathic pain developed normally in mice lacking Panx1 specifically in the macrophages/myeloid lineage, T cells, neurons and glia, this may reflect overlapping functions among the targeted cell types (e.g., amplifying or initiating innate inflammatory responses), or that functional redundancy may emerge when Panx1 is deleted from one cell type (e.g., allowing a different cell type to compensate). Alternatively, it is possible that a low level of residual Panx1 expression in one of these cell types is sufficient for pain development. Indeed, this possibility is supported by our viral re-expression experiments, where an average of ~7% of cells expressing Panx1 at ~5-10% of wild type levels was sufficient for restoration of the pain response. Thus, the Cre-mediated deletion, albeit often very efficient, may have not have reached the deletion threshold for effectiveness.

It is generally believed that channel activation is required for Panx1 signaling, and our experiments provide valuable insight into the mechanism of channel opening that is relevant for pain development. Specifically, we showed that Panx1 channels that are mutationally resistant to GPCR-mediated activation (52), but not to caspase cleavage-based activation (9,18), could not rescue neuropathic pain following bone marrow transplantation in Panx1-/- mice. The GPCR-specific activation mutation abrogates Panx1 activation by α1D adrenoceptors (52) and multiple additional Gq-linked receptors could potentially activate Panx1 channels in the context of neuropathic pain, including the histamine H1 receptor (53,148), P2Y1 (8,149), P2Y2 (75,150), P2Y6 (56,151), and Group 1 metabotropic glutamate receptors (152). P2Y6 and H1 receptors are of particular interest since they are prominently expressed in various immune cells (153,154). In addition, H1 receptor activation can induce Panx1-mediated ATP release from other cells (53). Finally, TNFα has been long-associated with neuropathic pain (155) and it is possible that TNFα may activate Panx1 channels via the same Tyr-198 residue mutated in our experiments (63).

Other potential channel activation mechanisms seem less likely. For example, Panx1 is described as a voltage-dependent channel, generating the largest currents at depolarized membrane potentials (10). However, a depolarization-dependent activation mechanism is doubtful since Trovan is as effective as CBX at preventing or remediating neuropathic pain, even though

Trovan blocks Panx1 channels only at hyperpolarized potentials (25). As mentioned previously, a P2X7-mediated Panx1 channel activation mechanism is unlikely since our mouse lines contained the C57BL/6 variant of P2X7-Leu451 unable to couple functionally to Panx1 (verified by differential restriction enzyme digest of a PCR-amplified P2X7; data not shown) (41,48). Although this precludes a requirement for P2X7 in the Panx1 activation relevant to nerve-injury induced pain, it does not rule out alternative mechanisms by which P2X7 could contribute to neuropathic pain. Finally, NMDA receptor activation can trigger Panx1 opening but this Src-dependent activation appears to target a different tyrosine residue (61,62).

Collectively, these data provide compelling genetic and pharmacological evidence that Panx1 plays an obligatory role in the development and maintenance of chronic pain following nerve injury that is linked to its expression in circulating bone marrow-derived cells. These studies also suggest that Panx1 is a potentially viable therapeutic target for neuropathic pain, a condition that has been notoriously refractory to the current treatment options.

CHAPTER 4

Pannexin 1 channels promote sleep

This chapter contains unpublished (and acknowledgeably, preliminary) data. It represents a novel physiologic context for pannexin channels.

4.1 Introduction

Sleep is arguably the most pervasive state of animal and human life (156). While the nature of sleep is different for every creature on the planet, we are all required to sleep at some time, and in some way, in order to stay alive. The exact function of sleep is debated but it is essential for cognitive processes including learning, memory and attention (157). Disorders of sleep in humans are incredibly common with a prevalence in the United States estimated to be upwards of 40% of adults experiencing problems with falling asleep or excessive daytime sleepiness (158). These disorders can be co-morbid features of other medical or psychiatric diseases (e.g., depression), or be the primary condition itself with profound effects on overall health and wellbeing (e.g., shift-work sleep disorder). It has even been suggested that increased pain may be related to sleep quality (and vice versa), and that sleep deprivation can attenuate the analgesic effects of some medicines (159).

Of particular clinical interest are the effects of sleep deprivation as this is a universal condition in humans. New parents, shift workers, healthcare employees and college students are all particularly susceptible to sleep deprivation. However this condition has affected all of us at one time or another and the well-known physiologic effects include cognitive impairment and delayed reaction time (160). There are also many long-term consequences of sleep deprivation, which include impaired homeostatic regulation of the immune system (161); this may account for the association between sleep and many chronic disease such as diabetes and cardiovascular disease (162).

On a molecular scale, increased periods of wakefulness are associated with an extracellular accumulation of adenosine in brain regions with known functions on controlling sleep such as the basal forebrain (163,164). This adenosine induces the physiologic pressure to sleep and promotes recovery from sleep deprivation as well (165). But where does this adenosine come from, and how does it get into the extracellular space? The kinetics of adenosine action suggest that ATP may be the molecule initially released which is then rapidly degraded into adenosine (166) but there may be direct effects of ATP on sleep as well (167). Potential sources of ATP/adenosine include synaptic co-release (168), concentration dependent release via transport mechanisms (169)), and also vesicular release from astrocytes (170). Surprisingly, there have been no published investigations regarding channel-mediated release mechanisms of ATP in sleep.

Panx1 channels are known mediators of ATP release from many brain cells including neurons, microglia and astrocytes (171). The channel is expressed in brain regions with identified roles in sleep-wake homeostasis including the basal forebrain and cortex (64,163,164). In addition, two independent groups have confirmed that mice lacking Panx1 function have learning and memory deficits (67,68). As learning and memory function is closely tied to sleep (157,160), we also wondered whether Panx1-deleted mice have an associated sleep dysfunction.

In this study, we used infrared mouse motion tracking technology as a preliminary means to investigate the sleep quality of global Panx1 knockout mice (*Panx1*$^{-/-}$) and their wild-type littermates (*Panx1*$^{+/+}$) both under normal conditions and after a 6 hour period of sleep deprivation. We found that under normal conditions, *Panx1*$^{-/-}$ mice demonstrated an increased duration to reach an immobile state immediately after the lights turned on, a crucial time for restorative sleep for these mostly nocturnal rodents. In addition, the mice were resistive to the effects of sleep deprivation, as they spent less time immobile and had a blunted drop in activity during the recovery phase. Although preliminary, this data suggests that Panx1 may have a function in normal sleep processes and that this channel is partially responsible for recovery from sleep deprivation.

4.2 Methods

4.2.1 Mice

Adult male *Panx1*$^{-/-}$ mice and their wild-type littermates were used in this study. These mice have been previously generated and described (Figure 3.1; (25)). All animal use was approved by the University of Virginia Animal Care and Use Committee, and all handling and procedures were performed in adherence to the National Institutes of Health Guide for the Care and Use of Laboratory Animals. Mice were housed individually and with standard 12 hour light/dark cycles.

4.2.2 Activity monitoring

The definitive method for analyzing mammalian sleep is EEG recordings, however immobility is often used as a surrogate measure when EEG recordings are not feasible (e.g., in phylogenetically lower species (172)). Activity of the mice as well as light intensity was recorded using MOUSE-E-MOTION cage top monitors (Hamburg, Germany). To determine the degree of activity or immobility for normal sleep-wake cycles, the mice were placed in the infrared-monitored cages and allowed to acclimate for at least 24 hours. After the acclimation period, the device recorded the number of seconds where a suprathreshold movement (as defined by the internal circuitry of the device) was detected within each 4 minute period. If there were no measurable movements within 4 minutes, this time period was

considered as “immobile” and the number of these immobile periods as well the total “activity” (summated activity counts) was recorded for the next 5-7 days. Figures display the activity counts as a percent of total possible counts (i.e., the number of seconds within each time period where a motion was logged by the mouse).

4.2.3 Sleep deprivation

After monitoring the mice under normal conditions for at least 5 days, the mice underwent 6 hours of sleep deprivation beginning at the start of the light cycle (see Figure 4.3A). Sleep deprivation was accomplished by presenting the mice with novel objects at frequent intervals or gently nudging the mice with a cotton swab when they stopped moving during the 6 hour period. This method of sleep deprivation was chosen as it minimizes contact with human animal handlers and reduces stress on the mice. At the end of the deprivation period, activity monitoring was allowed to proceed undisturbed for the next 18 hours (the recovery period).

4.2.4 Statistical analysis

All sleep deprivation and data analysis tasks were conducted by experimenters blinded to animal genotype. Data are presented as means ± s.e.m. Statistical comparisons were performed using GraphPad Prism using the indicated tests, with $p<0.05$ considered statistically significant.

4.3 Results

4.3.1 Panx1$^{-/-}$ mice exhibit delayed sleep initiation

We addressed whether Panx1 contributes to normal sleep-wake cycles using global Panx1 knockout mice and an infrared activity monitoring system that records beam breaks and light intensity. As expected for these nocturnal rodents, immobility durations were higher in the light (Figure 4.1A) while the activity counts were higher during the dark period (Figure 4.1B). With respect to genotype, immobility and activity of the *Panx1*$^{-/-}$ mice followed this same trend, however *Panx1*$^{-/-}$ mice did display overall greater activity counts during the dark period (Figure 4.1B).

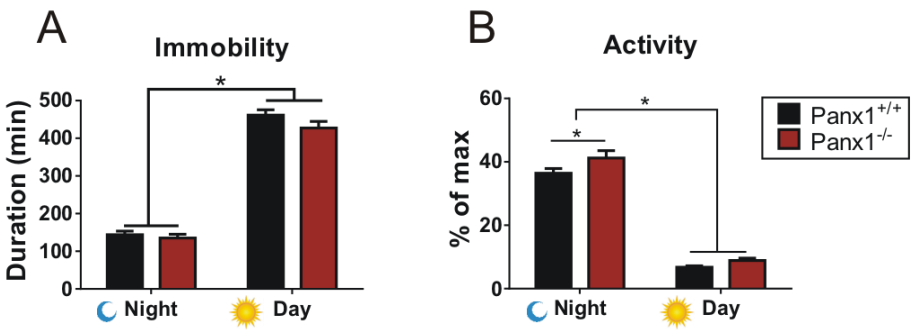

Figure 4.1 *Panx1*$^{-/-}$ mice have the same total immobility as wild-type littermates with slightly elevated nocturnal activity.

(A) Total duration of immobility (e.g., a 4 min period of no detected movement) and (B) activity over the 12 hour dark period or 12 over light period. (*$p<0.05$, two-way RM ANOVA followed by pairwise comparison, n = 18-26).

Next, we considered how activity and immobility would change over time with respect to light intensity. *Panx1*$^{-/-}$ mice were less immobile on average (and consequently more active) during the first two hours after lights came on (Figure 4.2A and B). Similarly, the duration until the first immobile period was longer for the *Panx1*$^{-/-}$ mice (Figure 4.2C). Because immobility can be indicative of sleep, this data suggests that Panx1 may have a role in initiation of sleep.

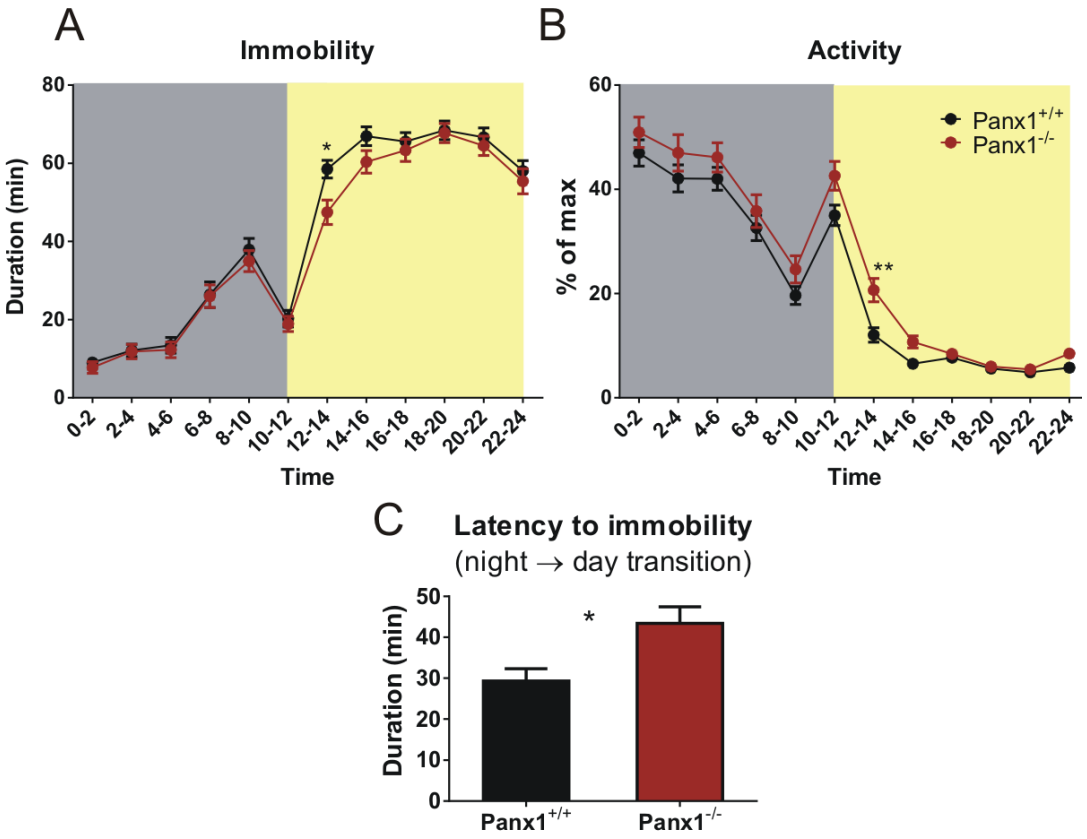

Figure 4.2 *Panx1*$^{-/-}$ mice are slow to initiate sleep in the beginning of the light cycle.

(A) Immobility or (B) activity summated into 2-hour blocks (* $p<0.05$, two-way RM ANOVA with pairwise comparison, n = 23-28). (C) Duration from the lights on until the first 4-min period of immobility. (*$p<0.05$, unpaired t-test, n=23-28).

4.3.2 Panx1$^{-/-}$ mice are resistant to recovery after sleep deprivation

To better relate these activity/immobility measures with actual sleep, we subjected the mice to a 6 hour period of sleep deprivation at the beginning of the light cycle (Figure 4.3A). As expected, *Panx1*$^{+/+}$ mice exhibited low immobility and high activity during the sleep deprivation period (orange bar and filled symbols, Figure 4.3B and Figure 4.3C). During the next 18 hours, the mice were allowed to sleep at will and *Panx1*$^{+/+}$ mice demonstrated several periods of increased immobility (Figure 4.3B) or decreased activity (Figure 4.3C) relative to their baselines with an overall 40% increase in immobility and a 38% drop in activity. With *Panx1*$^{-/-}$ mice, there were no periods of increased immobility (Figure 4.3D) and some periods of decreased activity (Figure 4.3E). Compared together, the genotypes exhibited differences in immobility (Figure 4.3F) and activity (Figure 4.3G) after sleep deprivation that was significant during the late light period and in the early dark period. Thus, although *Panx1*$^{-/-}$ mice do show some degree of sleep deprivation recovery, the overall response is blunted compared to *Panx1*$^{+/+}$ littermates.

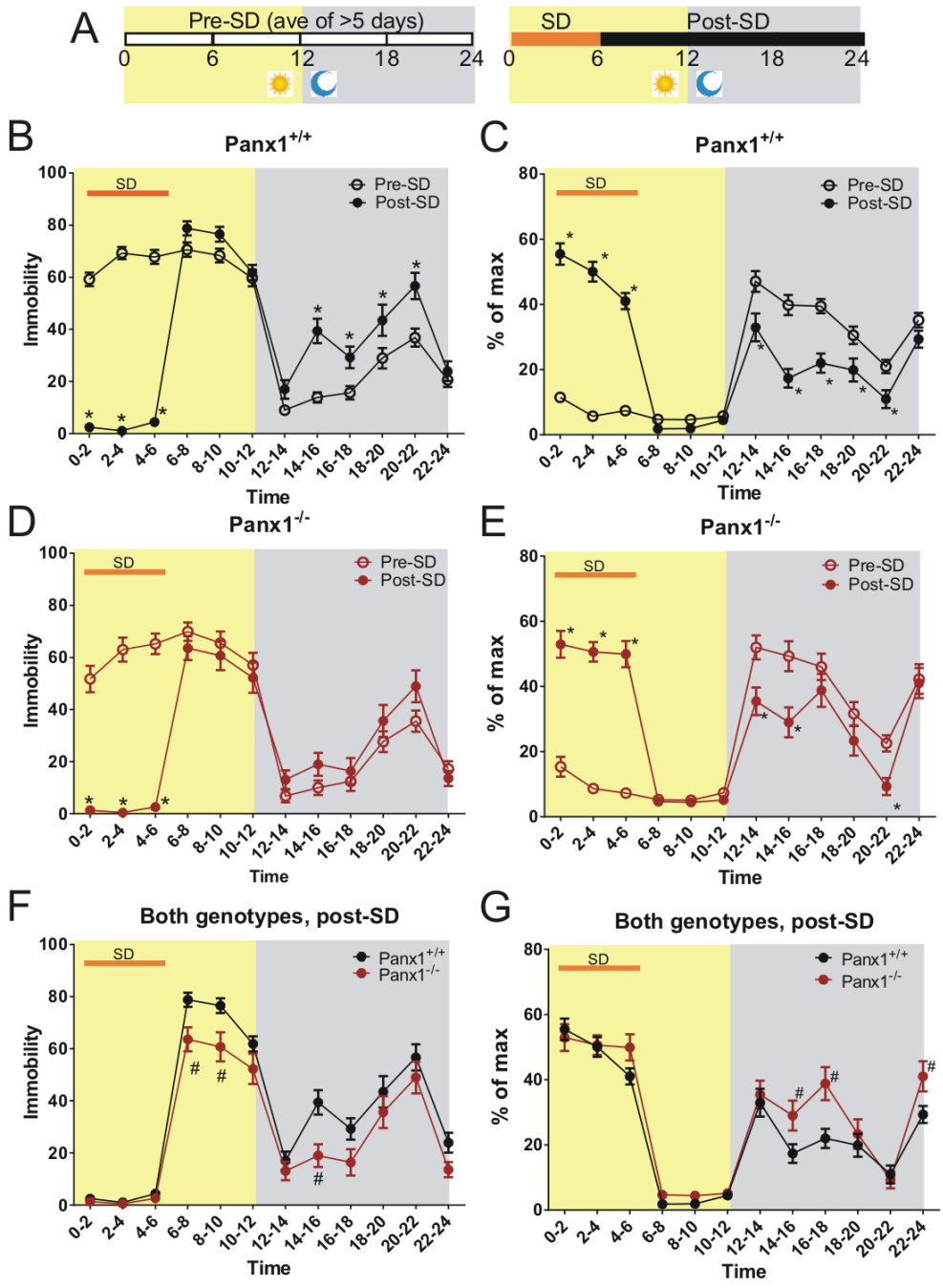

Figure 4.3 *Panx1*$^{-/-}$ mice resist sleep deprivation.

(A) Experimental design. (B) Immobility and (C) activity changes in *Panx1*$^{+/+}$ mice after sleep deprivation. (D) Immobility and (E) activity changes in *Panx1*$^{-/-}$ mice after sleep deprivation. (E) Genotype comparison after sleep deprivation with respect to immobility (F) and activity (G) (* or #, $p<0.05$, two-way RM ANOVA followed by pairwise comparison, n = 13-22).

4.4 Discussion

Using infrared motion sensing technology, we sought to determine whether Panx1 contributes to sleep or the recovery from sleep deprivation. While the normal sleep of *Panx1*$^{-/-}$ mice and wild-type littermates was largely unremarkable, mice lacking Panx1 took longer to reach a state of immobility at the start of the light cycle. After sleep deprivation, wild-type mice responded with increased immobility and decreased activity, and *Panx1*$^{-/-}$ mice exhibited blunted changes in these two parameters. These data suggest that Panx1 may have a role in sleep initiation and/or in the recovery response to sleep deprivation.

As mentioned above, accumulation of extracellular ATP/adenosine is closely associated with the physiologic drive to sleep. Among ATP/adenosine release mechanisms that have been examined, the evidence for vesicular release of adenosine is generally considered the strongest to-date based on the work of Halassa and colleagues (170). Although of great significance to our understandings of recovery from sleep deprivation, there are several key limitations of this work that remain unaddressed; these leave open the possibility of non-vesicular release mechanisms contributing to extracellular adenosine as well. For example, the authors generated a mouse that expressed a dominant negative SNARE (dnSNARE) construct to disrupt efflux of vesicular content from astrocytes in vivo and observed profound effects on the ability of the mice to recover from sleep deprivation. While this highlights the importance of gliotransmission in sleep, it does not necessarily exclude

other potential release mechanisms (including channel-mediated release). For instance, the trafficking of some channels to the plasma membrane is dependent on SNARE proteins (173-175), thus this experimental tool may have disrupted channel trafficking to the membrane as well. Finally, the selectivity of the dnSNARE for astrocytes has recently been called into question (176). For these reasons, we considered Panx1 as an alternative channel-mediated ATP release mechanism contributing to sleep and sleep deprivation recovery.

In this study, we used motion as a surrogate for EEG recordings, which is the optimal method for analyzing sleep structure (172). Motion detection is often used in organisms where EEG recordings are not possible and these studies have yielded valuable knowledge regarding sleep using organisms like drosophilia and zebrafish (e.g., (177-180)). In addition, motion detection has some advantages over EEG analysis, specifically the recordings can occur in freely moving animals without prior surgical manipulations, which are also known to alter sleep structure (181,182).

Motion detection methods do have limitations which necessitate confirmation of these findings with EEG recordings. In our work, we considered an immobile period to be an absence of activity detection in a 4 minute period. While this is most likely indicative of sleep, a lack of recorded activity could also occur with quiet awake activities such as grooming (unpublished observation, data not shown). Likewise, our activity outcome

has a large dynamic range as it summates the total activity over a given period of time. It is possible that a hyperactive mouse with no sleep deficits could result in significantly increased activity over the course of a few hours, leading to the erroneous conclusion that the mouse spent less time asleep. Here, we considered both activity and immobility as primary outcomes, as the binary nature of our immobility measurements lessens the possibility of these sorts of artifacts. Finally, sleep stages cannot be determined by motion detection, whereas EEG recordings in mice can distinguish up to 3 stages: slow wave sleep (SWS), rapid eye movement sleep (REM) and wakefulness (172). In order to better refine our determination of sleep states, our future work will require the use of EEG analysis.

Electrically, an extended period of wakefulness is associated with an increase in the low frequency component in the EEG signal of SWS (0.5-4 Hz range, termed slow-wave activity or SWA (183)). The increase in SWA is paralleled by an increase in adenosine in specific areas of the brain (163,164) which is thought to promote sleep by inhibiting wake-active neurons (184,185). Thus, the deficits observed in *Panx1*$^{-/-}$ mice may be related to altered SWA resulting from an absence of Panx1-mediated ATP efflux; a crucial test of this hypothesis will be to assess whether *Panx1*$^{-/-}$ mice fail to demonstrate the wake-related increase in adenosine.

Interestingly, most experimental manipulations that affect SWA such as deleting adenosine receptors from mice (186) or mice expressing a

dnSNARE construct in astrocytes (170) do not alter normal sleep; rather the significant differences are only observed after sleep deprivation. To date, our data challenges this status quo as we observed alterations in both the normal sleep-wake cycle and after sleep deprivation. ATP is generally thought to control sleep via its degradation to adenosine (166), however there may also be direct effects of ATP via activation of P2Y receptors (167). Because Panx1 promotes up-stream ATP efflux, Panx1 could have a broader contribution to sleep-wake homeostasis as compared to specific adenosine transporters. In addition, Panx1 can promote ATP release in neurons, glia and microglia (171,187), so perhaps this widespread expression of Panx1 confers a more extensive function in both sleep-wake homeostasis as well as in sleep deprivation recovery. More experiments, and in particular EEG recordings, will be vital to understand this question further.

Normal sleep in mice shares many components of human sleep, including an early prominence of SWS after the initiation of sleep and REM cycles occurring later in the night (or mostly in the daytime for mice) (172,188). In humans, sleep characteristics and the response to sleep deprivation vary widely, with a subsets of people who are resistant to the loss of performance associated with sleep deprivation (189) or have a "natural" shortened sleep duration (190). It would be interesting to test whether Panx1 expression or function in humans is related to these variations from average sleep characteristics.

Despite the limitations of this early work, these data represent tantalizing preliminary evidence for a role of Panx1 in normal sleep and sleep deprivation, and necessitate follow-up by future students.

CHAPTER 5
Conclusions and future work

In this dissertation, I have presented three novel sets of results regarding Panx1 channels. Although each is very different in content, they are related with respect to this compelling channel. Rather than reiterating the conclusions and discussions from the previous chapters, this last chapter will expand on ideas from each of the topics covered in this dissertation. Most importantly, it will critically examine some of the key assumptions that we have made and from these assumptions, propose several lines of future work.

5.1 S-nitrosylation, or something else?

At the time of publication, we did our best to ensure that all the proper controls and considerations were made in our paper on S-nitrosylation of Panx1 channels. However, there are two additional points that should have received more thought. These ideas warrant future consideration from anyone wishing to follow-up on our results.

The first issue involves a potential glutathionylation effect of GSNO compounds (191,192), which we did consider to some extent during preparation of the manuscript. As mentioned in Chapter 2, while GSNO is typically thought modify cysteine residues by S-nitrosylation, the compound is also capable of causing S-glutathionylation and this modification would also

yield a positive signal by the biotin switch assay (just like S-nitrosylation). These glutathionylation modifications are less well-known than nitrosylation events, but are also of biological importance in the context of redox stress. In addition, this modification does occur on other ion channels such as Kir1.6 (193,194), CFTR (195) and Cav1.2 (196), and induces functional changes in these channels as well.

Essentially, the modification consists of the addition of glutathione to the cysteine residue and will occur readily under oxidized condition (191,192). With respect to the GSNO compound specifically, it can decompose spontaneously into these species: GSH (reduced glutathione), GSSG (oxidized glutathione), and NO^+. Thus, it can facilitate either of the following reactions:

(1) S-nitrosylation: Protein-SH + NO^+ → Protein-S-NO

(2) S-glutathionylation: Protein-SH + GSSG → Protein-S-SG

In our studies, we accounted for this potential outcome by first using two different NO donors (GSNO and DEA NONOate) of which only GSNO can induce S-glutathionylation, and second, by incubating cells with extracellular GSH under oxidative conditions (i.e., with 100 μM H_2O_2 which induces S-glutationylation by producing GSSG). While DEA NONOate generated a signal in the biotin switch assay (Figure 2.2A) and inhibited Panx1-mediated ATP release (Figure 2.3D), the patch clamping results with the DEA NONOate were much less consistent than after GSNO application (see Results, page

41, Figure 2.4). In addition, GSH may not be membrane permeable (197), thus applying the compound extracellularly was not a stringent approach to ensure that the generated GSSG could have access to the intracellular cysteines of Panx1. In hindsight, the GSH should have been included in the patch pipette, and these experiments should have also been conducted on one of the channels mentioned above that are known to be glutathionylated as a positive control.

Thus, the results from our chosen approaches cannot completely rule out the possibility of glutathionylation as a functional modification of Panx1. But rather than negating the results of the study, this novel post-translational modification could be very exciting in addition to the effect of S-nitrosylation. Because this modification is implicated in counter-regulatory processes under oxidative conditions (191,192), glutathionylation and subsequent inhibition of Panx1 channels could represent a powerful protective reaction by a cell to stress. Whether this process does indeed inhibit Panx1 channels has yet to be determined.

Another important consideration with respect to the results of this study is the IV characteristics of various Panx1 mutant constructs which were not reported in the original publication. While the current density near the resting membrane potential in these constructs was identical (Figure 2.7), the two channels that were resistant to inhibition by S-nitrosylation (C40A and C346A) also had IV curves with more pronounced outward rectification

(Figure 5.1A). As in any mutagenesis study, it is difficult to know if the mutation somehow changed the channel in an unintended manner such that it could not be regulated independent of that cysteine moiety. However, it is important to note that S-nitrosylation inhibited the channel over the entire voltage range of the wild-type channel (including near the resting membrane potential), and the abnormal IV characteristics are marginalized when the IV curves are presented as I/I_{max} (Figure 5.1B). In addition, the mutant channels did respond normally to the Panx1 inhibitor CBX, suggesting that at least whatever aspects of the channel that are required for drug-mediated closure were still intact.

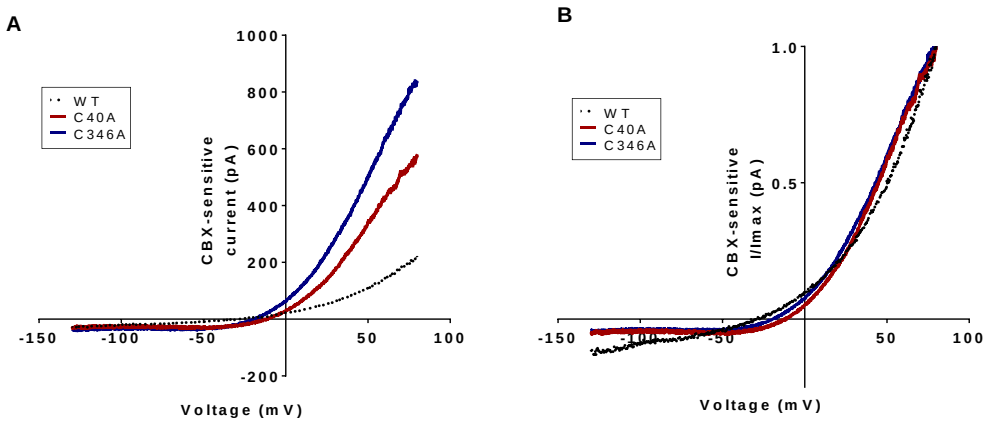

Figure 5.1 IV characteristics of WT Panx1 and two cysteine mutants.

(A) Example IV curves with respect to whole (unnormalized) currents. (B) Example IV curves with the y values normalized to the maximum current of each construct.

Nonetheless, additional work could be done to more definitively address this issue. S-nitrosylation, like other post-translational modifications, has a characteristic consensus sequence that spans several amino acids before and after the key cysteine residue (198). Thus, we hypothesized that mutations to this sequence which leave the cysteine intact may avert the problematic IVs observed in our initial mutant constructs. Under the guidance of Daniel Schwartz from the University of Connecticut, we identified the crucial consensus sequence around these cysteines, as well as the most likely substitutions that would disrupt S-nitrosylation while maintaining the presence of the cysteine residue. I generated two of these mutant constructs by site-directed mutagenesis (V38M and I41R) and these constructs had "normal" Panx1 whole-cell currents, however further analysis with these constructs has not been done in order to pursue other topics.

Lastly, a second group has published on nitric oxide modulation of Panx1 currents since the time of our original publication. However, this other work (as well as several others from this particular lab group) suffers from a non-conventional definition of Panx1 currents and recording conditions, and a lack of appropriate controls (199). The group did find reproducible inhibition of Panx1 currents in heterologous expression systems although they concluded that the mechanism of inhibition was via cGMP and phosphorylation of the channel. Further work in cell types with endogenous channel expression may help to provide clarification for this complex phenomenon and its mechanism of action.

5.2 Some loose ends from the pain project

There are three main topics which require additional discussion with respect to the pain project: the question of which Panx1-expressing cell type is involved, limitations associated with irradiation-replacement experiments (as well as viral reconstitutions), and the role of inflammation in recovery from injury.

A fundamental question regarding the pain project was which Panx1-expressing cell type promotes the development of pain. This question is crucial because it can be informative with respect to understanding the overall mechanism of Panx1 in the context of neuropathic pain, and perhaps in other situations as well. One of the first tasks that we initiated when I started in the lab was the development of cell-specific knockout mice in order to address this question. Five years and 5 novel mouse lines later, we still have not found a cell specific knockout mouse that reproduces the findings observed in the global knockout line.

There are a few possible explanations as to these results discussed in Chapter 3. First, there may be more than one cell type responsible for this phenotype, or we may simply have not yet tested the critical cell type. Second, a low-level of residual expression may be sufficient to compensate for the full channel function. And finally, in the absence of Panx1 in one cell type, another cell type with overlapping functions may make up for the deficiency.

To ascertain the best future approach, one has to consider the anticipated advancement in knowledge against the relative cost of pursuing these cell-specific knockout experiments. Does knowing the cell type preclude future drug development targeting Panx1 in neuropathic pain? Are we unable to define a mechanism for Panx1 without knowing the cell type? What is the likelihood that we would guess correctly with the next cell-specific knockout line, and how would our predictions change in consideration of dual cell knockout lines (e.g., a macrophage and T cell knockout)? Each of these questions suggests answers that steer away from further work on the cell type of interest. Specifically, we can understand the mechanism of Panx1 in pain by assaying overall features of the pathology (rather than cell-specific ones) and drug development can proceed with only the basic knowledge of whether the target is peripheral or hidden behind the blood-brain-barrier. In addition, there is no preliminary evidence or hint of any "next best" cell type at this time, therefore the construction of additional cell-specific knockout lines would be based entirely on instinct. Due to these facts, I can only conclude that we have made an adequate attempt to address the cell type question, but that the additional costs of more experiments in this regard cannot be justified by the potential knowledge to be gained from them.

One other aspect of this project that could use additional attention is the identification of the Panx1 activation mechanism in hematopoietic cells. Our results from irradiation-replacement experiments and viral reconstitutions strongly implicate a mechanism of opening channel that

depends on tyrosine 198 in the intracellular loop of the channel. While potentially powerful, our viral irradiation-replacement approaches have several intrinsic limitations that could be addressed using mouse lines that are already under construction by our collaborators for other purposes. The limitations specific to bone marrow transplantations include potential disruption of the blood-brain-barrier (200), development of graft-versus-host disease (201) and the requirement of using older mice in the final analysis (as the wait period for full reconstitution occurs over several weeks to months). In addition, viral reconstitution experiments have the added possibility of generating highly variable infection rates (see Figure 3.9) and, because they rely on retroviral vectors, have the potential to cause malignancy by aberrant integration into the host genome. While we are confident in our results because the included controls had the expected outcomes (e.g., pain development in the *Panx1*$^{+/+}$ to *Panx1*$^{+/+}$ bone marrow transfer, no pain with *Panx1*$^{-/-}$ to *Panx1*$^{-/-}$ mice, and no pain in the empty vector infected cells), additional experiments to confirm these findings would still be useful.

Luckily, ongoing work with our collaborators could facilitate the appropriate follow-up studies. Specifically, there are several lines of Cre-dependent knockin mice containing various mutant forms (or the wild-type form) of Panx1 that are currently under development. As these mice will not be subjected to the additional factors involved in bone marrow transplants and viral-mediated reconstitutions, they will be useful in confirming our

findings with a method free from our original limitations. In addition, the Cre-dependence of the mouse lines could also facilitate expression of mutant Panx1 in specific cell populations, which may be another method of addressing the earlier question regarding cell types.

Finally, if Panx1 inhibitors are indeed intended to become clinical drug targets, an additional question is how Panx1 affects inflammation, and if this could interfere with crucial healing processes after nerve injury. This could be particularly important with respect to other causes of neuropathic pain like metabolic insults, as the damage and subsequent healing process could be ongoing for years. To ascertain whether blocking Panx1 slows recovery from nerve injury, the best approach would be a more stringent mouse model of nerve injury such as sciatic nerve transection or crush injury and to conduct these models in our *Panx1*$^{-/-}$ mice and wild-type littermates (202-204). These operations would be easy to adapt from our current surgical techniques and assessment of recovery could include motor function, axon counting or recordings of evoked muscle action potentials. To me, these experiments on nerve regeneration after Panx1 inhibition are perhaps the most important for the potential translation of our findings into the clinic – if Panx1 inhibitors prevent healing, then the use of these inhibitors would need to be limited to allow patients to recover. This knowledge would be vital for clinicians to appropriately treat patients.

5.3 The sleep to-do list

While suggestive of a new, exciting role for pannexin channels, the sleep project is incomplete without EEG evidence. In addition to EEG analysis, there could be several other ongoing experiments related to this project.

5.3.1 Suggested task #1: Expression analysis

Although previous work has shown that Panx1 is expressed in the basal forebrain (64), the type of neurons or cells expressing Panx1 was not examined in this region. The subclass of neurons (cholinergic, excitatory, inhibitory, etc) as well as whether the channel is expressed in non-neuronal cells in this region (astrocytes, microglia) could be highly informative in the context of sleep. Ideally, this analysis would be performed using immunohistochemistry. The antibodies for Panx1, however, are notoriously inconsistent in immunohistochemistry experiments (34) and this may be further complicated by a downregulation of the channel within the brain after birth (205). Our lab has tried to reproduce basic immunohistochemical findings published by others in mouse brains with no success. We do have an RNAscope® probe designed for Panx1 in the laboratory and this tool may work well. It should be noted that this probe results in signal in the global knockout mouse, likely due to expression of the transcript distal to the floxed exon 3 and not necessarily a defect with the probe.

5.3.2 Suggested task #2: Adenosine accumulation

As noted above, specific regions of the brain accumulate adenosine in response to increasing durations of wakefulness (163,164). Given the ability of Panx1 to promote ATP efflux, we hypothesize that this adenosine accumulation would be lessened in Panx1 global knockout mice. Classically, groups identified adenosine accumulation using two tools: quantification by microdialysis (163,164) or by measuring the functional effects of adenosine blockers during patch clamp recordings of single cells (206). To date, our lab does not have any collaborators who are experts in microdialysis and it is my understanding that these are not simple experiments. Instead, we attempted to measure ATP in mouse brain slices using cyclic voltammetry with the help of collaborators at the University of Virginia; this was not successful largely due to challenges with personnel. We also attempted to derive a functional effect of adenosine antagonists by patch clamping cholinergic basal forebrain neurons (and thus, indirectly measuring adenosine accumulation and basal adenosine tone). While this was possible in patch clamping experiments using an interface chamber (206), we were unable to reproduce these results with our submersion-based recording chambers despite extensive attempts with various adenosine antagonist dosages, stop-flow recordings, ambient temperatures and sleep deprivation periods (of the mice prior to decapitation). It is possible that there was just simply too much liquid in the chamber that diluted out any local adenosine, so one future approach would be to set up an interface chamber and try these recordings again. Another

complicating factor in these recordings is the heterogeneity of neurons in the basal forebrain (207,208). We sought to mitigate this issue by using cholinergic reporter mice (mice that expressed mTomato downstream of choline acetyltransferase), however further subdivision of basal forebrain cholinergic neurons may be useful. With this approach, we did observe an average increase of 1.39 mV (± a s.e.m. of 0.56 mV, n=5 cells) after application of 2 μM of the A1 receptor antagonist 8-cyclopentyltheophylline. Given the spontaneous fluctuations in the membrane potential of these cells, this small change was not robust enough to convince us to continue with this method.

A more sophisticated approach would be to use an ATP fluorescent probe trafficked to the extracellular surface of cells, which could be expressed via viral vector injected into the brain of mice and subsequently imaged in awake mice. A plasma-membrane targeted luciferase has been described (209) and used *in vivo* (210); whether this sort of technique can be translated to the brain as well has yet to be determined.

5.3.3 Suggested task #3: EEG recordings

As discussed, EEG findings will be critical to connect the phenotype we observed in *Panx1*$^{-/-}$ mice to sleep. The central comparison is *Panx1*$^{-/-}$ versus wild-type littermates and this should be the initial experiment. The difficulty of these experiments is the sheer quantity of data required and subsequently

the time it will take to score the EEG recordings. Baselines alone will be 24 hours of data, and after recovery from sleep deprivation there will be another 18 hours to analyze. In our experience so far, scoring these sleep segments with the help of MATLAB® software took an equal time for each mouse as it took to originally collect it (and sometimes longer was needed for scoring depending on the quality of the recording).

There are a few strategies to help streamline this project. First, the above two tasks can be conducted simultaneously as the EEG recordings. Second, any additional comparisons can be tested in our motion detection system before committing to a full EEG analysis. For example, we currently have four relevant conditional knockout lines described in Chapter 3 – a macrophage/microglia knockout (crossed with a CX3CR1-cre), a T lymophocyte knockout (crossed with a CD4-cre), a glia knockout (crossed with a GFAP-cre) and a neuronal knockout (crossed with a Synapsin-cre). Instead of testing all those lines by EEG, they can first be screened on the motion detection system, and then the two most relevant mouse lines can continue on to EEG analysis. Even with streamlining this project, the EEG analysis will still be a major challenge, but the rewards of new knowledge relevant to sleep and sleep deprivation would be worthwhile.

5.4 Final thoughts

This dissertation has outlined several novel findings regarding Panx1. First, we identified S-nitrosylation as an inhibitory mechanism of Panx1 channels, and further defined the amino acid targets for this reversible post-translational modification. Next, we found that Panx1 promotes neuropathic pain development through its expression in hematopoietic cells and that systemic inhibition of the channel may be a viable therapeutic option for this otherwise intractable condition. In addition, pain development depended on the presence of tyrosine 198 in Panx1, a residue that has been implicated in G-protein mediated activation of the channel. Finally, I revealed a new physiological role for Panx1 in the initiation of sleep and in the recovery from sleep deprivation.

While these findings alone are of great significance, this work further suggests other exciting directions that were highlighted above. Specifically, is Panx1 subjected to modulation by glutathionylation? Does inhibiting Panx1 cause a harmful delay in the healing process? And do EEG analyses confirm our hypothesis on the role of Panx1 in sleep? These experiments are varied in nature, will push the technical limits of our laboratory, and could be a solid start to the next graduate dissertation project.

APPENDIX A: LIST OF PUBLICATIONS

The following is a comprehensive list of published projects (or prepared manuscripts) that I had the opportunity to contribute to while enrolled as a graduate student:

1. Weaver, J.L, Brown, G., Arandjelovic, S., Schappe, M., Mendu, S., Buckley, M.W., Chiu, Y.H., Shu, S., Kim, J.K., Chung, J., Jevtovic-Todorovic, V., Desai, B.N., Ravichandran, K.S., Bayliss, D.A. (2016). Hematopoietic pannexin 1 expression critically influences neuropathic pain. Manuscript in preparation.

2. Shi, Y., Abe, C., Holloway, B.B., Shu, S., Kumar, N.N., Weaver, J.L., Sen, J., Perez-Reyes, E., Stornetta, R., Guyenet, P.G., Bayliss, D.A (2016). NALCN is a "leak" sodium channel in retrotrapezoid nucleus that regulates neuronal excitability and breathing". Manuscript in preparation.

3. Obradovic, A.L., Scarpa, J., Osuru, H.P., Weaver, J.L., Park, J.Y., Pathiranthna, S., Peterkin, A., Lim, Y.H., Jagodic, M.M., Todorovic, S.M., & Jevtovic- Todorovic, V. (2015). Silencing the α2 subunit of GABAA receptors in rat dorsal root ganglia reveals its major role in antinociception post-traumatic nerve injury. Anesthesiology 123(3): 654-667. [PMID: 26164299]

4. Kumar, N.N., Velic, A., Soliz, J., Shi, Y., Li, K., Wang, S., Weaver, J.L., Sen, J., Abbott, S.B.G., Lazarenko, R.M., Ludwig, M., Perez-Reyes, E., Mohebbi, N., Bettoni, C., Gassmann, M., Suply, T., Seuwen, K., Guyenet,

P.G., Wagner, C.A., Bayliss, D.A. (2015). Regulation of breathing by CO2 requires the proton-activated receptor GPR4 in retrotrapezoid nucleus neurons. Science 348(6240): 1255-1260. [PMID: 26068853]

5. Morenilla-Palao, C., Luis, E., Fenandez-Pena, C., Quintero, E., Weaver, J.L., Bayliss, D.A., Viana, F. (2104). Ion channel profile of TRPM8 cold receptors reveals a novel role of TASK-3 potassium channels in thermosensation. Cell Reports 8(5):1571-1582. [PMID: 25199828]

6. Kenwood, BM., Weaver, J.L., Bajwa, A., Byrne, F.L., Murrow, B.A., Poon, I.K., Huang, L., Coleman, G., Saucerman, J., Santos, W.L., Lynch, K.R., Rogers, G.W., Ravichandran, K.S., Okusa, M.D., Bayliss, D.A., Hoehn, K.L. (2014). A novel mitochondria-selective protonophore uncoupler with a broad effective range. Molecular Metabolism 3(2): 114-123. [PMID: 24634817]

7. Lohman, A.W.*, Weaver, J.L.*, Billaud, M., Sandilos, J.K., Griffiths, R., Straub, A.C., Penuela, S., Leitinger, N., Laird, D.W., Bayliss, D.A., Isakson, B.E. (2012). S-nitrosylation inhibits pannexin 1 channel function. Journal of Biological Chemistry 287(27): 39602-12. [PMID: 24634817]

8. Naik, A.K.*, Latham, J.R.*, Obradovic, A., Jevtovic-Todorivic, V. (2011). Dorsal root ganglion application of muscimol prevents hyperalgesia and stimulates myelin protein expression following sciatic nerve injury in rats. Anesthesia and Analgesia 114(3): 674-82. [PMID: 22190549]

APPENDIX B: REFERENCES

1. Panchina Y, Kelmanson I, Matz M, Lukyanov K, Usman N, Lukyanov S. A ubiquitous family of putative gap junction molecules. *Curr Biol*. 2000;10(13):R473-R474.

2. Bruzzone R, Hormuzdi SG, Barbe MT, Herb A, Monyer H. Pannexins, a family of gap junction proteins expressed in brain. *Proc Natl Acad Sci U S A*. 2003;100(23):13644-13649.

3. Baranova A, Ivanov D, Petrash N, et al. The mammalian pannexin family is homologous to the invertebrate innexin gap junction proteins. *Genomics*. 2004;83(4):706-716.

4. Sosinsky GE, Boassa D, Dermietzel R, et al. Pannexin channels are not gap junciton hemichannels. *Channels (Austin)*. 2011;5(3):193-197.

5. Sahu G, Sukumaran S, Bera AK. Pannexins form gap junctions with electrophysiological and pharmacological properties distinct from connexins. *Sci Rep*. 2014;4:4955.

6. Penuela S, Bhalla R, Gong X, et al. Pannexin 1 and pannexin 3 are glycoproteins that exhibit many distinct characteristics from the connexin family of gap junction proteins. *J Cell Sci*. 2007;120(21):3772-3783.

7. Wang J, Ma M, Locovei S, Keane RW, Dahl G. Modulation of membrane channel currents by gap junction protein mimetic peptides: Size matters. *Am J Physiol Cell Physiol*. 2007;293(3):C1112-9.

8. Locovei S, Scemes E, Qiu F, Spray DC, Dahl G. Pannexin1 is part of the pore forming unit of the P2X7 receptor death complex. *FEBS Lett*. 2007;581(3):483-488.

9. Chekeni FB, Elliott MR, Sandilos JK, et al. Pannexin 1 channels mediate 'find-me' signal release and membrane permeability during apoptosis. *Nature*. 2010;467(7317):863-867.

10. Bao L, Locovei S, Dahl G. Pannexin membrane channels are mechanosensitive conduits for ATP. *FEBS Lett*. 2004;572(1-3):65-68.

11. Ma W, Compan V, Zheng W, et al. Pannexin 1 forms an anion-selective channel. *Pflugers Arch*. 2012;463(4):585-592.

12. Wang J, Ambrosi C, Qiu F, Jackson DG, Sosinsky G, Dahl G. The membrane protein Pannexin1 forms two open-channel conformations depending on the mode of activation. *Sci Signal*. 2014;7(335):ra69.

13. Chiu YH, Ravichandran KS, Bayliss DA. Intrinsic properties and regulation of pannexin 1 channel. *Channels (Austin)*. 2014;8(2):103-109.

14. Ma W, Hui H, Pelegrin P, Surprenant A. Pharmacological characterization of pannexin-1 currents expressed in mammalian cells. *J Pharmacol Exp Ther*. 2009;328(2):409-418.

15. Romanov RA, Bystrova MF, Rogachevskaya OA, Sadovnikov VB, Shestopalov VI, Kolesnikov SS. The ATP permeability of pannexin 1 channels in a heterologous system and in mammalian taste cells is dispensable. *J Cell Sci*. 2012;125(Pt 22):5514-5523.

16. Ambrosi C, Gassmann O, Pranskevich JN, et al. Pannexin1 and Pannexin2 channels show quaternary similarities to connexons and different oligomerization numbers from each other. *J Biol Chem*. 2010;285(32):24420-24431.

17. Wang J, Dahl G. SCAM analysis of Panx1 suggests a peculiar pore structure. *J Gen Physiol*. 2010;136(5):515-527.

18. Sandilos JK, Chiu Y, Chekeni FB, et al. Pannexin 1, an ATP release channel, is activated by caspase cleavage of its pore-associated C-terminal autoinhibitory region. *J Biol Chem*. 2012;287(14):11303-11311.

19. Dahl G, Qiu F, Wang J. The bizarre pharmacology of the ATP release channel pannexin1. *Neuropharmacology*. 2013;75:583-593.

20. Bruzzone R, Barbe MT, Jakob NJ, Monyer H. Pharmacological properties of homomeric and heteromeric pannexin hemichannels expressed in xenopus oocytes. *J Neurochem*. 2005;92(5):1033-1043.

21. Connors BW. Tales of a dirty drug: Carbenoxolone, gap junctions, and seizures. *Epilepsy Curr*. 2012;12(2):66-68.

22. Sigma Aldrich. Carbenoxolone disodium salt (C4790) - product information sheet. In: Saint Louis, Missouri, USA; 2003.

23. Silverman W, Locovei S, Dahl G. Probenecid, a gout remedy, inhibits pannexin 1 channels. *Am J of Physiol Cell Physiol*. 2008;295(3):C761-C767.

24. Sigma Aldrich. Probenecid (P8761) - product information sheet. In: Saint Louis, Missouri, USA; 2002.

25. Poon IKH, Chiu Y, Armstrong AJ, et al. Unexpected link between an antibiotic, pannexin channels and apoptosis. *Nature*. 2014;507(7492):329-334.

26. Paris MM, Hickey SM, Trujillo M, Shelton S, McCracken GH,Jr. Evaluation of CP-99,219, a new fluoroquinolone, for treatment of experimental penicillin- and cephalosporin-resistant pneumococcal meningitis. *Antimicrob Agents Chemother*. 1995;39(6):1243-1246.

27. Tocris. Product information trovafloxacin mesylate. In: Denver, Colorado, USA; 2016.

28. Dahl G. Gap Junction–Mimetic peptides do work, but in unexpected ways. *Cell Commun Adhes*. 2007;14(6):259-264.

29. Bhalla-Gehi R, Penuela S, Churko JM, Shao Q, Laird DW. Pannexin1 and pannexin3 delivery, cell surface dynamics, and cytoskeletal interactions. *J Biol Chem*. 2010;285(12):9147-9160.

30. Locovei S, Bao L, Dahl G. Pannexin 1 in erythrocytes: Function without a gap. *Proc Natl Acad Sci U S A*. 2006;103(20):7655-7659.

31. Penuela S, Bhalla R, Nag K, Laird DW. Glycosylation regulates pannexin intermixing and cellular localization. *Mol Biol Cell*. 2009;20(20):4313-4323.

32. Vanden Abeele F, Bidaux G, Gordienko D, et al. Functional implications of calcium permeability of the channel formed by pannexin 1. *J Cell Biol*. 2006;174(4):535-546.

33. Penuela S, Celetti SJ, Bhalla R, Shao Q, Laird DW. Diverse subcellular distribution profiles of pannexin 1 and pannexin 3. *Cell Commun Adhes*. 2008;15(1):133-142.

34. Cone AC, Ambrosi C, Scemes E, Martone ME, Sosinsky GE. A comparative antibody analysis of Pannexin1 expression in four rat brain regions reveals varying subcellular localizations. *Front Pharmacol*. 2013;4:6.

35. Lohman AW, Weaver JL, Billaud M, et al. S-nitrosylation inhibits pannexin 1 channel function. *J Biol Chem*. 2012;287(47):39602-39612.

36. Sandilos JK, Bayliss DA. Physiological mechanisms for the modulation of pannexin 1 channel activity. *J Physiol (Lond)*. 2012;590(24):6257-6266.

37. Penuela S, Harland L, Simek J, Laird DW. Pannexin channels and their links to human disease. *Biochem J*. 2014;461(3):371-381.

38. Burnstock G. Purinergic mechanisms and pain—An update. *Eur J Pharmacol*. 2013;716(1–3):24-40.

39. Alves LA, de Melo Reis RA, de Souza CAM, et al. The P2X7 receptor: Shifting from a low- to a high-conductance channel — an enigmatic phenomenon? *Biochim Biophys Acta*. 2014;1838(10):2578-2587.

40. Pelegrin P, Surprenant A. Pannexin-1 mediates large pore formation and interleukin-1beta release by the ATP-gated P2X7 receptor. *EMBO J*. 2006;25(21):5071-5082.

41. Sorge RE, Trang T, Dorfman R, et al. Genetically determined P2X7 receptor pore formation regulates variability in chronic pain sensitivity. *Nat Med*. 2012;18(4):595-599.

42. Iglesias R, Locovei S, Roque A, et al. P2X(7) receptor-Pannexin1 complex: Pharmacology and signaling. *Am J of Physiol Cell Physiol*. 2008;295(3):C752-C760.

43. Poornima V, Madhupriya M, Kootar S, Sujatha G, Kumar A, Bera AK. P2X7 receptor-pannexin 1 hemichannel association: Effect of extracellular calcium on membrane permeabilization. *J Mol Neurosci*. 2012;46(3):585-594.

44. Yan Z, Li S, Liang Z, Tomic M, Stojilkovic SS. The P2X7 receptor channel pore dilates under physiological ion conditions. *J Gen Physiol*. 2008;132(5):563-573.

45. Browne LE, Compan V, Bragg L, North RA. P2X7 receptor channels allow direct permeation of nanometer-sized dyes. *J Neuroscience.* 2013;33(8):3557-3566.

46. Cankurtaran-Sayar S, Sayar K, Ugur M. P2X7 receptor activates multiple selective dye-permeation pathways in RAW 264.7 and human embryonic kidney 293 cells. *Mol Pharmacol*. 2009;76(6):1323-1332.

47. Schachter J, Motta AP, de SZ, da Silva-Souza HA, Guimar├úes M,Zaluar P., Persechini PM. ATP-induced P2X7-associated uptake of large molecules involves distinct mechanisms for cations and anions in macrophages. *J Cell Sci*. 2008;121(19):3261-3270.

48. Adriouch S, Dox C, Welge V, Seman M, Koch-Nolte F, Haag F. Cutting edge: A natural P451L mutation in the cytoplasmic domain impairs the function of the mouse P2X7 receptor. *J Immunol*. 2002;169(8):4108-4112.

49. Stokes L, Fuller SJ, Sluyter R, Skarratt KK, Gu BJ, Wiley JS. Two haplotypes of the P2X(7) receptor containing the ala-348 to thr polymorphism exhibit a gain-of-function effect and enhanced interleukin-1beta secretion. *FASEB J*. 2010;24(8):2916-2927.

50. Xu XJ, Boumechache M, Robinson LE, et al. Splice variants of the P2X7 receptor reveal differential agonist dependence and functional coupling with pannexin-1. *J Cell Sci*. 2012;125(16):3776-3789.

51. Cheewatrakoolpong B, Gilchrest H, Anthes JC, Greenfeder S. Identification and characterization of splice variants of the human P2X7 ATP channel. *Biochem Biophys Res Commun*. 2005;332(1):17-27.

52. Billaud M, Chiu Y, Lohman AW, et al. A molecular signature in the pannexin1 intracellular loop confers channel activation by the α1 adrenoreceptor in smooth muscle cells. *Sci Signal*. 2015;8(364):ra17-ra17.

53. Pinheiro AR, Paramos-de-Carvalho D, Certal M, et al. Histamine induces ATP release from human subcutaneous fibroblasts, via pannexin-1 hemichannels, leading to Ca2+ mobilization and cell proliferation. *J Biol Chem*. 2013;288(38):27571-27583.

54. Godecke S, Roderigo C, Rose CR, Rauch BH, Godecke A, Schrader J. Thrombin-induced ATP release from human umbilical vein endothelial cells. *Am J Physiol Cell Physiol*. 2012;302(6):C915-23.

55. da Silva-Souza HA, de Lira MN, Patel NK, Spray DC, Persechini PM, Scemes E. Inhibitors of the 5-lipoxygenase pathway activate pannexin1 channels in macrophages via the thromboxane receptor. *Am J Physiol Cell Physiol*. 2014;307(6):C571-C579.

56. Timóteo MA, Carneiro I, Silva I, et al. ATP released via pannexin-1 hemichannels mediates bladder overactivity triggered by urothelial P2Y6 receptors. *Biochem Pharmacol*. 2014;87(2):371-379.

57. Sato M, Furuya T, Kimura M, et al. Intercellular odontoblast communication via ATP mediated by pannexin-1 channel and phospholipase C-coupled receptor activation. *Front Physiol*. 2015;6:326.

58. Seminario-Vidal L, Kreda S, Jones L, et al. Thrombin promotes release of ATP from lung epithelial cells through coordinated activation of rho- and

Ca2+-dependent signaling pathways. *J Biol Chem*. 2009;284(31):20638-20648.

59. Johnstone SR, Billaud M, Lohman AW, Taddeo EP, Isakson BE. Posttranslational modifications in connexins and pannexins. *J Membr Biol*. 2012;245(5):319-332.

60. Bunse S, Schmidt M, Prochnow N, Zoidl G, Dermietzel R. Intracellular cysteine 346 is essentially involved in regulating Panx1 channel activity. *J Biol Chem*. 2010;285(49):38444-38452.

61. Weilinger NL, Tang PL, Thompson RJ. Anoxia-induced NMDA receptor activation opens pannexin channels via src family kinases. *J Neurosci*. 2012;32(36):12579-12588.

62. Weilinger NL, Lohman AW, Rakai BD, et al. Metabotropic NMDA receptor signaling couples src family kinases to pannexin-1 during excitotoxicity. *Nat Neurosci*. 2016;advance online publication.

63. Lohman AW, Leskov IL, Butcher JT, et al. Pannexin 1 channels regulate leukocyte emigration through the venous endothelium during acute inflammation. *Nat Commun*. 2015;6:7965.

64. Ray A, Zoidl G, Weickert S, Wahle P, Dermietzel R. Site-specific and developmental expression of pannexin1 in the mouse nervous system. *Eur J Neurosci*. 2005;21(12):3277-3290.

65. Penuela S, Gehi R, Laird DW. The biochemistry and function of pannexin channels. *Biochim Biophys Acta*. 2013;1828(1):15-22.

66. Billaud M, Lohman AW, Straub AC, et al. Pannexin1 regulates α1-adrenergic receptor- mediated vasoconstriction. *Circ Res*. 2011;109(1):80-85.

67. Ardiles AO, Flores-Munoz C, Toro-Ayala G, et al. Pannexin 1 regulates bidirectional hippocampal synaptic plasticity in adult mice. *Front Cell Neurosci*. 2014;8.

68. Prochnow N, Abdulazim A, Kurtenbach S, et al. Pannexin1 stabilizes synaptic plasticity and is needed for learning. *PLoS One*. 2012;7(12):e51767.

69. Thompson RJ, Zhou N, MacVicar BA. Ischemia opens neuronal gap junction hemichannels. *Science*. 2006;312(5775):924-927.

70. Zhang L, Deng T, Sun Y, Liu K, Yang Y, Zheng X. Role for nitric oxide in permeability of hippocampal neuronal hemichannels during oxygen glucose deprivation. *J Neurosci Res*. 2008;86(10):2281-2291.

71. Bargiotas P, Krenz A, Hormuzdi SG, et al. Pannexins in ischemia-induced neurodegeneration. *Proc Natl Acad Sci U S A*. 2011;108(51):20772-20777.

72. Thompson RJ, Jackson MF, Olah ME, et al. Activation of pannexin-1 hemichannels augments aberrant bursting in the hippocampus. *Science*. 2008;322(5907):1555-1559.

73. Kim J, Kang T. The P2X7 receptor-pannexin-1 complex decreases muscarinic acetylcholine receptor-mediated seizure susceptibility in mice. *J Clin Invest*. 2011;121(5):2037-2047.

74. Jiang T, Long H, Ma Y, et al. Altered expression of pannexin proteins in patients with temporal lobe epilepsy. *Mol Med Rep*. 2013;8(6):1801-1806.

75. Zhang M, Piskuric NA, Vollmer C, Nurse CA. P2Y2 receptor activation opens pannexin-1 channels in rat carotid body type II cells: Potential role in amplifying the neurotransmitter ATP. *J Physiol*. 2012;590(17):4335-4350.

76. Gulbransen BD, Bashashati M, Hirota SA, et al. Activation of neuronal P2X7 receptor-pannexin-1 mediates death of enteric neurons during colitis. *Nat Med*. 2012;18(4):600-604.

77. Karatas H, Erdener SE, Gursoy-Ozdemir Y, et al. Spreading depression triggers headache by activating neuronal Panx1 channels. *Science*. 2013;339(6123):1092-1095.

78. Reigada D, Lu W, Zhang M, Mitchell CH. Elevated pressure triggers a physiological release of ATP from the retina: Possible role for pannexin hemichannels. *Neuroscience*. 2008;157(2):396-404.

79. Lutz SE, Gonzalez-Fernandez E, Ventura JC, et al. Contribution of pannexin1 to experimental autoimmune encephalomyelitis. *PLoS One*. 2013;8(6):e66657.

80. Gawlik M, Wagner M, Pfuhlmann B, Stober G. The role of pannexin gene variants in schizophrenia: Systematic analysis of phenotypes. *Eur Arch Psychiatry Clin Neurosci*. 2015.

81. Bravo D, Ibarra P, Retamal J, et al. Pannexin 1: A novel participant in neuropathic pain signaling in the rat spinal cord. *Pain*. 2014;155(10):2108-2115.

82. Zhang Y, Laumet G, Chen SR, Hittelman WN, Pan HL. Pannexin-1 up-regulation in the dorsal root ganglion contributes to neuropathic pain development. *J Biol Chem*. 2015;290(23):14647-14655.

83. Di Cesare Mannelli L, Marcoli M, Micheli L, et al. Oxaliplatin evokes P2X7-dependent glutamate release in the cerebral cortex: A pain mechanism mediated by pannexin 1. *Neuropharmacology*. 2015;97:133-141.

84. Bravo D, Maturana CJ, Pelissier T, Hernandez A, Constandil L. Interactions of pannexin 1 with NMDA and P2X7 receptors in central nervous system pathologies: Possible role on chronic pain. *Pharmacol Res*. 2015;101:86-93.

85. Bourinet E, Altier C, Hildebrand ME, Trang T, Salter MW, Zamponi GW. Calcium-permeable ion channels in pain signaling. *Physiol Rev*. 2014;94(1):81-140.

86. Dworkin RH, O'Connor AB, Audette J, et al. Recommendations for the pharmacological management of neuropathic pain: An overview and literature update. *Mayo Clin Proc*. 2010;85(3, Supplement):S3-S14.

87. Baron R, Binder A, Wasner G. Neuropathic pain: Diagnosis, pathophysiological mechanisms, and treatment. *Lancet Neurol*. 2010;9(8):807-819.

88. Berger A, Dukes EM, Oster G. Clinical characteristics and economic costs of patients with painful neuropathic disorders. *J Pain*. 2004;5(3):143-149.

89. Toth C, Lander J, Wiebe S. The prevalence and impact of chronic pain with neuropathic pain symptoms in the general population. *Pain Med*. 2009;10(5):918-929.

90. Trang T, Al-Hasani R, Salvemini D, Salter MW, Gutstein H, Cahill CM. Pain and poppies: The good, the bad, and the ugly of opioid analgesics. *J Neurosci*. 2015;35(41):13879-13888.

91. Institute of Medicine (US) Committee on Advancing Pain Research, Care, and Education. Relieving pain in america: A blueprint for transforming prevention, care, education, and research. In: Washington (DC): National Academies Press (US); 2011.

92. Ulmann L, Hatcher JP, Hughes JP, et al. Up-regulation of P2X4 receptors in spinal microglia after peripheral nerve injury mediates BDNF release and neuropathic pain. *J Neurosci*. 2008;28(44):11263-11268.

93. Coull JAM, Beggs S, Boudreau D, et al. BDNF from microglia causes the shift in neuronal anion gradient underlying neuropathic pain. *Nature*. 2005;438(7070):1017-1021.

94. Ueno S, Moriyama T, Honda K, Kamiya H, Sakurada T, Katsuragi T. Involvement of P2X2 and P2X3 receptors in neuropathic pain in a mouse model of chronic constriction injury. *Drug Dev Res*. 2003;59(1):104-111.

95. McGaraughty S, Wismer CT, Zhu CZ, et al. Effects of A-317491, a novel and selective P2X3/P2X2/3 receptor antagonist, on neuropathic, inflammatory and chemogenic nociception following intrathecal and intraplantar administration. *Br J Pharmacol*. 2003;140(8):1381-1388.

96. Chessell IP, Hatcher JP, Bountra C, et al. Disruption of the P2X7 purinoceptor gene abolishes chronic inflammatory and neuropathic pain. *Pain*. 2005;114(3):386-396.

97. Tozaki-Saitoh H, Tsuda M, Miyata H, Ueda K, Kohsaka S, Inoue K. P2Y12 receptors in spinal microglia are required for neuropathic pain after peripheral nerve injury. *J Neurosci*. 2008;28(19):4949-4956.

98. Adamson SE, Leitinger N. The role of pannexin1 in the induction and resolution of inflammation. *FEBS Lett*. 2014;588(8):1416-1422.

99. Makarenkova HP, Shestopalov VI. The role of pannexin hemichannels in inflammation and regeneration. *Front Physiol*. 2014;5:63.

100. Bennett MVL, Garré JM, Orellana JA, et al. Connexin and pannexin hemichannels in inflammatory responses of glia and neurons. *Brain Res*. 2012;1487(0):3-15.

101. Qu Y, Misaghi S, Newton K, et al. Pannexin-1 is required for ATP release during apoptosis but not for inflammasome activation. *J Immunol*. 2011;186(11):6553-6561.

102. Bao Y, Chen Y, Ledderose C, Li L, Junger WG. Pannexin 1 channels link chemoattractant receptor signaling to local excitation and global inhibition responses at the front and back of polarized neutrophils. *J Biol Chem*. 2013;288(31):22650-22657.

103. Woehrle T, Yip L, Elkhal A, et al. Pannexin-1 hemichannel–mediated ATP release together with P2X1 and P2X4 receptors regulate T-cell activation at the immune synapse. *Blood*. 2010;116(18):3475-3484.

104. Schenk U, Westendorf AM, Radaelli E, et al. Purinergic control of T cell activation by ATP released through pannexin-1 hemichannels. *Sci Signal*. 2008;1(39):ra6.

105. Ayna G, Krysko DV, Kaczmarek A, Petrovski G, Vandenabeele P, Fesus L. ATP release from dying autophagic cells and their phagocytosis are crucial for inflammasome activation in macrophages. *PLoS One*. 2012;7(6):e40069.

106. Pelegrin P, Barroso-Gutierrez C, Surprenant A. P2X7 receptor differentially couples to distinct release pathways for IL-1beta in mouse macrophage. *J Immunol*. 2008;180(11):7147-7157.

107. Wang H, Xing Y, Mao L, Luo Y, Kang L, Meng G. Pannexin-1 influences peritoneal cavity cell population but is not involved in NLRP3 inflammasome activation. *Protein Cell*. 2013;4(4):259-265.

108. Scholz J, Woolf CJ. The neuropathic pain triad: Neurons, immune cells and glia. *Nat Neurosci*. 2007;10(11):1361-1368.

109. Sorge RE, Mapplebeck JC, Rosen S, et al. Different immune cells mediate mechanical pain hypersensitivity in male and female mice. *Nat Neurosci*. 2015;18(8):1081-1083.

110. Liu T, van Rooijen N, Tracey DJ. Depletion of macrophages reduces axonal degeneration and hyperalgesia following nerve injury. *Pain*. 2000;86(1–2):25-32.

111. Boassa D, Ambrosi C, Qiu F, Dahl G, Gaietta G, Sosinsky G. Pannexin1 channels contain a glycosylation site that targets the hexamer to the plasma membrane. *J Biol Chem*. 2007;282(43):31733-31743.

112. Straub AC, Billaud M, Johnstone SR, et al. Compartmentalized connexin 43 S-Nitrosylation/Denitrosylation regulates heterocellular communication in the vessel wall. *Arterioscler Thromb Vasc Biol*. 2011;31(2):399-407.

113. Sun J, Xin C, Eu JP, Stamler JS, Meissner G. Cysteine-3635 is responsible for skeletal muscle ryanodine receptor modulation by NO. *Proc Natl Acad Sci U S A*. 2001;98(20):11158-11162.

114. Retamal MA, Cort├⌐s CJ, Reuss L, Bennett MVL, S├¡ez JC. S-nitrosylation and permeation through connexin 43 hemichannels in astrocytes: Induction by oxidant stress and reversal by reducing agents. *Proc Natl Acad Sci U S A*. 2006;103(12):4475-4480.

115. Asada K, Kurokawa J, Furukawa T. Redox- and calmodulin-dependent S-nitrosylation of the KCNQ1 channel. *J Biol Chem*. 2009;284(9):6014-6020.

116. Yoshida T, Inoue R, Morii T, et al. Nitric oxide activates TRP channels by cysteine S-nitrosylation. *Nat Chem Biol*. 2006;2(11):596-607.

117. Jaffrey SR, Snyder SH. The biotin switch method for the detection of S-nitrosylated proteins. *Sci STKE*. 2001;2001(86):pl1.

118. Lohman AW, Billaud M, Straub AC, et al. Expression of pannexin isoforms in the systemic murine arterial network. *J Vasc Res*. 2012;49(5):405-416.

119. Schwartz D, Chou MF, Church GM. Predicting protein post-translational modifications using meta-analysis of proteome scale data sets. *Mol Cell Proteomics*. 2009;8(2):365-379.

120. Swayne LA, Sorbara CD, Bennett SAL. Pannexin 2 is expressed by postnatal hippocampal neural progenitors and modulates neuronal commitment. *J Biol Chem*. 2010;285(32):24977-24986.

121. Ray A, Zoidl G, Wahle P, Dermietzel R. Pannexin expression in the cerebellum. *Cerebellum.* 2006;5(3):189-192.

122. Bunse S, Schmidt M, Hoffmann S, Engelhardt K, Zoidl G, Dermietzel R. Single cysteines in the extracellular and transmembrane regions modulate pannexin 1 channel function. *J Membr Biol*. 2011;244(1):21-33.

123. Sridharan M, Adderley SP, Bowles EA, et al. Pannexin 1 is the conduit for low oxygen tension-induced ATP release from human erythrocytes. *Am J Physiol Heart Circ Physiol*. 2010;299(4):H1146-H1152.

124. Ellsworth ML, Ellis CG, Goldman D, Stephenson AH, Dietrich HH, Sprague RS. Erythrocytes: Oxygen sensors and modulators of vascular tone. *Physiology*. 2009;24(2):107-116.

125. Beggs S, Salter MW. The known knowns of microglia–neuronal signalling in neuropathic pain. *Neurosci Lett*. 2013;557, Part A:37-42.

126. Yona S, Kim K, Wolf Y, et al. Fate mapping reveals origins and dynamics of monocytes and tissue macrophages under homeostasis. *Immunity*. 2013;38(1):79-91.

127. Shields SD, Eckert III WA, Basbaum AI. Spared nerve injury model of neuropathic pain in the mouse: A behavioral and anatomic analysis. *J Pain*. 2003;4(8):465-470.

128. Decosterd I, Woolf CJ. Spared nerve injury: An animal model of persistent peripheral neuropathic pain. *Pain*. 2000;87(2):149-158.

129. Sommer C, Schmidt C, George A, Toyka KV. A metalloprotease-inhibitor reduces pain associated behavior in mice with experimental neuropathy. *Neurosci Lett*. 1997;237(1):45-48.

130. Bennett GJ, Xie Y-. A peripheral mononeuropathy in rat that produces disorders of pain sensation like those seen in man. *Pain*. 1988;33(1):87-107.

131. Chaplan SR, Bach FW, Pogrel JW, Chung JM, Yaksh TL. Quantitative assessment of tactile allodynia in the rat paw. *J Neurosci Methods*. 1994;53(1):55-63.

132. Hargreaves K, Dubner R, Brown F, Flores C, Joris J. A new and sensitive method for measuring thermal nociception in cutaneous hyperalgesia. *Pain*. 1988;32(1):77-88.

133. Latham JR, Pathirathna S, Jagodic MM, et al. Selective T-type calcium channel blockade alleviates hyperalgesia in ob/ob mice. *Diabetes*. 2009;58(11):2656-2665.

134. Pear WS, Miller JP, Xu L, et al. Efficient and rapid induction of a chronic myelogenous leukemia-like myeloproliferative disease in mice receiving P210 bcr/abl-transduced bone marrow. *Blood*. 1998;92(10):3780-3792.

135. Jordan M. Genetic reconstitution of bone marrow for the study of signal transduction ex vivo. In: Ali H, Haribabu B, eds. Vol 332. Humana Press; 2006:331-342.

136. Zhang X, Goncalves R, Mosser DM. The isolation and characterization of murine macrophages. In: *Curr Protoc Immunol.* John Wiley & Sons, Inc.; 2008.

137. Jones SM, Novak AE, Elliott JP. Primary culture of cellular subtypes from postnatal mouse for in vitro studies of oxygen glucose deprivation. *J Neurosci Methods*. 2011;199(2):241-248.

138. Hilgenberg LGW, Smith MA. Preparation of dissociated mouse cortical neuron cultures. *J Vis Exp*. 2007(10):562.

139. Livak KJ, Schmittgen TD. Analysis of relative gene expression data using real-time quantitative PCR and the 2−ΔΔCT method. *Methods*. 2001;25(4):402-408.

140. Kreutzberg GW. Microglia: A sensor for pathological events in the CNS. *Trends Neurosci*. 1996;19(8):312-318.

141. Koltzenburg M. Painful neuropathies. *Curr Opin Neurol*. 1998;11(5):515-521.

142. Woolf CJ, Mannion RJ. Neuropathic pain: Aetiology, symptoms, mechanisms, and management. *Lancet*. 1999;353(9168):1959-1964.

143. Woehrle T, Yip L, Manohar M, et al. Hypertonic stress regulates T cell function via pannexin-1 hemichannels and P2X receptors. *J Leukoc Biol*. 2010;88(6):1181-1189.

144. Clausen BE, Burkhardt C, Reith W, Renkawitz R, Forster I. Conditional gene targeting in macrophages and granulocytes using LysMcre mice. *Transgenic Res*. 1999;8(4):265-277.

145. Ji R, Suter MR. p38 MAPK, microglial signaling, and neuropathic pain. *Molecular Pain*. 2007;3(1):1-9.

146. Scholz J, Broom DC, Youn D, et al. Blocking caspase activity prevents transsynaptic neuronal apoptosis and the loss of inhibition in lamina II of the dorsal horn after peripheral nerve injury. *J Neurosci*. 2005;25(32):7317-7323.

147. Jellinck PH, Monder C, McEwen BS, Sakai RR. Differential inhibition of 11β-hydroxysteroid dehydrogenase by carbenoxolone in rat brain regions and peripheral tissues. *J Steroid Biochem Mol Biol*. 1993;46(2):209-213.

148. Seltzer Z, Paran Y, Eisen A, Ginzburg R. Neuropathic pain behavior in rats depends on the afferent input from nerve-end neuroma including histamine-sensitive C-fibers. *Neurosci Lett*. 1991;128(2):203-206.

149. Barragán-Iglesias P, Pineda-Farias JB, Bravo-Hernández M, et al. Predominant role of spinal P2Y1 receptors in the development of neuropathic pain in rats. *Brain Res*.

150. Li N, Lu ZY, Yu LH, Burnstock G, Deng XM, Ma B. Inhibition of G protein-coupled P2Y2 receptor induced analgesia in a rat model of trigeminal neuropathic pain. *Mol Pain*. 2014;10:21-8069-10-21.

151. Barragan-Iglesias P, Pineda-Farias JB, Cervantes-Duran C, et al. Role of spinal P2Y6 and P2Y11 receptors in neuropathic pain in rats: Possible involvement of glial cells. *Mol Pain*. 2014;10:29-8069-10-29.

152. Jang JH, Kim D-, Sang Nam T, Se Paik K, Leem JW. Peripheral glutamate receptors contribute to mechanical hyperalgesia in a neuropathic pain model of the rat. *Neuroscience*. 2004;128(1):169-176.

153. Communi D, Parmentier M, Boeynaems J. Cloning, functional expression and tissue distribution of the human P2Y6Receptor. *Biochem Biophys Res Commun*. 1996;222(2):303-308.

154. Thurmond RL, Gelfand EW, Dunford PJ. The role of histamine H1 and H4 receptors in allergic inflammation: The search for new antihistamines. *Nat Rev Drug Discov*. 2008;7(1):41-53.

155. Leung L, Cahill CM. TNF-alpha and neuropathic pain--a review. *J Neuroinflammation*. 2010;7:27-2094-7-27.

156. Campbell SS, Tobler I. Animal sleep: A review of sleep duration across phylogeny. *Neurosci Biobehav Rev*. 1984;8(3):269-300.

157. Kirszenblat L, van Swinderen B. The yin and yang of sleep and attention. *Trends Neurosci*. 2015;38(12):776-786.

158. Hossain JL, Shapiro CM. The prevalence, cost implications, and management of sleep disorders: An overview. *Sleep Breath*. 2002;6(2):85-102.

159. Okifuji A, Hare BD. Do sleep disorders contribute to pain sensitivity? *Curr Rheumatol Rep*. 2011;13(6):528-534.

160. Lim J, Dinges DF. Sleep deprivation and vigilant attention. *Ann N Y Acad Sci*. 2008;1129(1):305-322.

161. Irwin MR. Why sleep is important for health: A psychoneuroimmunology perspective. *Annu Rev Psychol*. 2015;66:143-172.

162. Alvarez GG, Ayas NT. The impact of daily sleep duration on health: A review of the literature. *Prog Cardiovasc Nurs*. 2004;19(2):56-59.

163. Strecker RE, Morairty S, Thakkar MM, et al. Adenosinergic modulation of basal forebrain and preoptic/anterior hypothalamic neuronal activity in the control of behavioral state. *Behav Brain Res*. 2000;115(2):183-204.

164. Porkka-Heiskanen T, Strecker RE, McCarley RW. Brain site-specificity of extracellular adenosine concentration changes during sleep deprivation and spontaneous sleep: An in vivo microdialysis study. *Neuroscience*. 2000;99(3):507-517.

165. Basheer R, Porkka-Heiskanen T, Strecker RE, Thakkar MM, McCarley RW. Adenosine as a biological signal mediating sleepiness following prolonged wakefulness. *Neurosignals*. 2000;9(6):319-327.

166. Dunwiddie TV, Diao L, Proctor WR. Adenine nucleotides undergo rapid, quantitative conversion to adenosine in the extracellular space in rat hippocampus. *J Neurosci*. 1997;17(20):7673-7682.

167. Zhang J, Wang H, Ye C, et al. ATP released by astrocytes mediates glutamatergic activity-dependent heterosynaptic suppression. *Neuron*. 2003;40(5):971-982.

168. Kalinchuk AV, McCarley RW, Stenberg D, Porkka-Heiskanen T, Basheer R. The role of cholinergic basal forebrain neurons in adenosine-mediated homeostatic control of sleep: Lessons from 192 IgG–saporin lesions. *Neuroscience*. 2008;157(1):238-253.

169. Sims RE, Dale N. Activity-dependent adenosine release may be linked to activation of na(+)-K(+) ATPase: An in vitro rat study. *PLoS One*. 2014;9(1):e87481.

170. Halassa MM, Florian C, Fellin T, et al. Astrocytic modulation of sleep homeostasis and cognitive consequences of sleep loss. *Neuron*. 2009;61(2):213-219.

171. MacVicar BA, Thompson RJ. Non-junction functions of pannexin-1 channels. *Trends Neurosci*. 2010;33(2):93-102.

172. Brown RE, Basheer R, McKenna JT, Strecker RE, McCarley RW. Control of sleep and wakefulness. *Physiol Rev*. 2012;92(3):1087-1187.

173. Naren AP, Nelson DJ, Xie W, et al. Regulation of CFTR chloride channels by syntaxin and Munc18 isoforms. *Nature*. 1997;390(6657):302-305.

174. Kilisch M, Lytovchenko O, Schwappach B, Renigunta V, Daut J. The role of protein-protein interactions in the intracellular traffic of the potassium channels TASK-1 and TASK-3. *Pflugers Arch*. 2015;467(5):1105-1120.

175. Peters KW, Qi J, Johnson JP, Watkins SC, Frizzell R. Role of snare proteins in CFTR and ENaC trafficking. *Pflugers Arch*. 2001;443(1):S65-S69.

176. Fujita T, Chen MJ, Li B, et al. Neuronal transgene expression in dominant-negative SNARE mice. *J Neurosci*. 2014;34(50):16594-16604.

177. Cirelli C, Bushey D, Hill S, et al. Reduced sleep in drosophila shaker mutants. *Nature*. 2005;434(7037):1087-1092.

178. Bushey D, Tononi G, Cirelli C. Sleep and synaptic homeostasis: Structural evidence in drosophila. *Science*. 2011;332(6037):1576-1581.

179. Rogulja D, Young MW. Control of sleep by cyclin A and its regulator. *Science*. 2012;335(6076):1617-1621.

180. Appelbaum L, Wang G, Yokogawa T, et al. Circadian and homeostatic regulation of structural synaptic plasticity in hypocretin neurons. *Neuron*. 2010;68(1):87-98.

181. Yilmaz H, Iskesen I. Follow-up with objective and subjective tests of the sleep characteristics of patients after cardiac surgery. *Circ J*. 2007;71(10):1506-1510.

182. Weiergräber M, Henry M, Hescheler J, Smyth N, Schneider T. Electrocorticographic and deep intracerebral EEG recording in mice using a telemetry system. *Brain Res Protoc*. 2005;14(3):154-164.

183. Huber R, Deboer T, Tobler I. Topography of EEG dynamics after sleep deprivation in mice. *J Neurophysiol*. 2000;84(4):1888-1893.

184. Porkka-Heiskanen T, Strecker RE, Thakkar M, Bjorkum AA, Greene RW, McCarley RW. Adenosine: A mediator of the sleep-inducing effects of prolonged wakefulness. *Science*. 1997;276(5316):1265-1268.

185. Arrigoni E, Chamberlin NL, Saper CB, McCarley RW. Adenosine inhibits basal forebrain cholinergic and noncholinergic neurons in vitro. *Neuroscience*. 2006;140(2):403-413.

186. Stenberg D, Litonius E, Halldner L, Johansson B, Fredholm BB, Porkka-Heiskanen T. Sleep and its homeostatic regulation in mice lacking the adenosine A1 receptor. *J Sleep Res*. 2003;12(4):283-290.

187. Orellana JA, Montero TD, von Bernhardi R. Astrocytes inhibit nitric oxide-dependent Ca2+ dynamics in activated microglia: Involvement of ATP released via pannexin 1 channels. *Glia*. 2013;61(12):2023-2037.

188. Franken P, Malafosse A, Tafti M. Genetic determinants of sleep regulation in inbred mice. *Sleep*. 1999;22(2):155-169.

189. Kuna ST, Maislin G, Pack FM, et al. Heritability of performance deficit accumulation during acute sleep deprivation in twins. *Sleep*. 2012;35(9):1223-1233.

190. Grandner MA, Hale L, Moore M, Patel NP. Mortality associated with short sleep duration: The evidence, the possible mechanisms, and the future. *Sleep Med Rev*. 2009;14(3):191-203.

191. Martínez-Ruiz A, Lamas S. Signalling by NO-induced protein S-nitrosylation and S-glutathionylation: Convergences and divergences. *Cardiovasc Res*. 2007;75(2):220-228.

192. Grek CL, Zhang J, Manevich Y, Townsend DM, Tew KD. Causes and consequences of cysteine S-glutathionylation. *J Biol Chem*. 2013;288(37):26497-26504.

193. Yang Y, Shi W, Chen X, et al. Molecular basis and structural insight of vascular K(ATP) channel gating by S-glutathionylation. *J Biol Chem*. 2011;286(11):9298-9307.

194. Yang Y, Shi W, Cui N, Wu Z, Jiang C. Oxidative stress inhibits vascular K(ATP) channels by S-glutathionylation. *J Biol Chem*. 2010;285(49):38641-38648.

195. Wang W, Oliva C, Li G, Holmgren A, Lillig CH, Kirk KL. Reversible silencing of CFTR chloride channels by glutathionylation. *J Gen Physiol*. 2004;125(2):127-141.

196. Tang H, Viola HM, Filipovska A, Hool LC. Cav1.2 calcium channel is glutathionylated during oxidative stress in guinea pig and ischemic human heart. *Free Radic Biol Med*. 2011;51(8):1501-1511.

197. Grattagliano I, Wieland P, Schranz C, Lauterburg BH. Disposition of glutathione monoethyl ester in the rat: Glutathione ester is a slow release form of extracellular glutathione. *J Pharmacol Exp Ther*. 1995;272(2):484-488.

198. Ascenzi P, Colasanti M, Persichini T, et al. Re-evaluation of amino acid sequence and structural consensus rules for cysteine-nitric oxide reactivity. *Biol Chem*. 2000;381(7):623-627.

199. Poornima V, Vallabhaneni S, Mukhopadhyay M, Bera AK. Nitric oxide inhibits the pannexin 1 channel through a cGMP–PKG dependent pathway. *Nitric Oxide*. 2015;47:77-84.

200. Yuan H, Gaber MW, McColgan T, Naimark MD, Kiani MF, Merchant TE. Radiation-induced permeability and leukocyte adhesion in the rat blood–brain barrier: Modulation with anti-ICAM-1 antibodies. *Brain Res*. 2003;969(1–2):59-69.

201. Cui YZ, Hisha H, Yang GX, et al. Optimal protocol for total body irradiation for allogeneic bone marrow transplantation in mice. *Bone Marrow Transplant*. 2002;30(12):843-849.

202. Geuna S. The sciatic nerve injury model in pre-clinical research. *J Neurosci Methods*. 2015;243:39-46.

203. Griffin JW, Pan B, Polley MA, Hoffman PN, Farah MH. Measuring nerve regeneration in the mouse. *Exp Neurol*. 2010;223(1):60-71.

204. Wood MD, Kemp SWP, Weber C, Borschel GH, Gordon T. Outcome measures of peripheral nerve regeneration. *Ann Anat*. 2011;193(4):321-333.

205. Vogt A, Hormuzdi SG, Monyer H. Pannexin1 and Pannexin2 expression in the developing and mature rat brain. *Mol Brain Res*. 2005;141(1):113-120.

206. Rainnie DG, Grunze HC, McCarley RW, Greene RW. Adenosine inhibition of mesopontine cholinergic neurons: Implications for EEG arousal. *Science*. 1994;263(5147):689-692.

207. Aston-Jones G, Shaver R, Dinan T. Cortically projecting nucleus basalis neurons in rat are physiologically heterogeneous. *Neurosci Lett*. 1984;46(1):19-24.

208. Han S, Murchison D, Griffith WH. Low voltage-activated calcium and fast tetrodotoxin-resistant sodium currents define subtypes of cholinergic and noncholinergic neurons in rat basal forebrain. *Mol Brain Res*. 2005;134(2):226-238.

209. Pellegatti P, Falzoni S, Pinton P, Rizzuto R, Di Virgilio F. A novel recombinant plasma membrane-targeted luciferase reveals a new pathway for ATP secretion. *Mol Biol Cell*. 2005;16(8):3659-3665.

210. Furlow PW, Zhang S, Soong TD, et al. Mechanosensitive pannexin-1 channels mediate microvascular metastatic cell survival. *Nat Cell Biol*. 2015;17(7):943-952.